ISSN 2071-4726
2071-0305

Инженерно-строительный журнал

НАУЧНОЕ ИЗДАНИЕ

№1(69) 2017

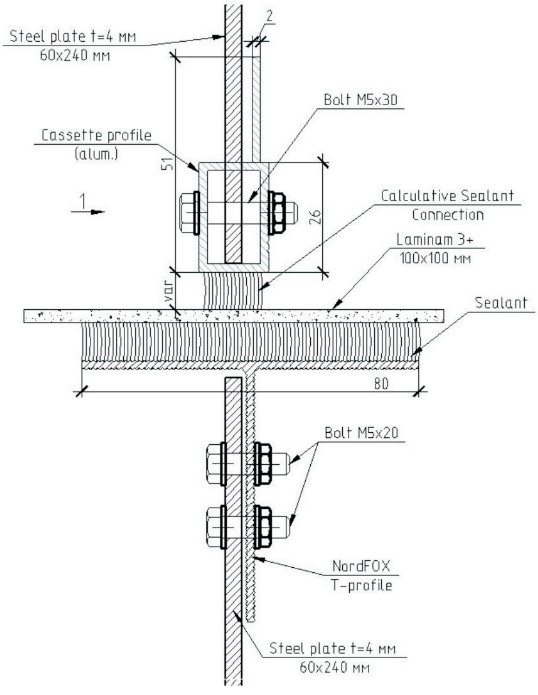

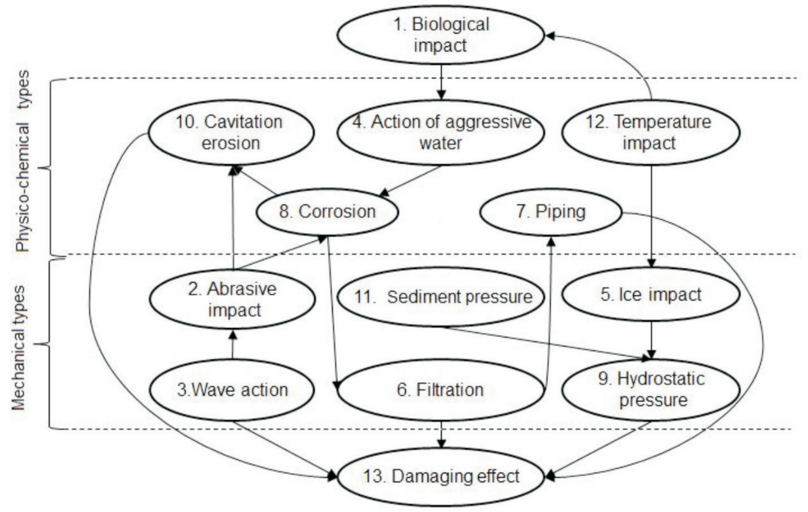

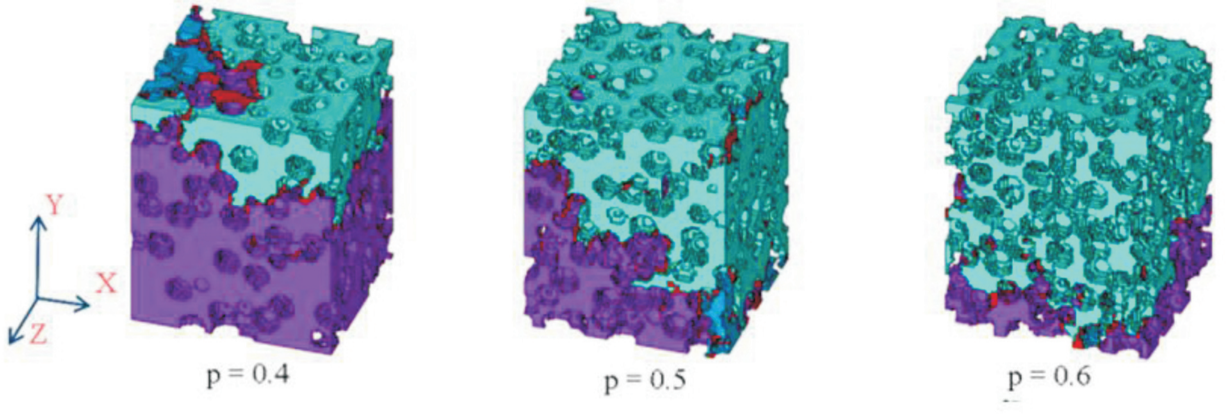

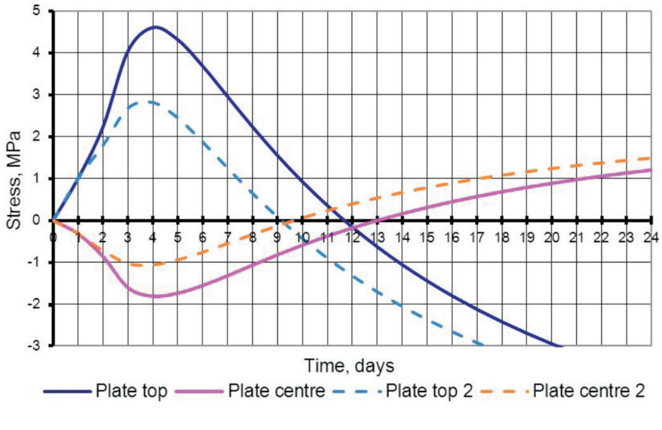

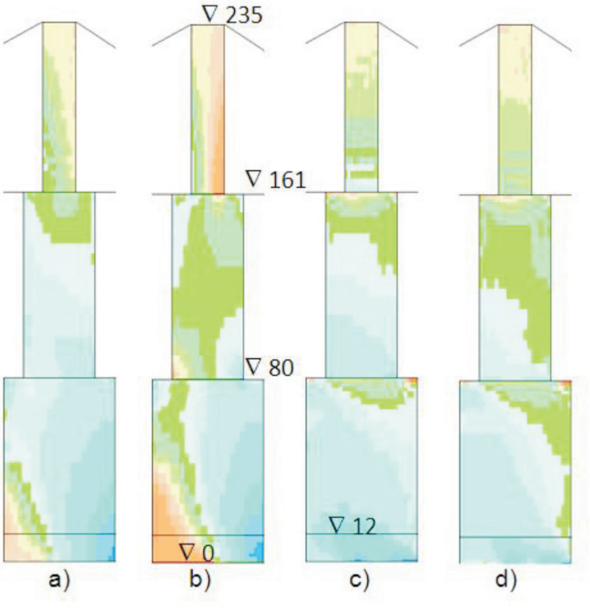

Федеральное государственное автономное образовательное учреждение
высшего образования
Санкт-Петербургский политехнический университет Петра Великого

ПОЛИТЕХ
Санкт-Петербургский политехнический университет Петра Великого

Инженерно-строительный институт
Центр дополнительных профессиональных программ

195251, г. Санкт-Петербург, Политехническая ул., 29,
тел/факс: 552-94-60, www.stroikursi.spbstu.ru,
stroikursi@mail.ru

Приглашает специалистов организаций, вступающих в СРО, на курсы повышения квалификации (72 часа)

Код	Наименование программы	Виды работ*
Курсы по строительству		
БС-01-04	«Безопасность и качество выполнения общестроительных работ»	**п.1,2, 3, 5, 6, 7, 9, 10, 11, 12, 13, 14**
БС-01	«Безопасность и качество выполнения геодезических, подготовительных и земляных работ, устройства оснований и фундаментов»	**1,2,3,5**
БС-02	«Безопасность и качество возведения бетонных и железобетонных конструкций»	**6,7**
БС-03	«Безопасность и качество возведения металлических, каменных и деревянных конструкций»	**9,10,11**
БС-04	«Безопасность и качество выполнения фасадных работ, устройства кровель, защиты строительных конструкций, трубопроводов и оборудования»	**12,13,14**
БС-05	«Безопасность и качество устройства инженерных сетей и систем»	**15,16,17,18,19**
БС-06	«Безопасность и качество устройства электрических сетей и линий связи»	**20,21**
БС-08	«Безопасность и качество выполнения монтажных и пусконаладочных работ»	**23,24**
БС-12	«Безопасность и качество устройства мостов, эстакад и путепроводов»	**29**
БС-13	«Безопасность и качество выполнения гидротехнических, водолазных работ»	**30**
БС-14	«Безопасность и качество устройства промышленных печей и дымовых труб»	**31**
БС-15	«Осуществление строительного контроля»	**32**
БС-16	«Организация строительства, реконструкции и капитального ремонта. Выполнение функций технического заказчика и генерального подрядчика»	**33**
Курсы по проектированию		
БП-01	«Разработка схемы планировочной организации земельного участка, архитектурных решений, мероприятий по обеспечению доступа маломобильных групп населения»	**1,2,11**
БП-02	«Разработка конструктивных и объемно-планировочных решений зданий и сооружений»	**3**
БП-03	«Проектирование внутренних сетей инженерно-технического обеспечения»	**4**
БП-04	«Проектирование наружных сетей инженерно-технического обеспечения»	**5**
БП-05	«Разработка технологических решений при проектировании зданий и сооружений»	**6**
БП-06	«Разработка специальных разделов проектной документации»	**7**
БП-07	«Разработка проектов организации строительства»	**8**
БП-08	«Проектные решения по охране окружающей среды»	**9**
БП-09	«Проектные решения по обеспечению пожарной безопасности»	**10**
БП-10	«Обследование строительных конструкций и грунтов основания зданий и сооружений»	**12**
БП-11	«Организация проектных работ. Выполнение функций генерального проектировщика»	**13**
Э-01	«Проведение энергетических обследований с целью повышения энергетической эффективности и энергосбережения»	
Курсы по инженерным изысканиям		
И-01	«Инженерно-геодезические изыскания в строительстве»	**1**
И-02	«Инженерно-геологические изыскания в строительстве»	**2,5**
И-03	«Инженерно-гидрометеорологические изыскания в строительстве»	**3**
И-04	«Инженерно-экологические изыскания в строительстве»	**4**
И-05	«Организация работ по инженерным изысканиям»	**7**

***(согласно приказам Минрегионразвития РФ N 624 от 30 декабря 2009 г.)**

По окончании курса слушателю выдается удостоверение о краткосрочном повышении квалификации установленного образца (72 ак. часа)

Для регистрации на курс необходимо выслать заявку на участие, и копию диплома об образовании по телефону/факсу: 8(812) 552-94-60, 535-79-92, , e-mail: stroikursi@mail.ru.

http://www.engstroy.spbstu.ru – полнотекстовая версия журнала в сети Интернет.
Бесплатный доступ, обновление с каждым новым выпуском

Инженерно-строительный журнал
НАУЧНОЕ ИЗДАНИЕ

ISSN 2071-4726

Свидетельство о государственной регистрации: ПИ №ФС77-38070, выдано Роскомнадзором

Специализированный научный журнал. Выходит с 09.2008.

Включен в Перечень ведущих периодических изданий ВАК РФ

Периодичность: 8 раз в год

Учредитель и издатель:

Санкт-Петербургский политехнический университет Петра Великого

Адрес редакции:

195251, СПб, ул. Политехническая, д. 29, Гидрокорпус-2, ауд. 227А

Содержание

На обложке: иллюстрации авторов к статьям номера

Установочный тираж 1000 экз.
Подписано в печать 05.05.2017. Формат 60x84/8, усл. печ. л. 11. Заказ №
Отпечатано в типографии СПбПУ. СПб, ул. Политехническая, д. 29

Контакты:

Тел. +7(812)535-52-47 E-mail: mce@ice.spbstu.ru
Web: http://www.engstroy.spbstu.ru

http://www.engstroy.spbstu.ru – full-text open-access version in Internet. It is updated immediately with each new issue.

Magazine of Civil Engineering
SCHOLAR JOURNAL

ISSN 2071-4726

Peer-reviewed scientific journal

Start date: 2008/09

8 issues per year

Publisher:

Peter the Great St. Petersburg Polytechnic University

Indexing:

Scopus, Russian Science Citation Index (WoS), Compendex, DOAJ, EBSCO, Google Academia, Index Copernicus, ProQuest, Ulrich's Serials Analysis System

Corresponding address:

227a Hydro Building, 29 Polytechnicheskaya st., Saint-Petersburg, 195251, Russia

Contents

On the cover: authors' illustrations

+7(812) 535-52-47

E-mail: mce@ice.spbstu.ru

Web: http://www.engstroy.spbstu.ru/eng/index.html

doi: 10.18720/MCE.69.1

Modeling of porous material fracture

Моделирование разрушения пористого материала

A.N. Levandovskiy,
B.E. Melnikov,
Peter the Great St. Petersburg Polytechnic University, St. Petersburg, Russia
A.A. Shamkin,
Corning SNG OOO, St. Petersburg, Russia

Младший науч. сотрудник А.Н. Левандовский,
д-р техн. наук, профессор Б.Е. Мельников,
Санкт-Петербургский политехнический университет Петра Великого, г. Санкт-Петербург, Россия
научный сотрудник А.А. Шамкин,
ООО «Корнинг СНГ», г. Санкт-Петербург, Россия

Key words: porous material; fracture; tomography; element deletion; element erosion; element size; fracture criterion; finite element; cordierite; cubic elements

Ключевые слова: пористый материал; разрушение; томография; удаление элементов; разрушение элементов; размер элемента; критерий разрушения; конечный элемент; кордиерит; кубические элементы

Abstract. Wide use of various porous materials in construction engineering applications requires development of up to date methods of non-destructive characterization and optimization of such materials. This work explores an approach to modeling of fracture of a brittle porous material. Available 3D digital data on the specimen geometry is converted into uniform finite element mesh consisting purely of elements of cubic shape. Fracture model is based on a series of linear solutions. Thus approach to linear modeling described in the previous papers could be utilized. Fracture is modeled by consecutive element erosion. A special element erosion criterion is established to avoid finite element size dependency. Two speed-up algorithms are proposed and tested. The approach described can be used for modeling fracture of uniform construction materials, also materials with inclusions under various mechanical and thermal loads.

Аннотация. Использование пористых материалов в промышленном строительстве требует разработки современных неразрушающих алгоритмов исследования и оптимизации эффективных механических свойств этих материалов. В настоящей работе рассмотрен подход к моделированию разрушения пористых материалов. Доступная трехмерная цифровая информация о структуре конвертируется в конечно-элементную модель, состоящую исключительно из одинаковых элементов кубической формы. Модель разрушения базируется на последовательности решений линейных задач. Таким образом, модели, разработанные ранее для моделирования линейных задач, могут обоснованно использоваться. Разрушение моделируется последовательным удалением элементов. Используется специальный критерий разрушения для удаления конечных элементов, который позволяет нивелировать сеточную зависимость. Так же предложены алгоритмы ускорения моделирования разрушения. Описываемый подход может использоваться для моделирования однородных строительных материалов, а так же материалов с включениями под воздействием различных температурно-механических нагрузок

Introduction

Porous structures based on brittle matrices are widely used in building construction and other engineering applications. The key ones to be mentioned: industrial ceramics including chemical- and corrosion-resistant materials, acid-proof wares, decorative tiles, refractory materials and products, bricks, road bricks, blown-out concrete, claydite and other fillers for light concrete, roof tiles, crucibles, troughs, molds for metal, glass, oxide fusion and forming, membranes and filters for mechanical and chemical (catalytic) liquid and gas cleaning [1–2], lined pipes, diesel and gasoline discharge gas filters, electronic high-temperature applications, bio-medical ceramics, domestic ceramics, sanitary earthenware.

The use of porous materials in modern civil engineering requires development of up-to-date methods and algorithms for non-destructive analysis of such materials and their thermo-mechanical property prediction.

Mechanical properties of porous materials were studied analytically, numerically and experimentally, at the most novel experimental facilities.

In the middle of the 20th century Gassmann wrote his equations, establishing a connection between the elastic parameters of porous matter, filled with liquid or gas [3]. Gassmann’s equations are used in geo-physics to estimate effective elastic properties of rocks.

During the last decades a number of papers were published, containing theoretical as well as half-empirical manipulations regarding effective linear properties of the porous structures of the specific kinds [4−9].

Numerical studies of the effective properties of the multi-phase and porous structures are conducted namely with the use of finite element method (FEM). The idea of the FEM was originally formulated more than 50 years ago [10]. A considerable contribution to the development of FEM was made by the Russian scientists and representatives of the St. Petersburg Polytechnic school [11−14].

Calculations on representative specimens of 3D non-periodic porous structures require a substantial amount of computer memory (of the order of tens of gigabytes). Therefore in most published papers authors only deal with periodic geometry structures, artificially generated (not existing in nature) on a computer with the use of some random algorithms [7, 15−20].

Only during the past years it became possible to directly simulate porous 3D structures. The problem had not been only with the computer power but also with the devices capable of digitizing the whole depth of the structures (not just surfaces) with extremely high resolution: median pore size in some could be as small as just a few microns. The first method to be mentioned here is the computer micro tomography [21]. With the use of tomography date the numerical studies of the microstructures are conducted [22−27]. Primarily those studies deal with bone properties. Some geological research may also be referred to [28].

The present investigation is based on the approaches to porous structure linear modeling described by the authors in the earlier papers [24]. The fracture models established here consist of series of linear runs similar to the ones used earlier to calculate the effective elasticity and thermal conductivity [24].

In [22, 23, 29, 30] attempts are made to simulate 2D material structures based on electronic microscopy and spectroscopy date.

Rarely is any special attention paid to the tomogram resolution and mesh convergence [17, 18, 24].

Besides traditional macroscopic experimental studies of the mechanical parameters of the porous structures [31, 32] for microstructure study special methods are developed and applied. The most useful of those is probably the neutron diffraction method to study deformation of the structures at micro-level [33−35, 7, 24, 37]. In the present study as examples of such methods tomography specimens of cordierite and aluminum titanate (AT) are considered. Aluminum titanate is a ceramic material that cannot be wetted by liquid aluminum and is also known for its excellent resistance to thermal shock. This makes it the ideal choice for use in aluminum foundries [36].Both cordierite and AT are thermal shock resistant and often used for components subject to high thermal stress levels. Potential consumers for such ceramics may be: energetic and industrial construction companies, in particular aluminum manufacturers, vendors and users of diesel particulate filters.

The aim of the current research is to develop a method of modeling fracture of a porous material when the material geometry is taken from 3D tomography images. The method should be invariant to the finite element (FE) mesh used. Since FE models used consist of identical FE of the cubic shape and the locations of the FE elements are prescribed (mesh could not be skewed etc.), there is only one important task that needs to be solved: the fracture model should give identical or convergent results on meshes with different FE sizes (e.g. meshes based on different tomography resolutions).

The modeling approach could then be used to model fracture of various porous construction materials or materials with inclusions, under mechanical and thermal loads.

Fracture is modeled under external uniaxial tension and compression by element deletion technique. The incrementally deleted (finite) elements approximately trace the crack initiation and propagation over the structure. Respective degradation of elasticity of the cracked body is evaluated at each step and so calculated stress-strain curves provide comprehensive information on effective Young's moduli, fracture toughness, tensile/compressive strength, and strain tolerance. The key of the simulation approach is the criterion for element deletion that delivers physically meaningful stress-strain curves with the results being stable at different finite element sizes (tomography resolutions).

Methods and materials

Material structures are presented by 3D arrays of solid cubic elements (voxels) of isotropic matter.

The following three types of materials are considered:

1. Virtual overlapped spherical pores structures of 100 x 100 x 100 = 10^6 voxels and total porosity of 0.3, 0.4, 0.5, and 0.6 (Figure 1)

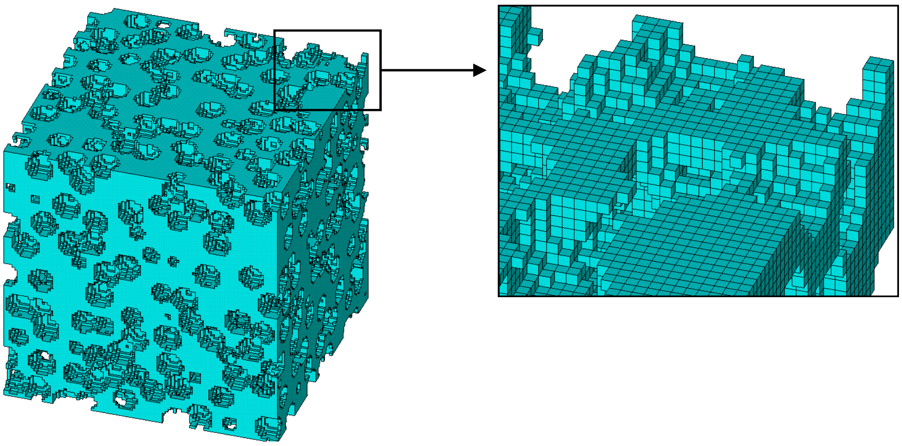

Figure 1. FE model of a virtual structure of overlapped spherical pores. Porosity = 0.5

2. Virtual overlapped spherical solids structures of 100 x 100 x 100 = 106 voxels and total porosity of 0.41, 0.52, and 0.63 (Figure 2). These structures have been obtained by inversing overlapped spherical pore structures. The procedure of inversion assumed "dust removal" for correct porosity evaluation, i.e. deleting the solid element cluster not connected to the main body that has originated from isolated pores inversion.

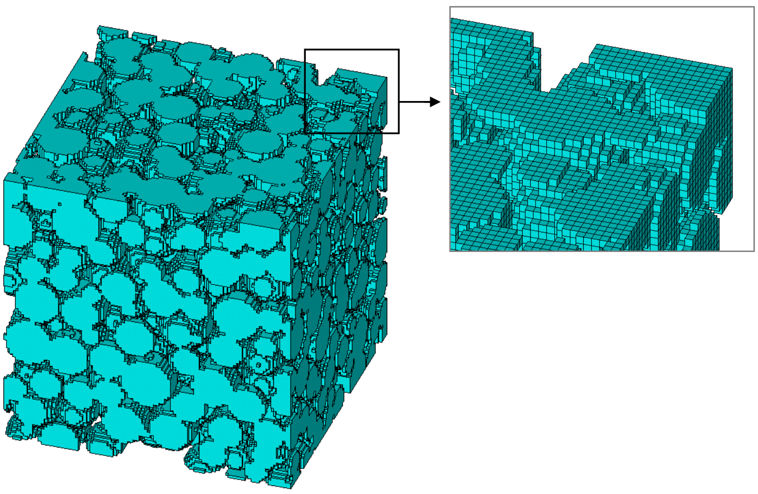

Figure 2. FE model of a virtual structure of overlapped solid spheres. Porosity = 0.5

3. 3D tomography samples of real materials. Cordierite JR1 and aluminum titanate AT (Figure 3).

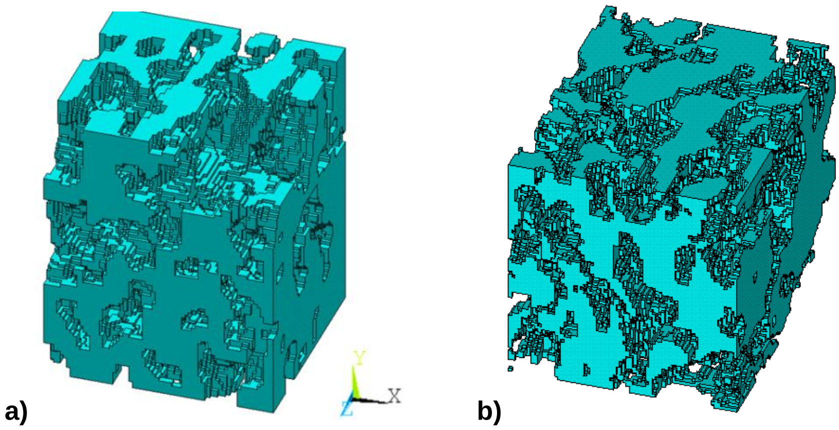

Figure 3. FE models of a quarter of cordierite sample JR1 (a) and an aluminum titanate sample AT (b)

Earlier papers are referenced here to give more details on the 3D FE models based on tomography data [24, 25, 37].

Figure 4 shows the statement used to calculate stress-strain response of the specimens at the macro-level. Out of a number of statements possible [38] the displacement BCs are used to be able to track material response after maximum stress is reached.

Specimen fracture is simulated by element deletion (erosion) approach: a structure is loaded until the critical value of the chosen criterion in a FE is reached. The criterion value in an FE is determined by averaging over all 8 nodes of the element. One linear task could be solved at any load and then scaled accordingly (Figure 5). Afterwards the element is removed and so on. In most simulations here an arbitrary trial value is taken for the critical criterion value for comparative analysis purposes. All tasks appear to be essentially linear. So all calculated stress-strain dependencies could be linearly scaled for any other critical criterion value. The absolute critical value for the criterion could be estimated once an experimental data set is available to fit the modeling data to.

ε^1 – the first principal strain norm is used in most simulations as a criterion typical for brittle materials. σ^1 – the first principal stress could also be applied.

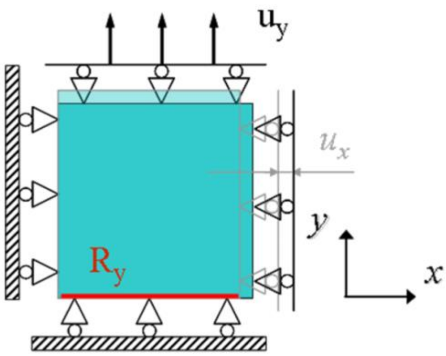

Figure 4. BCs used in the simulations (displacement is applied, reaction force is measured) to calculate stress-strain response of the specimens [7]

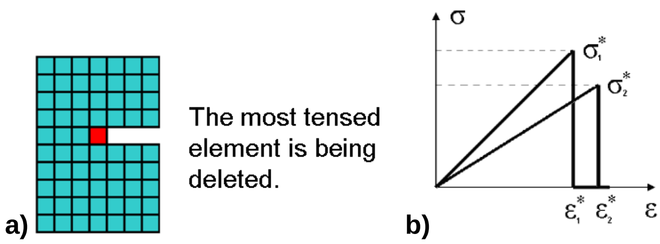

Figure 5. a) One step for crack propagation calculation b) Input properties of elements for different materials (1) and (2)

Numerical values of input parameters and their meanings will be noted in line with calculated results by specific material number from Table 1 below. Here the following notations are used:

ε^{*}_{crit}– critical value of first principal strain, at reaching which the element needs to be deleted,

γ– surface cleavage energy, corresponding to the critical value of the criterion, calculated from (4).

Table 1. Properties of the considered materials

Material	ε^{*}_{crit}, %	E, GPa	γ, J/m^2	Element size, μm
1	1.71	340	25	1.0
2	1.40	340	25	1.5
3	0.99	340	25	3
4	1.62	340	25	1.12
5	1.48	340	25	1.34
6	1.32	340	25	1.68
7	1.15	340	25	2.24
8	0.936	340	25	3.36
9	0.662	340	25	6.72
10	0.752	340	25	5.2
11	1.21	340	25	2
12	16.7	144	-	-

Results and Discussion

Crack initiation points

The effect of external load in JR1 structure is simulated as shown in Figure 4. The elements exceeding a certain strain could be selected, as shown in Figure 6, where “y” – vertical axis, “micro” and “macro” relate to values averaged over one FE or effectively over the whole structure. The probability density of the elementwise 1st principal strain distribution normalized by macroscopic (effective) uniaxial strain is shown in Figure 6 together with the picture showing space distribution of the most tensed elements. One can see that the elements are not concentrated in one location, they are rather randomly distributed through the volume, which means that we should expect multiple crack initiations and development in many locations simultaneously rather than a single crack propagation phenomena.

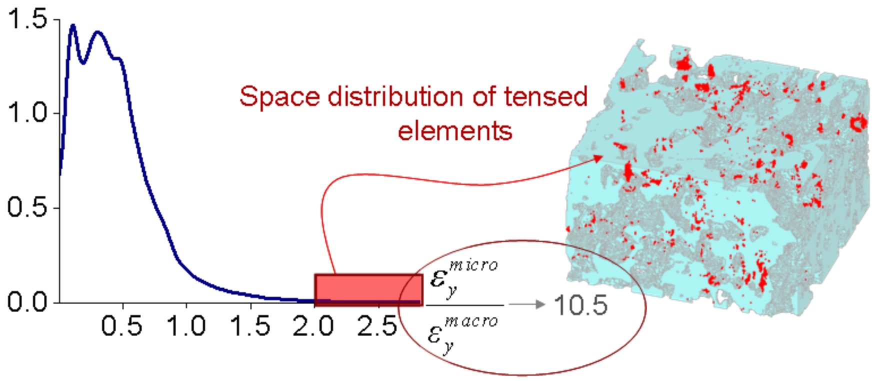

Figure 6. Strain probability distribution (left) and Space distribution of the most tensed elements in terms of the 1st principal strain value (right) for JR1. Since critical points are not concentrated, a single crack development would not occur; rather a lot of small sub-cracks can be expected

Number of elements to be deleted at each iteration

An attempt is made to speed up the solution. At first the number elements to be deleted at one step is estimated. The accurate way of fracture calculation is to delete the most stressed elements one by one and recalculating the strain distribution after each step. Calculations can be significantly increased if the number of elements being deleted at each step is more than one.

The diagram in Figure 7 illustrates a comparison of two stress-strain curves evaluated on the same tomogram, a quarter of JR1, with one and eight elements being deleted at one step. On the plot "y" denotes the axis of loading, "macro" – values recalculated from the BC and the effective reactions on the borders, ε^{*iso} – the critical value for the first principal strain element erosion criterion (see material #12 from Table 1).

In this particular case the curve difference looks negligible so the calculation speed up could be more valuable than accuracy.

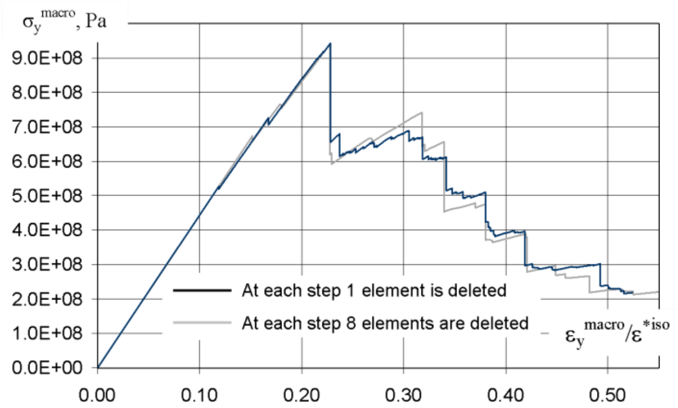

Figure 7. Tensile stress-strain curves for a quarter of JR1 specimen (85 x 70 x 65 voxels, 85 x 70 x 65 elements) with different number of elements deleted at one step. Material # 12.

Interestingly the deletion of elements begins at the strain level of approximately ten times less than the element strain tolerance. That implies high non-uniformity of micro strain/stress distribution in the pore structure.

Another alternative way to potentially speed up the process is to use a number of load steps. If the value of maximum load that the specimen can bare is approximately known, one could take a portion of that load and check if any of the FEs need to be deleted (using an element fracture criterion). When those elements are removed, another linear iteration is run with the load unchanged. The process repeats until there are zero elements to remove. Afterwards the next portion of the load is added and so on. The plot below (Figure 8) illustrates the quality of the results obtained with different speed-up techniques on an AT tomography specimen. It is clearly seen from Figure 8 that one can obtain reasonably good stress-strain results spending less than 6 % of the time needed for an "ideal" solution (1 deleted element per each linear solution). The most beneficial technology is the stepped load version of the algorithm.

Most of the results in the following paragraphs are obtained deleting 3 elements at each linear calculation iteration. The stepped load approach is not used in for the simulations described in this paper because historically it was developed later in particular for thermal fracture simulations.

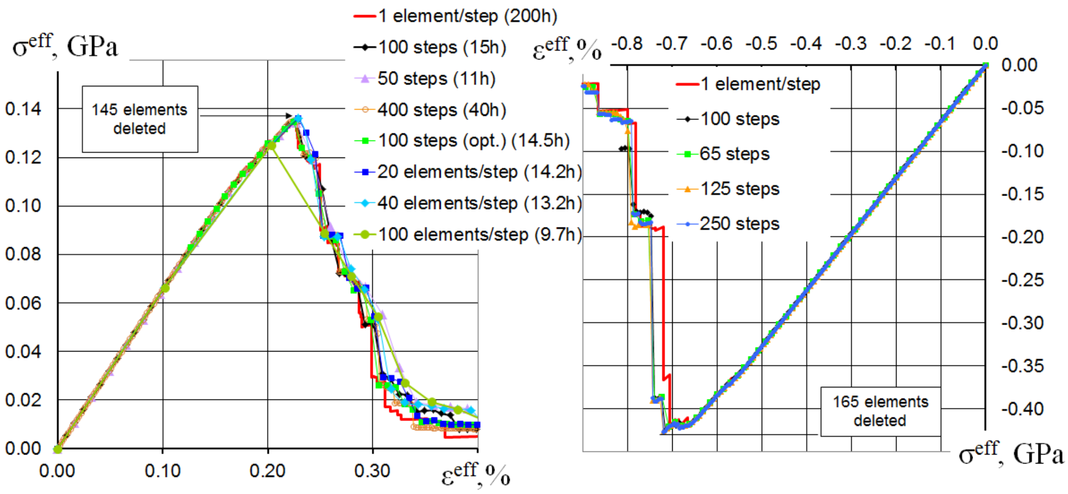

Figure 8. Tensile stress-strain curves for an AT specimen (E = 340 GPa, FE size is 5.2 μm), "x" direction. "Eff" denotes effective quantities

Stress-strain dependency for spherical pores/solids structures

In this section the results of fracture simulation with selected 1st principal stain criterion are shown for virtually generated structures. Simulated resolution (element size) is 1 micron at median pore size $d_{50} = 5.5$ microns. The structures with spherical pores have pore morphology parameter [24] m ~ 2, the 1st principal strain criterion assumed with the material properties corresponding to Material # 12 from Table 1.

Structure compressive and tensile strength both decrease with porosity and pore morphology factor (m). Tension always breaks the sample into two parts, whereas compression can produce more parts (Figures 9–12).

The ratio of tensile strength to compressive strength is about 3 at m = 2 (Figure 13) and tends to lower to the value of 2.4 at higher pore morphology m = 4.24 (Figure 14, see also table 5 at the end of the section).

Tensional strain tolerance (strain corresponding to the effective strength of the structure) increases with porosity at a constant m value and also increases with m at a constant porosity (Figures 13-14).

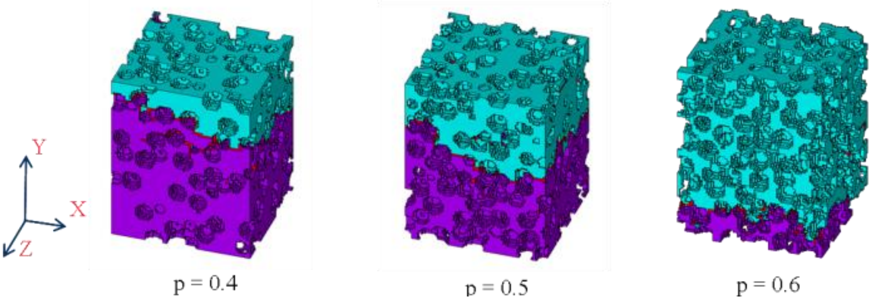

Figure 9. Overlapping spherical pores. Tension

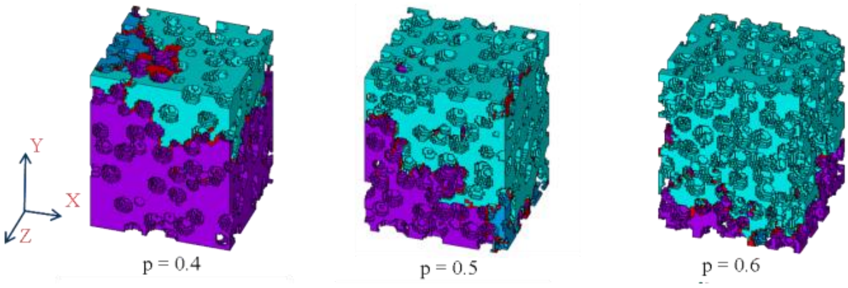

Figure 10. Overlapping spherical pores. Compression

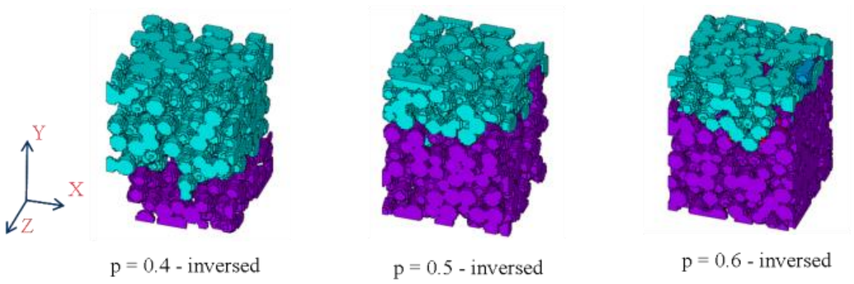

Figure 11. Overlapping spherical solids. Tension

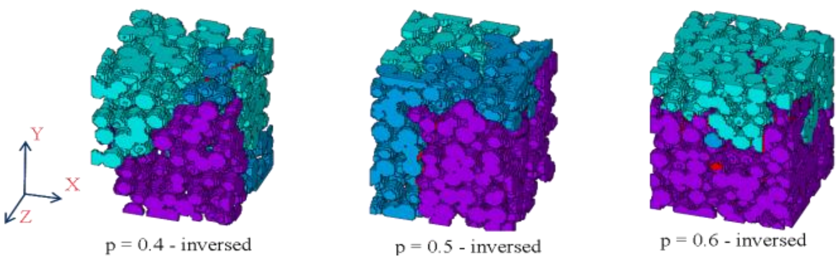

Figure 12. Overlapping spherical solids. Compression

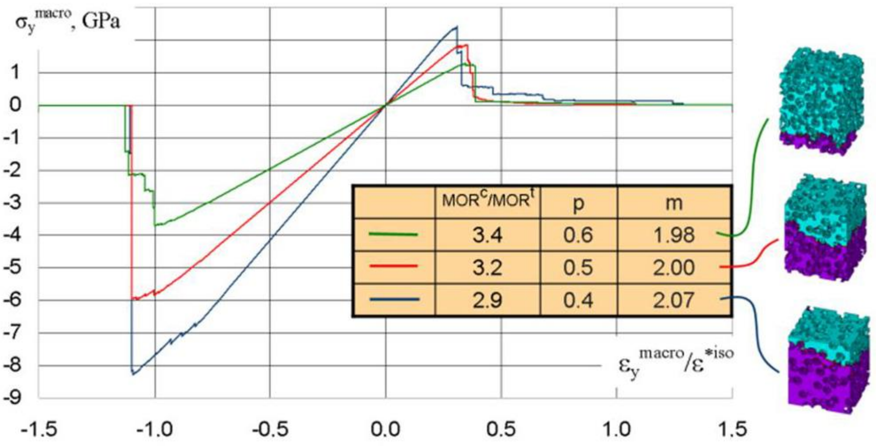

Figure 13. Overlapping spherical pores. Stress-strain curves. Material #12

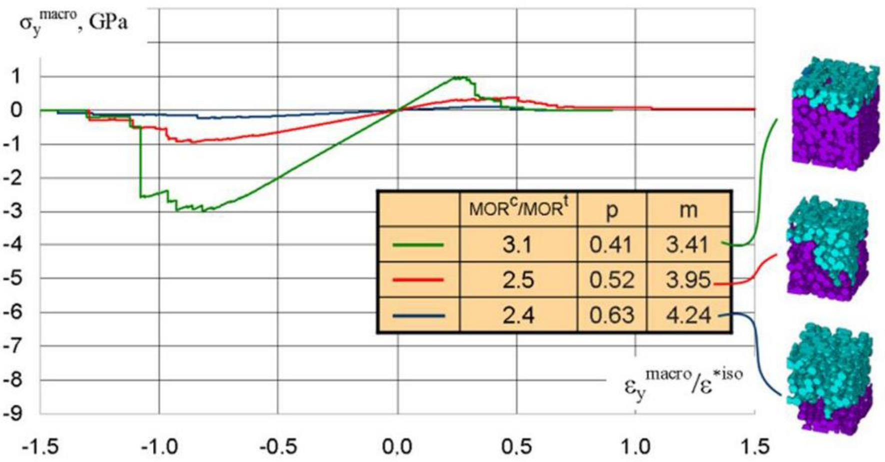

Figure 14. Overlapping spherical solids. Stress-strain curves. Material #12

Influence of extrusion process

As far as tensional strain tolerance increases with p, one can conclude that it is generally beneficial to use high-porosity materials in the applications where large thermal gradients exist, like exhaust filters.

It is also important the tensional strain tolerance increases with m. As shown in [39, 40], filter walls are weaker in the directions perpendicular to the extrusion axis. Taking into account that these are the directions of the highest thermal gradients [41, 42] the following conclusion is formulated: extrusion process itself has a positive influence on the overall thermal shock resistance of the filter structure. A solid statistical confirmation of this conclusion is a subject of future studies.

Element erosion criterion modifications to be used at different FE sizes

While simulating fracture of another part of JR1 – 120^3 piece (taken cube 120 x 120 x 120 1um voxels, and then coarsened to 6 um voxels) with 1st principal strain criterion at various element sizes, an approximately square root dependency of calculated MOR (maximum stress, effective strength of the specimens) on element size has been observed (Figures 15–17).

In Figure 15 the plots calculated for the same material structure and solid element properties (material #12) but different element sizes are shown. It can be seen that all the plots have similar shape but the scale is different. This is caused by the fact that element stresses/strains depend on the element size. For example element stresses and strains may reach infinite values (due to presence of re-entrant angles) if we take a zero volume of averaging – zero element size. The larger element size we take, the less the value of maximum element stresses/strains in the structure we have. So for larger elements we will have to apply larger macroscopic tension for the tensed elements to fail.

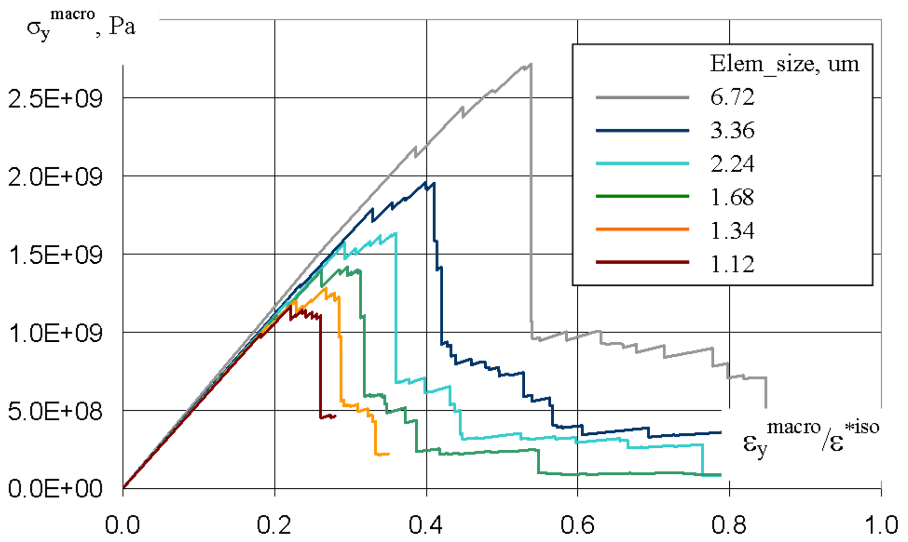

Figure 15. Stress-strain calculation dependence on cubic element size. Simple, element size independent, maximum strain criterion. Material #12

To exclude the dependency on FE size, the following modification of element failure criterion has been developed

As it is known from the general elasticity theory, in the field of macroscopic stresses in the vertices of the re-entrant corner there stresses and strains are not regular and tend to infinity [43]. In the vicinity of a vertex strain and stress tensor component are inversely proportional to the distance to the vertex r in a power λ:

$$\varepsilon_{ij} \sim \frac{1}{r^{\lambda}}, \qquad \sigma_{ij} \sim \frac{1}{r^{\lambda}} \tag{1}$$

For the exponent λ there is some theoretical data:

— in a crack tip it is equal to 0.5 [43];

— in a right corner tip it is 0.455 [43].

λ or <λ> is not easy to determine in our cases since FE models are of finite sizes and the type of defect vary for each stressed element.

It is proposed to check the 1st principal strain distribution in the elements that were deleted during fracture simulation of JR1 quarter (Figure 15). For each FE 1st principal strain is scaled such that macroscopic strain on the specimen is constant (1 % in this particular case). Then the median first principal strain is taken for each FE size (averaged among all deleted elements) and put on a plot (Figure 16). After power interpolation along the points on the plot (Figure 16) <λ> is obtained for the current structure.

In the Table 2 the results are given for median $<\varepsilon^1>$ and <λ> for the structures studied. All values are in the range 0.455–0.497.

Table 2. Median average values for ε^1 and λ for the structures studied

	Tension	Compression
JR1 (120^3 sample)	$\langle\lambda\rangle = 0.477$	$\langle\lambda\rangle = 0.455$
r, μm	$\langle\varepsilon^1\rangle$	$\langle\varepsilon^1\rangle$
6.72	$2.03\cdot 10^{-2}$	$7.87\cdot 10^{-3}$
3.36	$2.65\cdot 10^{-2}$	$1.05\cdot 10^{-2}$
2.24	$3.10\cdot 10^{-2}$	$1.27\cdot 10^{-2}$
1.68	$3.60\cdot 10^{-2}$	$1.42\cdot 10^{-2}$
1.34	$4.03\cdot 10^{-2}$	$1.62\cdot 10^{-2}$
1.12	$4.60\cdot 10^{-2}$	$1.80\cdot 10^{-2}$
JR1 (quarter sample)	$\langle\lambda\rangle = 0.497$	$\langle\lambda\rangle = 0.462$
r, μm	$\langle\varepsilon^1\rangle$	$\langle\varepsilon^1\rangle$
6.72	$2.72\cdot 10^{-2}$	$9.59\cdot 10^{-3}$
3.36	$3.91\cdot 10^{-2}$	$1.41\cdot 10^{-2}$
2.24	$4.68\cdot 10^{-2}$	$1.57\cdot 10^{-2}$

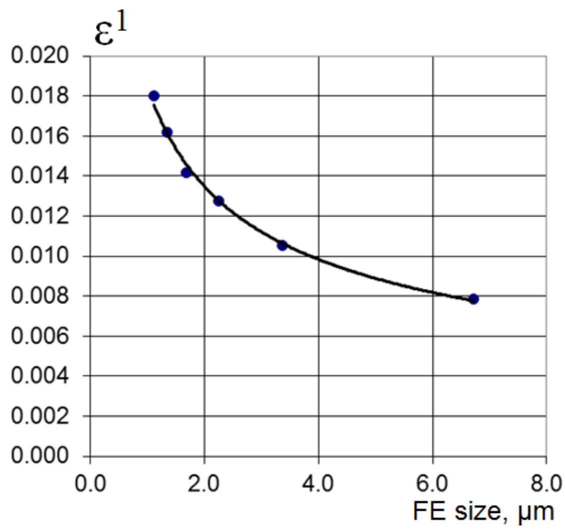

Figure 16. Median average values of ε^1 in the deleted elements in the special task described in the text. Specimen JR1 120x120x120. Compression. $\langle\lambda\rangle$ calculated is 0.455

Taking into account what is said above about σ(ε) scaling on different meshes with the constant criterion $\varepsilon^1 = \varepsilon^*$, a modified element erosion criterion is introduced, that depends on the FE size as follows:

$$\varepsilon^1 = \varepsilon^*(r),$$
$$\varepsilon^*(r) = \varepsilon^*(r_0)\left(\frac{r_0}{r}\right)^{\lambda}, \tag{2}$$
$$\varepsilon^*(r_0) = \varepsilon_0^*,$$

where r – FE element edge length;

r_0 – base FE element edge length, for which critical $\boldsymbol{\varepsilon_0^*}$ is assumed to be known;

λ – average power exponent (singular exponent), determined by the geometry and BC;

λ = 0.5 is suggested for simplicity and only small potential inaccuracy for very different FE sizes ($\frac{1}{r^{\lambda}}$ varies by no more than 10 % at even 10 times changes of r – FE element edge length).

Test simulation results below (Figures 17–20) show that the modified criterion of element fracture yields comparable and converging results at different meshes.

The value of ε_0^* could be determined if suitable experimental data is available. The data could be either a macro stress-strain dependency for tension or compression of a specimen of a known material (material for which typical geometry information is available, e.g. through 3D tomography). Then a trial FE simulation based on the known geometry (with ε_0^* of an arbitrary choice) is compared against the experimental data. Based on that comparison the value of ε_0^* is chosen that provides the best fit of the experimental data.

Another option could be used when fracture of a thermally microcracked material [37] is simulated. Such materials consist of orthotropic domains and are intact (have no cracks) at some reference temperature (typically around 1200 °C). The material structure and thermally induced microcracking upon cooling could be simulated. If effective Young's modulus on temperature dependency $E^{eff}(T)$ for the material is known then it could be compared to the simulation results. Based on that comparison the value of ε_0^* is chosen that provides the best fit of the experimental data.

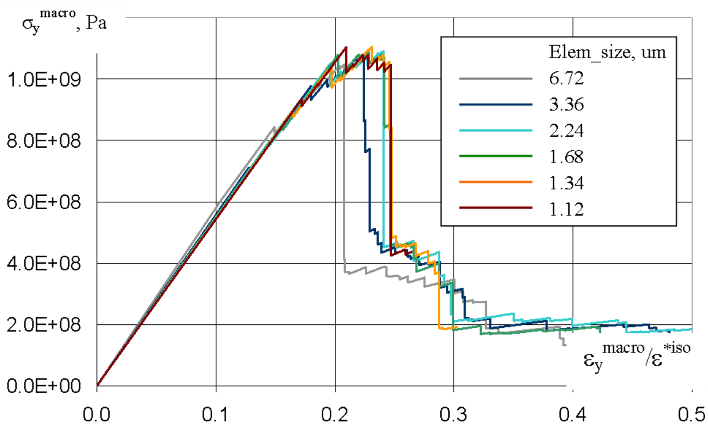

Figure 17. Stress strain curve. Critical criterion value scaled as the square root of element size (2), (4)

Another explanation to the criterion modification for different FE sizes could be suggested.

Based on Griffith's theory we state here that element fails when energy of tension reaches the energy of crack surface development and present the event by the energy balance equation as follows

$$\frac{1}{2}E\cdot\varepsilon^*\cdot\sigma^*\cdot d^3 = 2\gamma\cdot d^2 \tag{3}$$

where d – element size, E – Young's module, ε* – strain of element fracture, σ* – stress of element fracture, γ – surface (cleavage) energy, are the properties of cubic element.

The critical values are given by:

$$\varepsilon^* = \sqrt{\frac{4\gamma}{E\cdot d}} \tag{4}$$

In the formulas above factor "2" (3, right side) is due to the fact that when a crack develops typically 2 free surfaces are created. Ideally speaking in our case there should be come variable between 1 and 4, corresponding to the amount of free surface created when a FE is deleted. Also ε and σ should be considered to be tensors and their scalar product will be a scalar, inversely proportional to so some power of d (element size). The power will be the same for all tensor components. Then anyway this power will be obtained from (4) and will be equal to 0.5.

One can see that new element failure criterion (scaled element failure criterion or "Gamma criterion") for stress-strain simulation depends on square root of element size. This criterion is expected to provide consistent results at similar meshes with different element size.

We found in the previous research [24] that solid element size for accurate estimation of Young's modulus and fluidic permeability of pore structures should be less than median pore size d_{50}. The developed Gamma criterion would bring an additional condition related to correct strength estimation, namely determining the critical element size for accurate evaluation of the both elasticity and fracture. We will test the criterion in a range of element sizes and determine the ranges of criterion validity regarding pore size, porosity, and pore morphology.

FE size for JR1 sample

A precise look on images of crushed sample (Figures 18–19), a quarter of JR1 (85 x 70 x 65 voxels, 85 x 70 x 65 elements), and relative stress-strain curves (Figure 20) with element sizes d = 2.24-6.72 microns (but the same geometry corresponding to voxel size of 6.72 microns) at pore size d_{50} = 20 micron (material # = 7, 9 respectively) has shown that tension breaks a porous sample into two pieces (Figure 18) and looks very similar for all element sizes. However one can see more branching cracks for fine elements than for coarse elements (Figure 18).

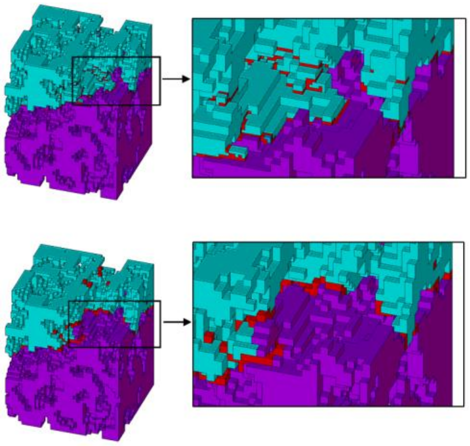

Figure 18. JR1. Tension. Different element sizes (top-2um, bottom-6 um) used on the same geometry

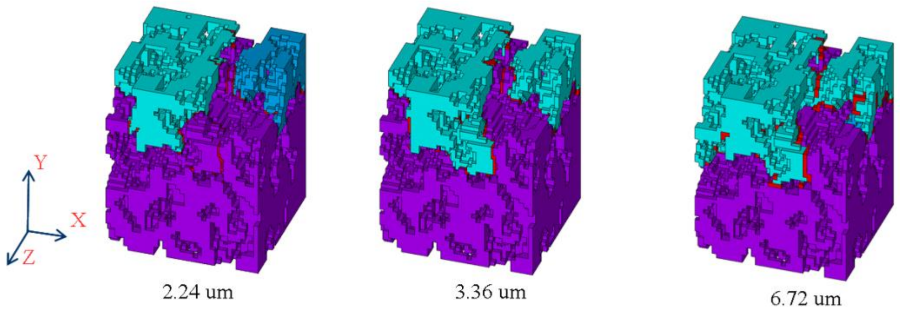

Figure 19. JR1. Different element sizes used on the same geometry. Compression

The stress-strain plots for the structure are very similar to each other as well and the tensile strength obtained with the gamma criterion is the same essentially for all element sizes (Figures 20–21).

Compression test shows three pieces for small elements and two parts for coarse elements (Figure 19). Crack path variation on element size is higher at compression than at tension. However all three predicted compressive strength values are very consistent, and a nearly identical match is observed for material # 7 and 8.

The data has shown that results of strength estimation coincide for element sizes less than half of mid pore size.

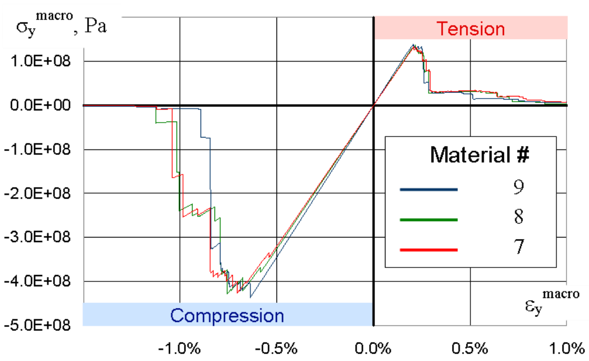

Figure 20. JR1. Different element sizes used on the same geometry. Stress-strain curves

Levandovskiy A.N., Melnikov B.E., Shamkin A.A. Modeling of porous material fracture. *Magazine of Civil Engineering*. 2017. No. 1. Pp. 3–22. doi: 10.18720/MCE.69.1

A larger sub-sample of JR1 – 120^3 piece (taken cube 120 x 120 x 120 1 um original voxels, but then coarsened to 6 um voxels) – was chosen to investigate the stress-strain curves dependence on a wider range of element sizes. Again in this test (simulated coarsened) pore geometry does not change, gamma criterion is used, alumina properties are taken as solid matter input: E = 340 GPa, ν = 0.23, γ = 25 J/m^2

The plot from Figure 21 shows the results of the calculations. Important fact is that the curves for finer elements are closer than for coarse mesh, which means we have “mesh convergence”. The calculations have confirmed that Material # 7 (element size 2.24 microns) and lower provide very consistent estimations of tensile strength and strain tolerance and good estimations for compressive values.

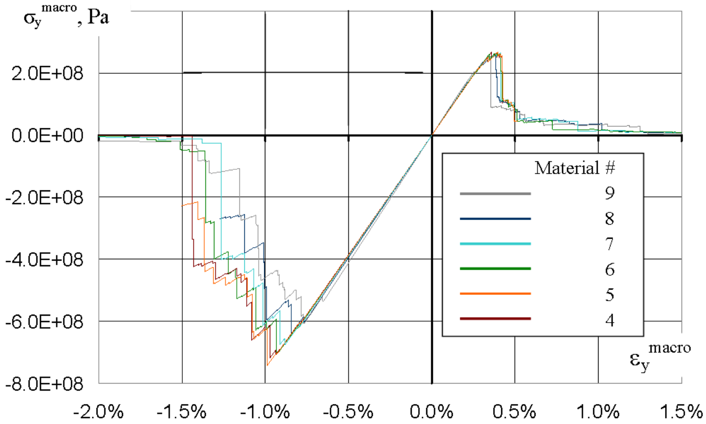

Figure 21. Stress-strain curves for JR1 120^3 – good match for tensile strength. For compression, curves look similar with some offset. The curves for finer elements are closer to each other, than for coarse mesh – “mesh convergence”

FE size for overlapping spherical pore/solid structures

For overlapping pore structures (simulated pore size 5.5 micron, voxel 1 um) the stress-strain curves have been obtained with gamma criterion on various porosities between 0.3–0.6. Alumina properties assumed are E = 340 GPa, ν = 0.23, γ = 25 J/m^2, element size = voxel size = 1 um, ε* = 1.71 %.

For the structure with 0.3 porosity, coarser resolution of 2 um was simulated as well. The difference of calculated MORs is 10 % for compression and 9 % for tension (Figure 22).

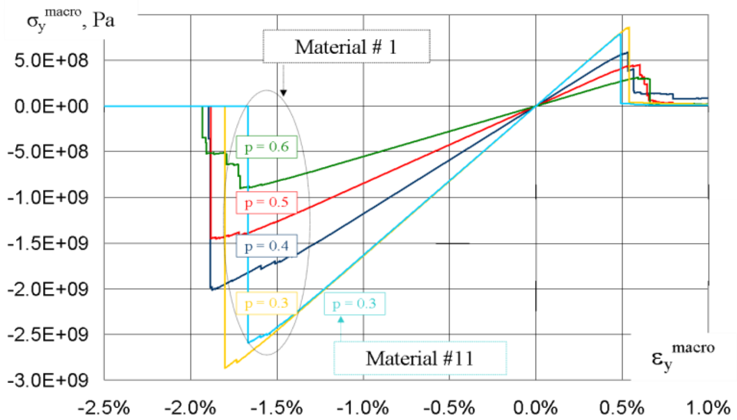

Figure 22. Virtual structures with different porosities. For p = 0.3 the calculations are also done with simulated coarser resolution – one voxel = 2 um with element size of 2 um.

The following plot (Figure 23) shows the comparison between the above curves (Figure 22, shown in shadow in Figure 23) and another set of calculated curves for larger pieces of the virtual structures (100^3 vs 80^3) for porosities of 0.4, 0.5 and 0.6 (top-down respectively) . The element sizes are 3, 1.5 and 1 um (top-down respectively). Voxel size is 3 um.

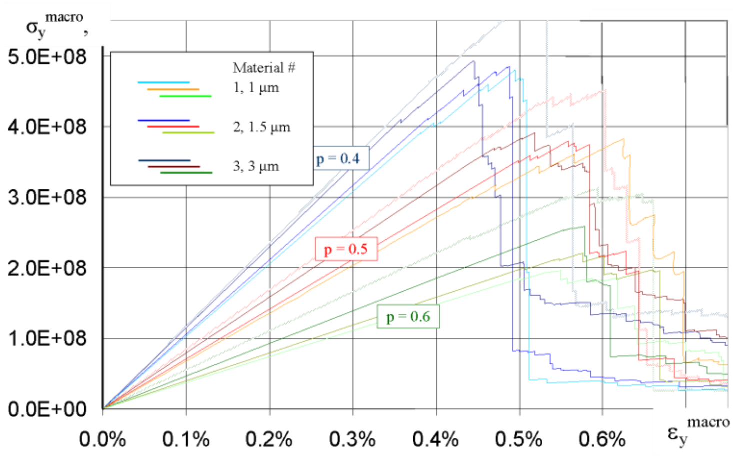

Figure 23 Spherical pore structures with various porosities. Stress-strain curves for tension

Tables 5 and 6 and Figures 24-25 show the results of the numerical experiments described above. One can observe that MOR values calculated with different element sizes for each structure fall in 10 % for tension and 20 % for compression except 35 % in case of overlapping spherical pores at p = 0.6. The difference between two neighboring values is lower than 10 % in all cases except 25 % in case of overlapping spherical pores at p = 0.6. The larger difference for p = 0.6 can be attributed to the fact that we have thinner walls between the pores in this case and more elements are needed per each wall.

Based on the comparison of 100 micron and 80 micron size sample simulation results (shadowed and solid lines in Figure 23), one can conclude that at the size of 100 micron and above the effective Young's moduli are not going to experience any significant change. In other words samples of overlapping spherical pores and conversely overlapping spherical solids (as far as both could be considered a mutual inversion) are representative when their linear dimensions are 8–10 larger than their median pore size d_{50}. Presumably natural structures with irregularly shaped pores should require larger sample size to produce stable mechanical property calculation/experimental results.

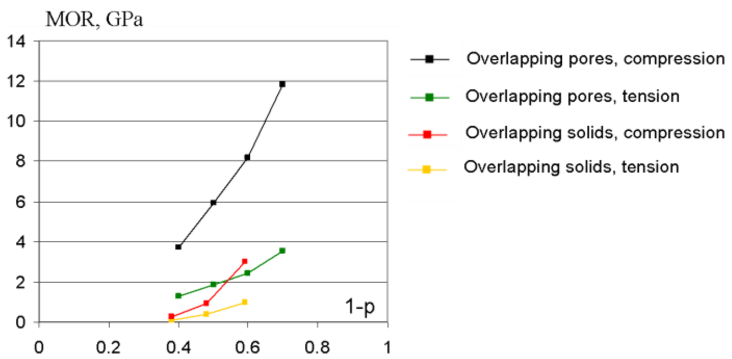

Figure 24. Strength of spherical pore and spherical solids structures with various porosities under tension and compression.

A few series of simulations on structures with the same voxel and element sizes were carried out to develop insight into a model of strength dependence on pore structure. We have simulated four overlapping spherical pore structures with voxel size of 1 um and element size 1 um and also three structures of overlapping solid spheres all with structure voxel size of 1 um, element size 1 um and input of material properties # 12 (see Tables 3–6).

The obtained data show steady non-linear dependence of calculated strength on porosity.

It was found that the strength is proportional to factor $(1\text{-}p)^m$ in each data series with a standard deviation about 4 % for compression and 10 % for tension (see Table 6).

Based on the preliminary model interpretation, calculated strength dependence on porosity and pore morphology is given by

$$Strength(p,m) = S_0 \cdot (1-p)^m \tag{5}$$

Levandovskiy A.N., Melnikov B.E., Shamkin A.A. Modeling of porous material fracture. *Magazine of Civil Engineering.* 2017. No. 1. Pp. 3–22. doi: 10.18720/MCE.69.1

Interestingly the strength model obtained here has the same dependence on p and m as the dependence for Young's modulus.

The value of the S_0 parameter in equation (5) has a physical sense of the strength at zero porosity. It is known to depend on grain size and material tensile strength. Presumably the S_0 value simulated in tension must be equal to the value $\sigma^* = E \cdot \varepsilon^* = 24$ GPa. It is not quite the case here. The parameter calculated as $S_0 = \text{Strength}/(1-p)^m$ stays constant versus porosity within one data set for a specific structure. However a difference is observed between the data sets, which need physical interpretation in future.

Whereas the average values in Tables 3-5 look similar for different structures as compared separately at tension or at compression, the compressive values are about three times higher than the respective tensile values. The ratio slowly decreases with m as demonstrated at Figure 25.

Table 3. MOR and strain tolerance at various voxel, element and pore size

	Tension	*voxel size*	*FE-size*	d_{50}	*MOR*	*ε(MOR)*
	Mat #	um	um	um	GPa	
JR1 120³	4	6.72	1.12	22	0.268	0.359
	5	6.72	1.34	22	0.269	0.396
	6	6.72	1.68	22	0.266	0.392
	7	6.72	2.24	22	0.265	0.413
	8	6.72	3.36	22	0.259	0.384
	9	6.72	6.72	22	0.255	0.356
JR1, quarter	7	6.72	2.24	22	0.132	0.210
	8	6.72	3.36	22	0.137	0.218
	9	6.72	6.72	22	0.136	0.210
Virtual structures	p = 0.3					
	1	1.00	1.00	5.5	0.861	0.540
	11	2.00	2.00	5.5	0.784	0.490
	p = 0.4					
	1	3.00	1.00	5.5	0.480	0.495
	2	3.00	1.50	5.5	0.485	0.448
	3	3.00	3.00	5.5	0.492	0.446
	p = 0.5					
	1	3.00	1.00	5.5	0.383	0.625
	2	3.00	1.50	5.5	0.379	0.558
	3	3.00	3.00	5.5	0.392	0.519
	p = 0.6					
	1	3.00	1.00	5.5	0.196	0.549
	2	3.00	1.50	5.5	0.216	0.602
	3	3.00	3.00	5.5	0.259	0.579

Table 4. Compressive strength and strain tolerance

	Compression	voxel size	FE-size	d_{50}	MOR, GPa	ε(MOR)
	Mat #	um	um	um	GPa	
JR1 120^3	4	6.72	1.12	22	-0.72	-0.973
	5	6.72	1.34	22	-0.74	-0.988
	6	6.72	1.68	22	-0.70	-0.934
	7	6.72	2.24	22	-0.68	-0.881
	8	6.72	3.36	22	-0.64	-0.845
	9	6.72	6.72	22	-0.61	-0.770
JR1, quarter	7	6.72	2.24	22	-0.43	-0.757
	8	6.72	3.36	22	-0.43	-0.706
	9	6.72	6.72	22	-0.44	-0.639
Virtual structures	p = 0.3					
	1	1.00	1.00	5.5	-2.87	-1.800
	11	2.00	2.00	5.5	-2.59	-1.670
	p = 0.4					
	1	3.00	1.00	5.5	-1.52	-0.156
	2	3.00	1.50	5.5	-1.52	-0.150
	3	3.00	3.00	5.5	-1.62	-0.157
	p = 0.5					
	1	3.00	1.00	5.5	-1.02	-0.164
	2	3.00	1.50	5.5	-1.13	-0.174
	3	3.00	3.00	5.5	-1.23	-0.162
	p = 0.6					
	1	3.00	1.00	5.5	-0.50	-0.151
	2	3.00	1.50	5.5	-0.62	-0.166
	3	3.00	3.00	5.5	-0.74	-0.178

Table 5. Summary of calculated mechanical parameters for synthetic structures (input Material #12)

Overlapping pores	m	MOR^{compr}, GPa	MOR^{tens}, GPa	MOR^{compr}/ MOR^{tens}
p = 0.30	2.04	11.85	3.55	3.34
p = 0.40	1.98	8.19	2.42	3.38
p = 0.50	2.00	5.93	1.86	3.19
p = 0.60	2.07	3.71	1.29	2.88
Overlapping solids				
p = 0.41	3.41	3.01	0.98	3.07
p = 0.52	3.95	0.95	0.38	2.50
p = 0.63	4.24	0.25	0.09	2.78

Table 6. Calculated average strength (GPa) and statistical deviations (in brackets)

Average strength, GPa	Tension	Compression
Overlapping spherical pores	7.5 (11 %)	23.9 (4 %)
Overlapping spherical solids	6.3 (8 %)	17.5 (4 %)

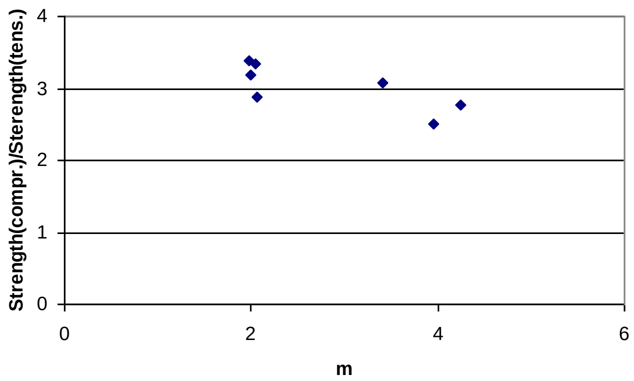

Figure 25. Compressive/Tensile Strength ratio as function of pore morphology

Conclusions

1. A number of FEM simulations on virtually generated and real tomography 3D pore structures has been performed to search for a feasible way to numerically study the influence of pore structure on mechanical strength of ceramics structures

2. The 3D simulation of structure stress-strain dependence by element deletion technique delivers numerical estimates of specific structure strength and provides valuable insight in the fracture mechanism. The key point of the strength evaluation is feasible. Element failure criterion has been developed in accordance with Griffith's theory to address strength dependence on dense material physical properties such as cleavage energy and elasticity, as well as the dependence of FEM calculation method on element size (gamma criterion). The criterion worked well for simulation of compressive and tensile strength and will be used further to study various materials pore structures.

3. The element deletion technique with gamma criterion can be recommended for usage in comparative simulations of complex 3D structure failures at various load modes and meshes.

4. A previous conclusion [24] has been confirmed for the tomography resolution required to adequately simulate porous structures in 3D. With the resolution being finer than the median pore size $V < D50_{\min}$, one should obtain consistent results suitable for comparative analyses.

5. Samples of overlapping spherical pores/overlapping spherical solids are representative when their linear dimensions are 8–10 larger than their median pore size d_{50}. Natural structures with irregularly shaped pores should require larger relative sample sizes to produce stable mechanical property calculation or experimental results.

References

1. Krivoshapkina Ye.F., Krivoshapkin P.V., Dudkin B.N. Mikroporistaya keramika kordiyeritovogo sostava na osnove prirodnogo syrya [Microporous cordierite ceramics on a natural raw material]. *Izvestiya Komi nauchnogo tsentra UrO RAN.* 2011. No. 7. Pp. 27–32. (rus)
2. Solovyev S.A. Okislitelnaya konversiya metana na strukturirovannykh katalizatorakh Ni–Al2O3/Kordierit [Oxidative methane conversion on structural catalysts Ni–Al2O3/Cordierite]. *Catalysis in Industry.* 2011. No. 4. Pp. 31–42. (rus)
3. Gassmann F. Uber Die elastizitat poroser medien. *Vier der Natur Gesellschaft.* 1951. No. 96. Pp. 1–23.
4. Kachanov M., Tsukrov I., Shafiro B. Effective Moduli of Solids With Cavities of Various Shapes. *Applied Mechanics Reviews.* 1994. Vol. 47(1S). Pp. 151–174.
5. Kachanov M., Sevostianov I., Shafiro B. Explicit cross-property correlations for porous materials with anisotropic microstructures. *Journal of the Mechanics and Physics of Solids.* 2001. Vol. 49(1). Pp. 1–25.
6. Knudsen F.P. Dependence of Mechanical Strength of Brittle Polycrystalline Specimens on Porosity and Grain Size. *Journal of the American Ceramic Society Volume.* 1959. Vol. 42(8). Pp. 376–387.
7. Bruno G., Efremov A.M., Levandovskyi A.N., Clausen B. Connecting the macro- and microstrain responses in

Литература

1. Кривошапкина Е.Ф., Кривошапкин П.В., Дудкин Б.Н. Микропористая керамика кордиеритового состава на основе природного сырья. // Известия Коми научного центра УрО РАН. 2011. № 7. С. 27–32.
2. Соловьев С.А. Окислительная конверсия метана на структурированных катализаторах Ni–Al2O3/Кордиерит // Катализ в промышленности. 2011. № 4. С. 31–42.
3. Gassmann F. Uber Die elastizitat poroser medien // Vier der Natur Gesellschaft. 1951. № 96. Pp. 1–23.
4. Kachanov M., Tsukrov I., Shafiro B. Effective moduli of solids with cavities of various shapes // Applied Mechanics Reviews. 1994. Vol. 47(1S). Pp. 151–174.
5. Kachanov M., Sevostianov I., Shafiro B. Explicit cross-property correlations for porous materials with anisotropic microstructures // Journal of the Mechanics and Physics of Solids. 2001. Vol. 49(1). Pp. 1–25.
6. Knudsen F.P. Dependence of Mechanical Strength of Brittle Polycrystalline Specimens on Porosity and Grain Size // Journal of the American Ceramic Society Volume. 1959. Vol. 42(8). Pp. 376–387.
7. Bruno G., Efremov A.M., Levandovskyi A.N., Clausen B. Connecting the macro- and microstrain responses in technical porous ceramics: modeling and experimental validations // Journal of Materials Science. 2011. Vol. 46(1).

technical porous ceramics: modeling and experimental validations. *Journal of Materials Science*. 2011. Vol. 46(1). Pp. 161–173.

8. Roberts A., Garboczi E.J. Elastic properties of model porous ceramics. *Journal of the American Ceramic Society.* 2000. Vol. 83(12). Pp. 3041–3048.
9. Shmitko Ye.I., Rezanov A.A., Bedarev A.A. Multiparametricheskaya optimizatsiya struktury yacheistogo silikatnogo betona [Multi-parametric optimization of the silicate cell concrete structure]. *Magazine of Civil Engineering.* 2013. No. 3. Pp. 15–23. (rus)
10. Courant R. Variational methods for the solution of problems of equilibrium and vibrations. *Bulletin of American Mathematic Society.* 1943. Vol. 49. Pp. 1–23.
11. Galerkin B.G. *Sobraniye sochineniy* [Collected works]. Vol. I. M.: Izdatelstvo AN SSSR, 1952. 391 p. (rus)
12. Timoshenko S.P., Voynovskiy-Kriger S. *Plastiny i obolochki* [Plates and shells]. M.: Nauka, 1966. 635 p. (rus)
13. Rozin L.A. *Sterzhnevyye sistemy kak sistemy konechnykh elementov* [Beam systems as systems of finite elements]. L.: Izd-vo LGU, 1976. 232 p. (rus)
14. Asheychik A.A., Polonskiy V.L. *Raschet detaley mashin metodom konechnykh elementov* [Machinery details processing by the finite element method]. SPb.: Izd-vo SPbGPU, 2016. 243 p. (rus)
15. Roberts A.P., Garboczi E.J. Elastic properties of model random three-dimensional open-cell solids. *Journal of the Mechanics and Physics of Solids.* 2002. Vol. 50(1). Pp. 33–55.
16. Roberts A., Garboczi E.J. Computation of the linear elastic properties of random porous materials with a wide variety of microstructure. *Proceedings of the Royal Society. Series A: Mathematical, Physical and Engineering Sciences.* 2002. Vol. 458(2021). Pp. 1033–1054.
17. Charles P. Ursenbach Simulation of elastic moduli for porous materials. *CREWES Research Report.* 2001. Vol. 13. Pp. 83–98.
18. Bauer J.S., Sidorenko I., Mueller D., Baum T. Prediction of bone strength by µCT and MDCT-based finite-element-models: How much spatial resolution is needed? *European Journal of Radiology.* 2014. Vol. 83(1). Pp. 36–42.
19. Shtern M.B., Kuzmov A.V., Frolova Ye.G., Vdovichenko A.V. Issledovaniye uprugogo povedeniya poroshkovykh materialov s ploskimi porami metodom pryamogo kompyuternogo modelirovaniya na elementarnoy yacheyke [Study of the elastic behavior of the powder materials with flat pores by direct computer modeling on an elementary cell]. *Naukovi notatki Zbirnik naukovikh prats.* 2005. No. 17. Pp. 390–398. (rus)
20. Garboczi E.J., Day A.R. An algorithm for computing the effective linear elastic properties of heterogeneous materials: 3D results for composites with equal phase Poisson ratios. J*ournal of the Mechanics and Physics of Solids.* 1995. Vol. 43. Pp. 1349–1362.
21. Razina I.S., Semenova S.G., Sattarov A.G., Musin I.N. Primeneniye mikrotomografii dlya issledovaniya novykh materialov. Obzor [Micro tomography use for new materials study. A review]. *Vestnik Kazanskogo gosudarstvennogo tekhnologicheskogo universiteta. Kazan: Izd-vo Kazanskogo gosudarstvennogo tekhnologicheskogo universiteta.* 2013. Vol. 16. No. 19. Pp. 163–169. (rus)
22. Garboczi E.J. Bentz D.P., Martys N.S. *Digital images and computer modeling in "Methods of the Physics of Porous Media".* Ed. P.-z. Wong. San Diego: Academic Press, 1999. Vol. 35(1). Pp. 1–41.
23. Garboczi E.J. *Finite element and finite difference programs for computing the linear electric and elastic properties of digital images of random materials* [Elektronnyy resurs] Sistem requirements: Adobe Acrobat Reader. URL: ftp: //ftp.nist.gov/pub/bfrl/garbocz/FDFEMANUAL/MANUAL.pdf (data obrashcheniya: 20.11.2016)

Pp. 161–173.

8. Roberts A., Garboczi E.J. Elastic properties of model porous ceramics // Journal of the American Ceramic Society. 2000. Vol. 83(12). Pp. 3041–3048.
9. Шмитько Е.И., Резанов А.А., Бедарев А.А. Мультипараметрическая оптимизация структуры ячеистого силикатного бетона // Инженерно-строительный журнал. 2013. № 3. С. 15–23.
10. Courant R. Variational methods for the solution of problems of equilibrium and vibrations // Bulletin of American Mathematic Society. 1943. Vol. 49. Pp. 1–23.
11. Галеркин Б.Г. Собрание сочинений. Том I. М.: Издательство АН СССР, 1952. 391 с.
12. Тимошенко С.П., Войновский-Кригер С. Пластины и оболочки. М.: Наука, 1966. 635 с.
13. Розин Л.А. Стержневые системы как системы конечных элементов. Л.: Изд-во ЛГУ, 1976. 232 с.
14. Ашейчик А.А., Полонский В.Л. Расчёт деталей машин методом конечных элементов. СПб.: Изд-во СПбГПУ, 2016. 243 с.
15. Roberts A.P., Garboczi E.J. Elastic properties of model random three-dimensional open-cell solids // Journal of the Mechanics and Physics of Solids. 2002. Vol. 50(1). Pp. 33–55.
16. Roberts A., Garboczi E.J. Computation of the linear elastic properties of random porous materials with a wide variety of microstructure // Proceedings of the Royal Society. Series A: Mathematical, Physical and Engineering Sciences. 2002. Vol. 458(2021). Pp. 1033–1054.
17. Charles P. Ursenbach Simulation of elastic moduli for porous materials // CREWES Research Report. 2001. Vol. 13. Pp. 83–98.
18. Bauer J.S., Sidorenko I., Mueller D., Baum T. Prediction of bone strength by µCT and MDCT-based finite-element-models: How much spatial resolution is needed? // European journal of radiology. 2014. Vol. 83(1). Pp. 36–42.
19. Штерн М.Б., Кузьмов А.В., Фролова Е.Г., Вдовиченко А.В. Исследование упругого поведения порошковых материалов с плоскими порами методом прямого компьютерного моделирования на элементарной ячейке // Наукові нотатки Збірник наукових праць. 2005. № 17. С. 390–398.
20. Garboczi E.J., Day A.R. An algorithm for computing the effective linear elastic properties of heterogeneous materials: 3D results for composites with equal phase Poisson ratios // Journal of the Mechanics and Physics of Solids. 1995. Vol. 43. Pp. 1349–1362.
21. Разина И.С., Семенова С.Г., Саттаров А.Г., Мусин И.Н. Применение микротомографии для исследования новых материалов. Обзор // Вестник Казанского государственного технологического университета. Казань: Изд-во Казанского государственного технологического университета; 2013. Т. 16. № 19. С. 163–169.
22. Garboczi E.J. Bentz D.P., Martys N.S. Digital images and computer modeling in "Methods of the Physics of Porous Media" // San Diego: Academic Press, 1999. Vol. 35(1). Pp. 1–41.
23. Garboczi E.J. Finite element and finite difference programs for computing the linear electric and elastic properties of digital images of random materials [Электронный ресурс] Систем. требования: Adobe Acrobat Reader. URL: ftp: //ftp.nist.gov/pub/bfrl/garbocz/FDFEMANUAL/MANUAL.pdf (дата обращения: 20.11.2016)
24. Levandovskiy A., Melnikov B. Finite element modeling of porous material structure represented by a uniform cubic mesh // Applied Mechanics and Materials. 2015. Vol. 725–726. Pp. 928–936.
25. Levandovskiy A.N., Efremov A.M., Bruno G. Macro to micro stress and strain conversion in porous ceramics // Materials

24. Levandovskiy A., Melnikov B. Finite element modeling of porous material structure represented by a uniform cubic mesh. *Applied Mechanics and Materials.* 2015. Vol. 725–726. Pp. 928–936.
25. Levandovskiy A.N., Efremov A.M., Bruno G. Macro to micro stress and strain conversion in porous ceramics. *Materials Science Forum.* 2012. Vol. 706–709. Pp. 1667–672.
26. Huang Y., Yang Z., Ren W., Liu G. 3D meso-scale fracture modelling and validation of concrete based on in-situ X-ray computed tomography images using damage plasticity model. *International Journal of Solids and Structures.* 2015. Vol. 67. Pp. 340–352.
27. Emerson J.E., Matt J.C., Reilly G.C., Amaka C. Offiah Geometrically accurate 3D FE models from medical scans created to analyze the causes of sports injuries. *Procedia Engineering.* 2011. Vol. 13. Pp. 422–427.
28. Roshchin P.V., Rogachev M.K., Vaskes Kardenas L.K., Kuzmin M.I., Litvin V.T., Zinovyev A.M. Issledovaniye kernovogo materiala Pecherskogo mestorozhdeniya prirodnogo bituma s pomoshchyu rentgenovskogo kompyuternogo mikrotomografa SKYSCAN 1174V2 [Kern material study of the Pecherski field with the computer micro tomograph SKYSCAN 1174 v2]. *Mezhdunarodnyy nauchno-issledovatelskiy zhurnal.* 2013. No. 8(15). Part 2. Pp. 45–48. (rus)
29. Yiotis A.G., Kainourgiakis M.E., Eustathios S. Kikkinides, Stubos A.K. Application of the Lattice-Boltzmann method to the modeling of population blob dynamics in 2 D porous domains. *Computers & Mathematics with Applications.* 2010. Vol. 59(7). Pp. 2315–2325.
30. Mo L.T., Huurman M., Wu S.P., Molenaar A.A.A. 2D and 3D meso-scale finite element models for ravelling analysis of porous asphalt concrete. *Finite Elements in Analysis and Design.* 2008. Vol. 44(4). Pp. 186–196.
31. Gorshkov A.S., Vatin N.I. Svoystva stenovykh konstruktsiy iz yacheistobetonnykh izdeliy avtoklavnogo tverdeniya na poliuretanovom kleyu [Wall structures properties made of cell concrete on polyurethane glues]. *Magazine of Civil Engineering.* 2013. No. 5. Pp. 5–19. (rus)
32. Gorshkov A.S., Vatin N.I. Innovatsionnaya tekhnologiya vozvedeniya stenovykh konstruktsiy iz gazobetonnykh blokov na poliuretanovyy kley [Wall structures properties made of cell concrete on polyurethane glues]. *Construction of Unique Buildings and Structures.* 2013. No. 8. Pp. 20–28. (rus)
33. Nikitin A.N., Ivankina T.I., Sobolev G.A., Shefftsyuk K., Frishbutter A., Valter K. Neytronograficheskiye issledovaniya vnutrikristallicheskikh deformatsiy i napryazheniy v obraztse mramora pri povyshennykh temperaturakh i vneshnikh mekhanicheskikh nagruzkakh [Neutron studies of the crystal deformations and stresses in marble under high temperature and mechanical loading]. *Izvestia. Physics of the Solid Earth.* M.: Nauka, 2004. No. 1. Pp. 88–92. (rus)
34. Frishbutter A., Neov D., Scheffzuk C., Vrana M., Walther K. Lattice strain measurements on sandstones under load using neutron diffraction. *Journal of Structural Geology*. 2000. Vol. 22(11–12). Pp. 1587–1600.
35. Darling T.W, TenCate J.A, Brown D.W., Clausen B., Vogel S.C. Neutron diffraction study of the contribution of grain contacts to nonlinear stress-strain behavior. *Geophysical Research Letters.* 2004. Vol. 31(16/L16604). Pp. 1–4.
36. *Electronic source: CeramTec GmbH* [Electronic source]. URL: https://www.ceramtec.com/alutit/ (date: 01.02.2017).
37. Bruno G., Efremov A.M., Levandovskiy A.N., Pozdnyakova I., Hughes D.J., Clausen B. Thermal and mechanical response of industrial porous ceramics. *Materials Science Forum.* 2010. Vol. 652. Pp. 191–196.
38. Kouznetsova V.G. *Computational homogenization for the multi-scale analysis of multi-phase materials*: doctoral dissertation: 9.12.02. Kouznetsova Varvara. Eindhoven, 2002. 134 p.

Science Forum. 2012. Vol. 706–709. Pp. 1667–672.
26. Huang Y., Yang Z., Ren W., Liu G. 3D meso-scale fracture modelling and validation of concrete based on in-situ X-ray computed tomography images using damage plasticity model // International Journal of Solids and Structures. 2015. Vol. 67. Pp. 340–352.
27. Emerson J.E., Matt J.C., Reilly G.C., Amaka C. Offiah Geometrically accurate 3D FE models from medical scans created to analyze the causes of sports injuries // Procedia Engineering. 2011. Vol. 13. Pp. 422–427.
28. Рощин П.В., Рогачев М.К., Васкес Карденас Л.К., Кузьмин М.И., Литвин В.Т., Зиновьев А.М. Исследование кернового материала Печерского месторождения природного битума с помощью рентгеновского компьютерного микротомографа SKYSCAN 1174V2 // Международный научно-исследовательский журнал. 2013. № 8(15). Ч. 2. С. 45–48.
29. Yiotis A.G., Kainourgiakis M.E., Eustathios S. Kikkinides, Stubos A.K. Application of the Lattice-Boltzmann method to the modeling of population blob dynamics in 2 D porous domains. // Computers & Mathematics with Applications. 2010. Vol. 59(7). Pp. 2315–2325.
30. Mo L.T., Huurman M., Wu S.P., Molenaar A.A.A. 2D and 3D meso-scale finite element models for ravelling analysis of porous asphalt concrete // Finite Elements in Analysis and Design. 2008. Vol. 44(4). Pp. 186–196.
31. Горшков А.С., Ватин Н.И. Свойства стеновых конструкций из ячеистобетонных изделий автоклавного твердения на полиуретановом клею // Инженерно-строительный журнал. 2013. № 5. С. 5–19.
32. Горшков А.С., Ватин Н.И. Инновационная технология возведения стеновых конструкций из газобетонных блоков на полиуретановый клей // Строительство уникальных зданий и сооружений. 2013. № 8. С. 20–28.
33. Никитин А.Н., Иванкина Т.И., Соболев Г.А., Шеффцюк К., Фришбуттер А., Вальтер К. Нейтронографические исследования внутрикристаллических деформаций и напряжений в образце мрамора при повышенных температурах и внешних механических нагрузках // Физика Земли. М.: Наука, 2004. № 1. С. 88–92.
34. Frishbutter A., Neov D., Scheffzuk C., Vrana M., Walther K. Lattice strain measurements on sandstones under load using neutron diffraction // Journal of Structural Geology. 2000. Vol. 22(11–12). Pp. 1587–1600.
35. Darling T.W, TenCate J.A, Brown D.W., Clausen B., Vogel S.C. Neutron diffraction study of the contribution of grain contacts to nonlinear stress-strain behavior // Geophysical Research Letters. August 2004. Vol. 31(16/L16604). Pp. 1–4.
36. Электронный источник: CeramTec GmbH [Электронный ресурс]. Систем. требования: IE. URL: https://www.ceramtec.com/alutit/ (дата обращения: 01.02.2017).
37. Bruno G., Efremov A.M., Levandovskiy A.N., Pozdnyakova I., Hughes D.J., Clausen B. Thermal and mechanical response of industrial porous ceramics // Materials Science Forum. 2010. Vol. 652. Pp. 191–196.
38. Kouznetsova V.G. Computational homogenization for the multi-scale analysis of multi-phase materials: doctoral dissertation: 9.12.02 / Kouznetsova Varvara. Eindhoven, 2002. 134 p.
39. Bubeck C. Direction dependent mechanical properties of extruded cordierite honeycombs // Journal of the European Ceramic Society. 2009. Vol. 29(15). Pp. 3113–3119.
40. Wereszczak A., Fox E., Lance M., Ferber M. Failure stress and apparent elastic modulus of diesel particulate filter ceramics // SAE International Journal of Materials and Manufacturing. 2012. Vol. 5(2012-01-1252). Pp. 517–527.
41. Boger T., Tilgner I.C., Shen M., Jiang Y. Oxide based particulate filters for light-duty diesel applications – impact of the filter length on the regeneration and pressure drop

39. Bubeck C. Direction dependent mechanical properties of extruded cordierite honeycombs. *Journal of the European Ceramic Society.* 2009. Vol. 29(15). Pp. 3113–3119.
40. Wereszczak A., Fox E., Lance M., Ferber M. Failure stress and apparent elastic modulus of diesel particulate filter ceramics. *SAE International Journal of Materials and Manufacturing.* 2012. Vol. 5(2012-01-1252). Pp. 517–527.
41. Boger T., Tilgner I.C., Shen M., Jiang Y. Oxide based particulate filters for light-duty diesel applications – impact of the filter length on the regeneration and pressure drop behavior. *SAE International Journal of Fuels and Lubricants.* 2008. Vol. 1(2008-01-0485). Pp. 252–264.
42. Ingram-Ogunwumi R.S., Dong Q., Murrin T.A., Bhargava R.Y., Warkins J.L., Heibel A.K. Performance evaluations of aluminum titanate diesel particulate filters. *SAE Technical Paper.* 2007. No. 2007-01-0656.
43. Williams M.L. Stress singularities resulting from various boundary conditions in angular corner plates in extension. *Journal of Applied Mechanics.* 1952. Vol. 19. Pp. 526–528.

behavior // SAE International Journal of Fuels and Lubricants. 2008. Vol. 1(2008-01-0485). Pp. 252–264.
42. Ingram-Ogunwumi R.S., Dong Q., Murrin T.A., Bhargava R.Y., Warkins J.L., Heibel A.K. Performance evaluations of aluminum titanate diesel particulate filters // SAE Technical Paper. 2007. No. 2007-01-0656.
43. Williams M.L. Stress singularities resulting from various boundary conditions in angular corner plates in extension // Journal of Applied Mechanics. 1952. Vol. 19. Pp. 526–528.

Andrey Levandovskiy,
+7(904)5157287; levandovan@corning.com

Boris Melnikov,
+7(812)5526303; kafedra@ksm.spbstu.ru

Artemiy Shamkin,
+7(911)7366391; shamkinaa@corning.com

Андрей Николаевич Левандовский,
+7(904)5157287;
эл. почта: levandovan@corning.com

Борис Евгеньевич Мельников,
+7(812)5526303;
эл. почта: kafedra@ksm.spbstu.ru

Артемий Александрович Шамкин,
+7(911)7366391;
эл. почта: shamkinaa@corning.com

doi: 10.18720/MCE.69.2

Computational modelling of random distribution of stresses for wooden structures

Численное моделирование случайного распределения напряжений для деревянных конструкций

I.K. Rasha,
Design and consulting firm "Strojrekonstrukcija" OOO, St. Petersburg, Russia
O.N. Pertseva,
A.Yu. Lazareva,
G.V. Martynov,
Peter the Great St. Petersburg Polytechnic University, St. Petersburg, Russia

Канд. техн. наук, главный инженер И.К. Раша,
ООО «Проектно-консалтинговая фирма «Стройреконструкция», г.Санкт-Петербург, Россия
студент О.Н. Перцева,
студент А.Ю. Лазарева,
студент Г.В. Мартынов,
Санкт-Петербургский политехнический университет Петра Великого, г. Санкт-Петербург, Россия

Key words: restoration; wooden structures; Monte Carlo simulation; timber; probabilistic analysis

Ключевые слова: реставрация; деревянные конструкции; метод Монте-Карло; вероятностный анализ

Abstract. Stochastic allocation is the main characteristic of processes which can be described in wooden structures. Random distribution of stresses and deformations in such structures is mostly based on timber imperfections, such as different curvature of sticks, presence of knots, twigs and gnarls. Due to restoration works using of test methods and experiments in wooden structures, especially in architectural monuments, is limited because of high labor contribution and restrictions for protection of historic cultural heritage. Therefore, for decreasing efforts application of statistical methods with help of software tools is necessary and highly important in case of restoration of wooden structures. In particular, this article describes solution of design problem in choosing the optimal step of wall dowels with help of Monte Carlo method by the time of restoration in the Church of the Transfiguration on Kizhi Island. For analysis of stresses in cribbed panel wall an analytical model, which describes structural behavior sticks and dowels according to all imperfections, with three different dowels steps (0.67 m, 1.0 m and 1.67 m) was created in SCAD software. Stick curvature has been changed longitudinal direction and after that calculation of stresses was performed. As the result the most optimal dowel step is one meter, such as it produces minimal stresses due to the minimum intervention in the structure.

Аннотация. Вероятностное распределение является основной характеристикой процессов, которые могут быть описаны в деревянных конструкций. Случайное распределение напряжений и деформаций в таких конструкциях основывается на присутствии дефектов древесины, таких как различие кривизны брусков, узлы, ветки и свилеватость. Реставрационные работы с использованием экспериментальных методов, особенно в архитектурных памятниках, ограничены из-за трудозатратности и правил охраны исторического культурного наследия. Поэтому при восстановлении деревянных конструкций необходимо применение статистических методов и программных средств. Целью данного исследования является обоснование нового способа проектирования в ходе реконструкции сооружений, зависящих от вероятностных факторов, путем введения метода Монте-Карло в процедуру моделирования методом конечных элементов.В частности, в данной статье описывается выбор оптимального шага стеновых дюбелей с помощью метода Монте-Карло во время реставрации в церкви Преображения Господня на острове Кижи. Для анализа напряжений панельной стены в программе SCAD была создана аналитическая модель, которая описывает поведение брусков и дюбелей в соответствии со всеми несовершенствами, с тремя различными шагами нагелей (0,67 м., 1,0 м и 1,67 м). Изгиб брусков изменяли в продольном направлении, после чего проводили расчет напряжений. Было выявлено, что самый оптимальный шаг дюбелей – один метр, так как он вызывает наименьшие напряжения

Раша И.К., Перцева О.Н., Лазарева А.Ю., Мартынов Г.В. Численное моделирование случайного распределения напряжений для деревянных конструкций // Инженерно-строительный журнал. 2017. № 1(69). С. 23–33.

при минимальном вмешательстве в конструкцию. Результаты были сравнены с законом непрерывного распределения и законом распределения Гаусса. Таким образом, была разработана новая методика для решения конструктивных задач методом Монте Карло и доказана ее корректность.

Introduction

Historically, timber is the most wide spread material in most of the countries for different types of structures, such as residentional houses, household buildings and even temples or castles (for example, Buddhist temple Hōryū-ji in Nara, Japan). The main reasons of such common timber usage are relatively simple processing of materials and, of course, a high accessibility timber from woods. In comparison with concrete structures, lifetime of the timber is not very high; therefore wooden structures are not durable. That is why survived until present days from last centuries wooden structures can be estimated as architectural monuments and considering this part of the cultural heritage is of outstanding interest and therefore need to be preserved as part of the world heritage of mankind as a whole.

Problem of restoration of architectural monuments, especially churches and temples, is one of the most significant around the world. It belongs not only to the Central Europe [1, 2] but also to Southeast Asia [3], South America [4] and East Asia [5]. In Russian Federation the most famous and significant historical complex of wooden structures is a national open-air museum Kizhi Pogost which consists of more than 80 historical wooden structures and belongs to UNESCO World Heritage site. Since 1980th the Church of the Transfiguration which is the central architectural object in this ensemble is under restoration processes [6]. Nowadays a lot of structural zones are restored and it’s required to pick up the most optimal scheme of dowel bars planting zones and their number. It is important for the complete enforcing of a middle quadrangle located at the top of the octagon. For this purpose it is supposed to perform the natural experiment but such kind of tests are restricted from the point of view conservation the structure as much as possible. Moreover, it is very wasteful and requires a lot of efforts [7].

Worldwide experience provides different kinds of solutions for problem of safety restoration works. For example, non-destructive techniques enable conduct an inspection of wooden structures of protected buildings without affection disturbances of structures. Such non-destructive techniques as ultrasound and thermography are used in inspections of the wooden roofs of buildings to identify dampness, deterioration, density loss and defects as a means of assessing their conservation status. Thermography identifies different materials and moisture content while ultrasound detects the various degrees of deterioration and density-loss in areas of the wood with high moisture content [8]. According to non-destructive inspection of the Church of the Transfiguration it was found out that the walls of the main octagon are not stiff enough and should be bound by rigid connections (dowels) for prevention of buckling in the vertical direction. Choosing of the number and step of such dowels is the main purpose of this research and highly important for continuation of restoration works. Additionally to difficulties of natural experiment that were mentioned above restoration of architectural monuments is complicated because of the difficulties in restoration site. Cultural monuments should not be closed for visitors for a long period from the financial point of view [9]. The same procedure is now going on the restoration site of the Church of the Transfiguration what makes restoration process more complicated.

Implementation of modern methods of simulation and modelling in vast number of cases allows to come up with the solution of engineering problems without conducting any experiments. For example, BIM technologies may represent the three-dimensional compounds of the building [10] and the several phases of restoration work in a fixed schedule [11]. And in order to predict the structural damage and deformed configuration of the building under the loading it is reasonable to use FEM modelling as the most convenient and accurate.

However, in case of restoration engineers should work with probability factors, which cannot be considered by software for simulation because of the vast number of information. For the studied wall from the Church of the Transfiguration which was mentioned above it is impossible to simulate behavior of every timber beam because of the different curvature of every part and different stiffness characteristic of every trunk. The most appropriate way to consider the contribution of every trunk in the work of a whole structure is usage of probabilistic methods. One of the most usable probabilistic methods in engineering is a Monte-Carlo method. It is known that Monte Carlo simulation can be used for evaluation of efficiency, reliability and capacity of different models [12]. Monte-Carlo simulation is already applied for evaluation of restoration costs [13], seismic reliability assessment of classical columns [14], production assurance analyses in subsea production system [15]. This method helps to consider corrosion damaging [16] and develop strategies for the restoration of structure [17]. But application of Monte Carlo simulation for choosing the geometry of structure for improving stiffness is not so widely used as it should be though it allows changing the geometry without any natural experiments, disturbance of restored building and high efforts [18]. Moreover, Monte Carlo simulation is successfully used for analysis of wooden structures, such as glued timber roofs [19] and bolted timber joints [20]. Therefore, Monte Carlo simulation in collaboration with FEM truss system should be used for modelling of the structure of a middle quadrangle located at the top of the octagon and choosing of the optimal number and step of dowels for its enforcing.

Taking the foregoing into consideration, let us formulate the purpose and objectives of the research.

The purpose of this study is substantiation of the new method for structural design during renovation of systems which depend on probabilistic factors by introducing Monte Carlo simulation in finite element modelling procedure. The Church of the Transfiguration should be used as an example for design task with octagon walls which is described in the next section.

It can be done by achieving the following objectives:

1. Modelling of the system with conditional dowels and equivalent stiffness;

2. FEM simulation of probabilistic factors for every design scheme;

3. Deriving of characteristics for Monte Carlo simulation;

4. Reliability evaluation of performed numerical experiments by comparison with normal probability law and by the law of the uniform density

5. Choosing the most rational and efficient design scheme of dowels for further modernization of the octagon walls.

Methods

The Church of the Transfiguration was built in 1714. It consists of the one main octagon in which four walls are connected with the earth and the res four walls are suspension. This octagon bears loads from a whole structure as main support for 22 different domes and two smaller octagons. This building is unique because it does not have any nails. Nowadays it has following deformations [21]:

– displacements of a primary tilt are from 15 to 30 cm because of the differential settlement;
– displacements of a secondary tilt are from 32 to 36 cm because of the deformation in the main octagon;
– main octagon is inclined for 35 cm in the north direction and for 55 cm in the east direction;
– local buckling of the walls of the main octagon is up to 35 cm;
– deflections in beams achieve 16 cm.

Such high deformations show that the local and global stiffness of the structure and its separate parts (trunks) is not sufficient. It can be a consequence of very various reasons. First is a weak bond of trunks in the horizontal direction and the absence of dowels in a longitudinal direction. Second reason is an accumulation of deformation due to the impact of temporary loads throughout a long time period. The next reason is the humidity difference of inside and outsides layers of the walls. Due to the swelling of outsides layers trunks bend out. Finally, seasonal temperature changes cause uneven heating of inside and outside surfaces what also increases deflections of trunks due to the time.

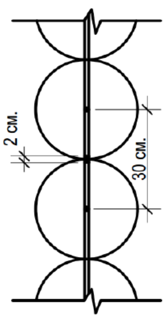

Figure 1. Fragmant of installation of dowels in the trunks for determination of the length of functional part

In order to increase stiffness of the octagon in a horizontal direction it is necessary to put some dowels along a whole wall. Such vertical bonds will prevent any buckling of trunks. But it is necessary to take into account all impacts which cause deformations and, moreover, most of imperfections of timber and trunks' geometry should be considered.

Solution of such problem was derived by Monte Carlo simulation. The basis of the design scheme is an east diagonal wall of the main octagon. Its trunks have diameter from 20 to 30 cm. Curvature along the trunk is also various (3–5 cm). The length of the wall is 6 meters. There are also imperfections such as knots, twigs and gnarls.

Following assumptions have been applied:

- the log panel consists of 7 trunks with length 5 meters and diameter 30 cm;
- loads act only in vertical direction;
- step of dowels should be no more than 2 m and no less than 0.5 m;
- according to [22] for such step of dowels the diameter of every dowel was prescribed as 2.4 cm;
- horizontal and vertical trunks are modelled as trusses with a reduced cross sections;
- in the spans trunks are supported on each other in n points. This points are the places of dowels installation;
- dowels are modelled by vertical trusses;
- system deformability is based on dowel bendings.

In order to model dowels correctly the reduced cross section of dowels was calculated. Diameter of dowel $D =$ 2.4 cm. Mostly it is rigidly fixed but in the central part (effective part) it works on a slice and a bend. The length of this central part depends on the gap between of trunks, the height of the shear zone, the grade of wood ant etc. The conditional length was assigned by Figure1. Stiffness of the dowel with the length 30 cm is not the same for dowel with the length of 2 cm, that is why for design scheme conditional values of stiffness (equivalent stiffness) were used instead of real values.

Schema A **Schema B**

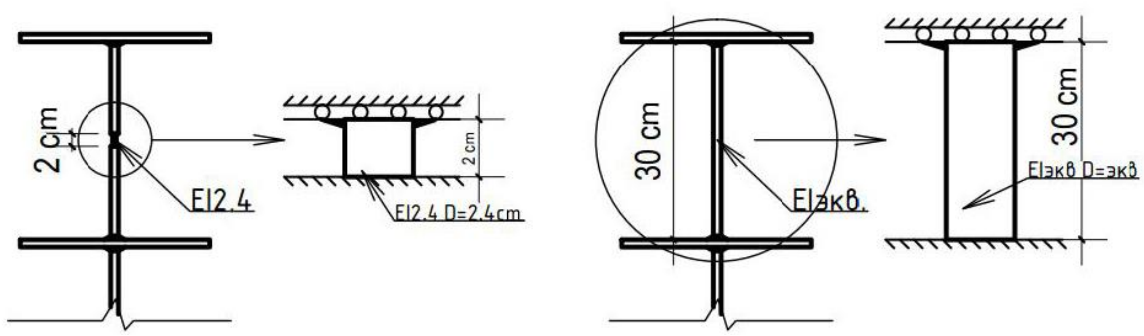

Figure 2. Schemes of equivalent stiffness

Stiffness of conditional dowel δ_{eq} should be larger than stiffness of the real dowel $\delta_{2,4}$. This difference is proportional to the relation of their lengths to the third power:

$$\delta_{eq} = \frac{l_{eq}^3}{3EJ_{eq}}; \quad \delta_{2,4} = \frac{l_{2,4}^3}{3EJ_{2,4}} \quad \textit{and} \quad \delta_{eq} = \delta_{2,4}, \tag{1}$$

where $l_{2,4} = 2cm$ and $l_{eq} = 30cm$ are the length of effective part of the dowel and the length of the equivalent dowel respectively; $E = 100000\ kg/cm$ is an elasticity modulus; J_{eq} and $J_{2,4}$ are the moments of inertia of effective part of the dowel and the equivalent dowel respectively. Moment of inertia for effective part of the dowel can be calculated through the dimeter:

$$J_{2,4} = 0.05D^4 = 0.05 \cdot 2.4^4 = 1.66\ cm^4 \tag{2}$$

Therefore, from Eq. (1) J_{eq} can be derived:

$$J_{eq} = \frac{l_{eq}^3 \cdot 3EJ_{2,4}}{3El_{2.4}^3} = \frac{l_{eq}^3 \cdot J_{2,4}}{l_{2.4}^3} = \frac{30^3 \cdot 1.66}{2^3} = 5602 \ cm^4 \tag{3}$$

Diameter of equivalent dowel can be calculated from Equation (2):

$$D_{eq} = \sqrt[4]{\frac{J_{eq}}{0.05}} = \sqrt[4]{\frac{5602}{0.05}} = 18 \ cm \tag{4}$$

For modeling of design scheme FEM tools were used. Design scheme was simulated as a truss model in the SCAD software for three different steps of dowels (1 m, 1.67 m and 0.71 m), which are represented in Figures 3, 4 and 5 respectively. Stiffness for truss elements were modelled by means of numerical descriptions: EF is a longitudinal stiffness, where $F = \pi D^2/4$ is the area of element; $EI_z = EI_y$ is a bending stiffness, where $I_z = I_y = \pi D^4/64$ are the moments of inertia; GI_k is a torsional stiffness, where $G = E/2(1+\mu)$ and $I_k = \pi D^4/32$; $GF_y = GF_z$ is a shear stiffness. All these characteristics for logs, dowels and the cuttings (bonds) were calculated and provided in Table 1, where numbers in brackets (*) are the number of stiffness types. It should be also noticed, that truss element for cuttings are modelled as trusses in three dimensional space with infinite stiffness.

Applied loads were derived from corresponding projects and reports of LLC "DCF "Stroyrekonstruktsiya". Since overall load for 7 trunk of the main octagon is approximately equal $9.8 \ kN$ output internal forces for dowels are very small (third order values). Such as the main task is to choose step of dowels conditional load ($98 \ kN$) was prescribed. This assumption enables to evaluate probabilistic characteristics not as thousandths but as decimal values.

Table 1. Calculated parameters for simulation of element stiffness

	Log	Dowel	Cutting
$EF, \ [kN]$	692370	249253	98000000
$EI_z = EI_y$, $[kN \cdot m^2]$	3894.52	548.99	3894.52
GI_k, $[kN \cdot m^2]$	2614.64	341.04	-
$GF_y = GF_z, \ [kN]$	233877	84197	233877

After modelling of every case in SCAD software for every design model the calculations without prescribed displacements in Y-direction were produced. After that according to Monte Carlo method in every design model trunks curvature was changed in longitudinal direction. Calculations were produced after every modification and the dowel with maximal internal force was registered. Consistently, curvatures of other dowels were changed up to the moment when selection became representative. For solution of this problem overall 99 calculations were performed for every design scheme.

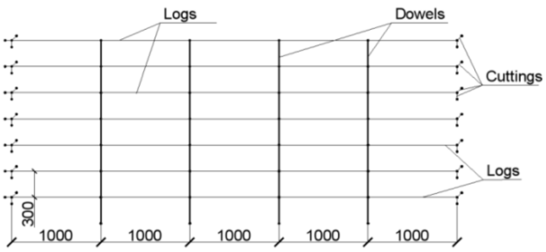

Figure 3. Design scheme for step of dowels 1 m

Figure 4. Design scheme for 1.67 m

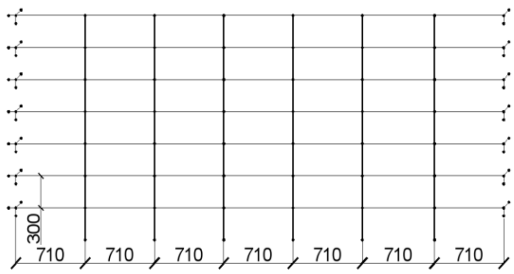

Figure 5. Design scheme for step of dowels 0.71 m

Results and Discussion

By derived above values tables with completed ranking were created for every design scheme. For the step of dowels 1 m maxim value of random variables (internal forces in dowels) $x_{i\min} = 1.7$ and the maximum value $x_{i\max} = 9.08$. For the step 1.67 m these values were equal 1.86 and 16.25 respectively. And for the step of dowels 0.71 m random variables took the values from $x_{i\min} = 0.57$ to $x_{i\max} = 9.08$ In Table 2 maximum and minimum values of random variables (internal forces in dowels) are provided. After that all range of variables was divided into intervals (J_i) and by the frequency of occurrence (m_i) corresponding probability of the emergence of a random variable (p_i^*) was calculated. Then histograms of the distribution were created and provided in Figures 6, 7 and 8.

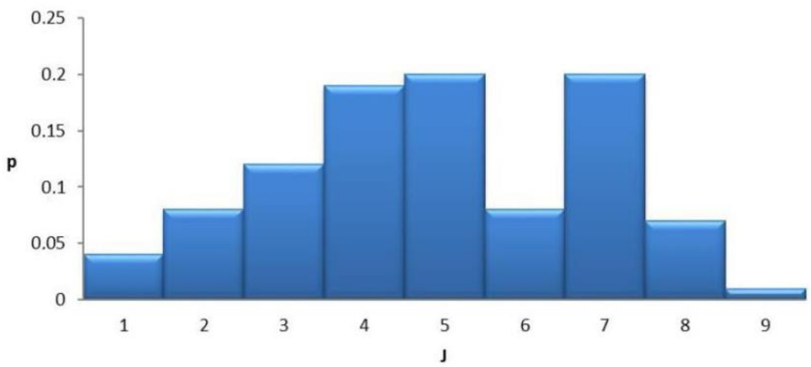

Figure 6. Histogram of the distribution for step of dowels 1 m (9 intervals)

Rasha I.K., Pertseva O.N., Lazareva A.Yu., Martynov G.V. Computational modelling of random distribution of stresses for wooden structures. *Magazine of Civil Engineering*. 2017. No. 1. Pp. 23–33. doi: 10.18720/MCE.69.2

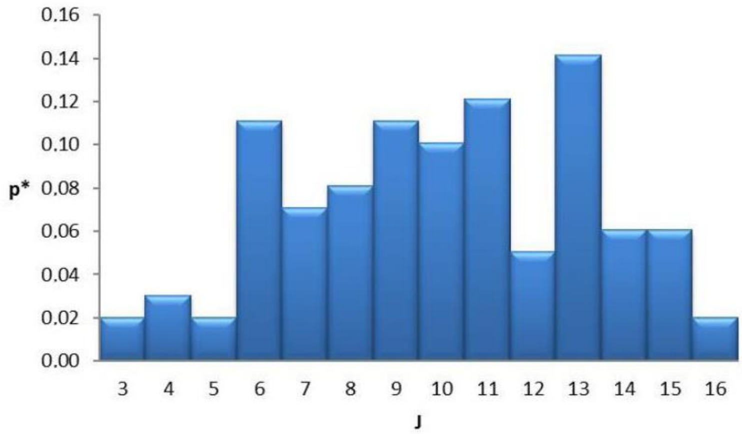

Figure 7. Histogram of the distribution for step of dowels 1.67 m (14 intervals)

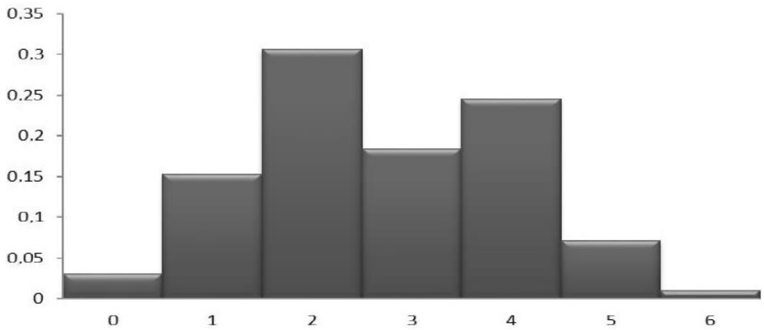

Figure 8. Histogram of the distribution for step of dowels 0.71 m (6 intervals)

For complete analysis of this discrete distribution such numerical characteristics as the statistical average value $(\overline{x_n})$, the standard deviation (σ_n), dispersion (D) and the coefficient of variation (COV) were calculated [23]. For comparison with recent researches reliability indexes β according to first order reliability method (FORM) were calculated [24].

Calculated numerical characteristics are provided in the Table 2.

Table 2. Numerical characteristics of the discrete distribution variables for different steps of dowels

Characteristics	Step of dowels		
	1 m	1.67 m	0.71 m
Number of tests	99	99	99
$\overline{x_n}$	5.415	10.43	3.18
σ_n	1.87	3.21	1.29
D	3.506	10.33	1.67
COV	0.345	0.307	0.406
β	2.896	3.249	2.465

Alignment of the statistical series was held by the normal probability law and by the law of the uniform density. The law of the normal probability is:

$$f(x) = \frac{1}{\sigma_n \cdot \sqrt{2\pi}} \cdot e^{\frac{1}{2}\left(\frac{x_i - \bar{x}^2}{\sigma_n}\right)^2}, \tag{5}$$

where σ_n is a standard deviation; x_i are numerical values of the random variable X and $\bar{x}$ is a statistical average value. And the law of the uniform density has a following form:

$$f(x) = \frac{(J_{i+1} - J_i)}{\overline{\Delta J}} p_i^*. \tag{6}$$

For verification of the distribution laws Person criteria were applied. For this purposes distribution curve was combined with every histogram and the measure of divergence was calculated with help of the following formula:

$$\chi^2 = \sum_{i=1}^{n} \frac{(m_i - np_i)^2}{np_i}, \tag{7}$$

where χ^2 is the criterion of consent; m_i is a measure of occurrence; p_i is the corresponding probability of occurrence and n is the number of tests. Then number of degrees of freedom (r) was calculated as a difference between the number of bits (k) and the number of imposed bonds (s). After that by Table 4 probability (p) was found. If the value of p is very small applied hypothesis is considered as implausible. If the value of p is very large the hypothesis should be considered as not contradicting to test data. The question is how small should be probability p for reconsideration of the hypothesis is quite undefined as soon as the question howl small should be the probability of occurrence for its impossibility [25]. Person criteria allow to appreciate reliability of applied model (hypothesis) and compare results numerically [26]. Results of performed calculations are provided in Table 3 for the law of uniform density and in Table 4 for the law of the normal probability.

Table 3. Evaluation of convergence by the law of uniform density

Characteristics	**Step of dowels**		
	1 m	1.67 m	0.71 m
$p_i = f(x)$	0.11	0.1	0.166
χ^2	37.65	9.01	45.94
k	9	14	7
s	3	3	3
r	6	11	4
Measure of convergence	0.00	0.68	0.00

Table 4. Evaluation of convergence by the law of the normal probability

Characteristics	Step of dowels		
	1 m	1.67 m	0.71 m
χ^2	14.53	16.72	45.94
k	9	14	7
s	3	3	3
r	6	11	4
Measure of convergence	0.038	0.16	0.77

In published works of other authors, the problem of finding the most appropriate design scheme with help of probabilistic theory in general and particularly a detailed comparison of dowel step for enforcing were not touched upon. Therefore, the comparison with other researches should be performed for reliability of the application Monte Carlo simulation for different engineering tasks [27]. In case with glued timber roofs [19] results provided by Monte Carlo simulation vary from results provided by Eurocodes from 6.4 % to 27.81 %. In case with bolted timber joints [20] Monte Carlo simulation was compared with experimental results and for different cases results varied from 10 % to 30 %.

In the present study results were compared with the law of uniform density distribution and with the law of normal probability. For the step of dowels 1m both laws do not provide any convergence (0 % by the law of uniform density and 3.8 % by the law of the normal probability) and more complicated theories should be applied. For the step of 1.67 m. the law of uniform density provides convergence 68 % while convergence by the law of normal probability is only 16 %. In the case when step of dowels is 0.71 m. the law of normal probability yields convergence 77 % whereas the law of uniform density does not provide any convergence (0 %). Therefore, application of Monte Carlo simulation for determination of the most appropriate design scheme provides high reliability and the range of applicability for Monte Carlo simulation can be extended.

Moreover, if we consist moderate consequences of failure and average cost for upgrading the safety level [28] the target reliability index β_t will be equal 4.2 what is larger than all reliability indexes for every design scheme. It means that possibility of failure is equal 0.27 %, 0.098 % and 0.68 % for dowel steps 1.0 m, 1.67 m and 0.71 m respectively. It means that all design schemes are safety and probabilities of failure are very small.

It means that the choice of the optimal step of dowels should be based on produced internal forces for every case, but also technical efforts (cost of construction, materials) should be taken into account. For the step of dowels 1 m. average value of internal forces is 53.07 kN and maximum value is 88.98 kN. For the step of dowels 1.67 m. average value of the internal forces is equal 102.21 kN whereas maximum value is 159.25 kN. In the last case (step of dowels is 0.71 m.) average value of the internal forces is 31.16 kN and maximum value is 60.07 kN. Obviously that the most optimal step of dowels is 1 m since it creates small internal forces as the case with step 1.67 m. and doesn’t require too much material and installation efforts like the case with the step equal 0.71 m.

Conclusions

Influence of imperfections of wooden structures to the internal forces in dowels was analyzed as soon as the zones of the bonding logs and dowels. New algorithm for the simulation and choice of design scheme and structural elements which allows considering all imperfections of structure was created. For three different cases of steps of dowels (1 m., 1.67 m. and 0.71 m.) design scheme in FEM software was modelled and internal forces were calculated. According to Monte Carlo simulation discrete distribution with its main characteristics were derived. Convergence of every distribution for internal forces was estimated by Person criteria. According to resulted convergences assumption that internal forces comply to the law of the normal probability is proven. Optimal step of dowels for walls in the main octagon in the Church of the Transfiguration was calculated and equal 1 m. It provides small stresses by the time of relatively low construction efforts and cost. It was shown that Mote Carlo simulation provides high reliability not only for evaluation of strength of timber details but also for solution of structural problems and finding the most efficient one. Created calculation algorithm and recommended step of dowels will be used for restoration of the Church of the Transfiguration. Moreover, it can be applied for restoration of other wooden structures.

References

1. Tribulová T., Kotlík P. Material studies within the scope of pre-project preparations for restoration of a significant Czech country Church. *International Journal of Architectural Heritage*. 2015. No. 9. Pp. 352–366.
2. Serrano-Lanzarote B., Fenollosa Forner E., Arnau Paltor F. Damage assessment and restoration actions in the church of San Nicolas by Eduardo Torroja (Gandia, 1962). *Informes de la Construccion*. 2016. No. 541. e130.
3. Zolkafli U.K., Yahya Z., Zakaria N., Akashah F.W., Ali A.S.

Литература

1. Tribulová T., Kotlík P. Material studies within the scope of pre-project preparations for restoration of a significant Czech country Church // International Journal of Architectural Heritage. 2015. № 9. Pp. 352–366.
2. Serrano-Lanzarote B., Fenollosa Forner E., Arnau Paltor F. Damage assessment and restoration actions in the church of San Nicolas by Eduardo Torroja (Gandia, 1962) // Informes de la Construccion. 2016. № 541. e130.
3. Zolkafli U.K., Yahya Z., Zakaria N., Akashah F.W., Ali A.S. Restoration of historical timber building: a Malaysian case

Restoration of historical timber building: a Malaysian case study. *Structural Survey.* 2015. No. 33. Pp. 309–321.

4. Petrozzi G.R., Carbajal F., Schexnayder C.J. Restoration of a historic adobe church. *Practice Periodical on Structural Design and Construction*. 2015. No. 20. 04014026.
5. Qiao G., Li T., Frank Chen Y. Assessment and retrofitting solutions for an historical wooden pavilion in China. Construction and Building Materials. 2016. No. 105. Pp. 435–447.
6. Opolovnikov A.V. *Sokrovishcha Russkogo Severa* [Treasures of the Russian North]. Moskow: Stroyizdat, 1989. 367 p. (rus)
7. Luzhin O.V., Zlochevskiy A.B. *Obsledovaniye i ispytaniye sooruzheniy* [Insperction and testing of buildings and structures]. Moskow: Stroyizdat, 1987. 263 p. (rus)
8. Liñán C.R., Morales Conde M.J., De Hita P.R., Gálvez F.P. Application of non-destructive techniques in the inspection of wooden structures of protected buildings: The case of nuestra señora de los dolores church (Isla Cristina, Huelva). *International Journal of Architectural Heritage.* 2015. No. 9. Pp. 324–340.
9. Rodríguez-Mayorga E., Yanes-Bustamante E., Sáez-Pérez A. Analysis and diagnosis of the church of Santiago in Jerez de la Frontera (Spain). *Informes de la Construccion*. 2015. No. 67. e127.
10. Carlo B., Pietro C., Vincenzo D., Nora F. Towards the BIM implementation for historical building restoration sites. *Automation in Construction*. 2016. № 71.
11. Carlo B., Pietro C., Vincenzo D., Nora F. IT procedures for simulation of historical building restoration site. *32nd International Symposium on Automation and Robotics in Construction and Mining: Connected to the Future.* Oulu: IAARC. 2015. Pp. 1–8.
12. Onen A., Jung J., Dilek M., Cheng D., Broadwater R., Scirbona C., Cocks G., Hamilton S., Wang X. Model-centric distribution automation: Capacity, reliability, and efficiency. *Electric Power Components and Systems.* 2016. No. 44. Pp. 495–505.
13. Seo J., Park H. Seismic restoration cost curve of curved steel bridges. *Forensic Engineering 2015: Performance of the Built Environment – Proceedings of the 7th Congress on Forensic Engineering.* Miami: ASCE, 716-726 (2015)
14. Stefanou I., Fragiadakis M., Psycharis I.N. Seismic reliability assessment of classical columns subjected to near source ground motions. *Computational Methods in Applied Sciences*. 2015. No. 37. Pp. 61–82.
15. Aven T., Pedersen L.M. On how to understand and present the uncertainties in production assurance analyses, with a case study related to a subsea production system. *Reliability Engineering and System Safety.* 2014. No. 124. Pp. 165–170.
16. De León D., González-Pérez C.A., Díaz S., Delgado D., Arteaga J.C. Time variation of bridges structural reliability due to corrosion in Mexico. *Bridge Maintenance, Safety, Management, Resilience and Sustainability – Proceedings of the Sixth International Conference on Bridge Maintenance, Safety and Management.* Stresa: CRC Press. 2012. Pp. 2225–2229.
17. Yuan J.L., Yan Y.D., Huang D., Du C. Restoration strategies of urban road network after earthquake based on corrected component probabilistic importance. *Applied Mechanics and Materials*. 2014. No. 694. Pp. 95–101.
18. Quiroga L.M., Schnieder E. Monte Carlo simulation of railway track geometry deterioration and restoration. *Journal of Risk and Reliability.* 2012. No. 226. Pp. 274–282.
19. Domański T. Reliability of glued timber roofs belonging to CC3 class consequences of failure. Technical transactions architecture. *Architecture.* 2014. No. 8-A. Pp. 41–48.
20. Sawata, K., Yasumura, M. *Evaluation of yield strength of*

study // Structural Survey. 2015. № 33. Pp. 309–321.

4. Petrozzi G.R., Carbajal F., Schexnayder C.J. Restoration of a historic adobe church // Practice Periodical on Structural Design and Construction. 2015. № 20. 04014026.
5. Qiao G., Li T., Frank Chen Y. Assessment and retrofitting solutions for an historical wooden pavilion in China // Construction and Building Materials. 2016. № 105. Pp. 435–447.
6. Ополовников А.В. Сокровища Русского Севера. М.: Стройиздат, 1989. 367 с.
7. Лужин О.В., Злочевский А.Б. Обследование и испытание сооружений. М.: Стройиздат, 1987. 263 с.
8. Liñán C.R., Morales Conde M.J., De Hita P.R., Gálvez F.P. Application of non-destructive techniques in the inspection of wooden structures of protected buildings: The case of nuestra señora de los dolores church (Isla Cristina, Huelva) // International Journal of Architectural Heritage. 2015. № 9. 324–340.
9. Rodríguez-Mayorga E., Yanes-Bustamante E., Sáez-Pérez A. Analysis and diagnosis of the church of Santiago in Jerez de la Frontera // Informes de la Construccion. 2015. № 67. e127.
10. Carlo B., Pietro C., Vincenzo D., Nora F. Towards the BIM implementation for historical building restoration sites. Automation in Construction // Automation in Construction. 2016. № 71.
11. Carlo B., Pietro C., Vincenzo D., Nora F. IT procedures for simulation of historical building restoration site // 32nd International Symposium on Automation and Robotics in Construction and Mining: Connected to the Future. Oulu: IAARC. 2015. Pp. 1–8.
12. Onen A., Jung J., Dilek M., Cheng D., Broadwater R., Scirbona C., Cocks G., Hamilton S., Wang X. Model-centric distribution automation: Capacity, reliability, and efficiency // Electric Power Components and Systems. № 44. 2016. Pp. 495–505.
13. Seo J., Park H. Seismic restoration cost curve of curved steel bridges // Forensic Engineering 2015: Performance of the Built Environment – Proceedings of the 7th Congress on Forensic Engineering. Miami: ASCE. 2015. Pp. 716–726.
14. Stefanou I., Fragiadakis M., Psycharis I.N. Seismic reliability assessment of classical columns subjected to near source ground motions // Computational Methods in Applied Sciences. № 37. 2015. Pp. 61–82.
15. Aven T., Pedersen L.M. On how to understand and present the uncertainties in production assurance analyses, with a case study related to a subsea production system // Reliability Engineering and System Safety. 2014. № 124. Pp. 165–170.
16. De León D., González-Pérez C.A., Díaz S., Delgado D., Arteaga J.C. Time variation of bridges structural reliability due to corrosion in Mexico // Bridge Maintenance, Safety, Management, Resilience and Sustainability - Proceedings of the Sixth International Conference on Bridge Maintenance, Safety and Management. Stresa: CRC Press. 2012. Pp. 2225–2229.
17. Yuan J.L., Yan Y.D., Huang D., Du C. Restoration strategies of urban road network after earthquake based on corrected component probabilistic importance // Applied Mechanics and Materials. 2014. № 694. Pp. 95–101.
18. Quiroga L.M., Schnieder E. Monte Carlo simulation of railway track geometry deterioration and restoration // Journal of Risk and Reliability. 2012. № 226. Pp. 274–282.
19. Domański T. Reliability of glued timber roofs belonging to CC3 class consequences of failure. Technical transactions architecture // Architecture. 2014. № 8-A. Pp. 41–48.
20. Sawata, K., Yasumura, M. Evaluation of yield strength of bolted timber joints by Monte-Carlo simulation [Электронный ресурс]. Систем. требования:

bolted timber joints by Monte-Carlo simulation [Online]. System requirements: AdobeAcrobatReader. URL: http://timber.ce.wsu.edu/Resources/papers/1-4-4.pdf (date of application: 02.03.2017)

21. Chusov A.A., Skopin V.A., Lyubimtsev A.Yu. O restavratsii tserkvi preobrazheniya gospodnya na o. Kizhi [About restoration of the Church of the Transfiguration on Kizhi island]. *Tserkov preobrazheniya gospodnya na ostrove Kizhi: 300 let na zaonezhskoy zemle* [Church of the Transfiguration on Kizhi Island: 300 years on earth Zaonezhie]. Petrozavodsk: Museum-reserve "Kizhi" Press, 2014. Pp. 148–157. (rus)
22. *SP 64.13330.2011.* Derevyannyie konstrukcii [Timber structures]. 2011. (rus)
23. Venttsel Ye.S. *Teoriya veroyatnostey* [Theory of probabilities]. Moskow: Nauka, 1969. 576 p. (rus)
24. Köhler J. *Reliability of timber structures* [Online]. System requirements: AdobeAcrobatReader. URL: http://e-collection.library.ethz.ch/eserv/eth:2337/eth-2337-01.pdf (date of application: 01.03.2017)
25. Mitropolskiy A.K. *Tekhnika statisticheskikh vychisleniy* [The technique of statistical calculations]. Moskow: Nauka, 1971. 576 p. (rus)
26. Vatin N.I., Volodin V.V., Zolotareva E.A., Petrov K.V., Zhmarin E.N. Rekonstruktsiya krysh Sankt-Peterburga na osnove legkikh stalnykh tonkostennykh konstruktsiy i antiobledenitelnoy sistemy [Reconstruction of roofs of St. Petersburg on the basis of light steel thin-walled structures and anti-icing system]. *Magazine of Civil Engineering*. 2010. No. 2. Pp. 59–64. (rus)
27. Oliynyk O., Murgul V.A. Strategy for energy efficient reconstruction of residential low-rise buildings. *Construction of Unique Buildings and Structures.* 2016. No. 1. Pp. 112–124.
28. *Joint Committee of Structural Safety*. Probabilistic Model Code. [Online]. System requirements: AdobeAcrobatReader. URL: http://www.jcss.byg.dtu.dk/Publications/Probabilistic_Model_Code.aspx (date of application: 02.03.2017)

AdobeAcrobatReader. URL: http://timber.ce.wsu.edu/Resources/papers/1-4-4.pdf (дата обращения: 02.03.2017).

21. Чусов А.А., Скопин В.А., Любимцев А.Ю. О реставрации церкви преображения господня на о. Кижи // Церковь преображения господня на острове Кижи: 300 лет на заонежской земле. Петрозаводск: Изд-во музея-заповедника «Кижи», 2014. С. 148–157.
22. СП 64.13330.2011. Деревянные конструкции. 2011.
23. Вентцель Е.С. Теория вероятностей. М.: Наука, 1969. 576 с.
24. Köhler J. Reliability of timber structures, [Электронный ресурс]. Систем. требования: AdobeAcrobatReader. URL: http://e-collection.library.ethz.ch/eserv/eth:2337/eth-2337-01.pdf (дата обращения: 01.03.2017)
25. Митропольский А.К. Техника статистических вычислений. М.: Наука, 1971. 576 с.
26. Ватин Н.И., Володин В.В., Золотарева Е.А., Петров К.В., Жмарин Е.Н. Реконструкция крыш Санкт-Петербурга на основе легких стальных тонкостенных конструкций и антиобледенительной системы // Инженерно-строительный журнал. 2010. № 2. С. 59–64.
27. Олейник О., Мургул В.А. Стратегия энергоэффективной реконструкции жилых малоэтажных зданий // Строительство уникальных зданий и сооружений. 2016. № 1. С. 112–124. (eng)
28. Joint Committee of Structural Safety. Probabilistic Model Code. [Электронный ресурс]. Систем. требования: AdobeAcrobatReader. URL: http://www.jcss.byg.dtu.dk/Publications/Probabilistic_Model_Code.aspx (дата обращения: 02.03.2017)

Iosif Rasha,
+7(921)9983692; oslik1939@rambler.ru

Olga Pertseva,
+7(953)1711053; olya_perceva@mail.ru

Alena Lazareva,
+7(911)0134854; lazareva101@mail.ru

Gleb Martynov,
+7(911)7333721; martynovgleb@rambler.ru

Иосиф Кириллович Раша,
+7(921)9983692;
эл. почта: oslik1939@rambler.ru

Ольга Николаевна Перцева,
+7(953)1711053;
эл. почта: olya_perceva@mail.ru

Алёна Юрьевна Лазарева,
+7(911)0134854;
эл. почта: lazareva101@mail.ru

Глеб Вадимович Мартынов,
+7(911)7333721;
эл. почта: martynovgleb@rambler.ru

Раша И.К., Перцева О.Н., Лазарева А.Ю., Мартынов Г.В. Численное моделирование случайного распределения напряжений для деревянных конструкций // Инженерно-строительный журнал. 2017. № 1(69). С. 23–33.

doi: 10.18720/MCE.69.3

Lifetime of earth dams

Срок эксплуатации грунтовых плотин

T.S. Titova,
Petersburg State Transport University,
St. Petersburg, Russia
A. Longobardi,
Università degli Studi di Salerno, Salerno, Italy
R.G. Akhtyamov,
E.S. Nasyrova,
Petersburg State Transport University,
St. Petersburg, Russia

Д-р техн. наук, заведующая кафедрой, проректор по научной работе Т.С. Титова,
Петербургский государственный университет путей сообщения Императора Александра I, Санкт-Петербург, Россия
PhD, профессор А. Лонгобарди,
Университет г. Салерно, г. Салерно, Италия
канд. техн. наук, доцент Р.Г. Ахтямов, аспирант Э.С. Насырова,
Петербургский государственный университет путей сообщения Императора Александра I, Санкт-Петербург, Россия

Key words: construction; hydraulic engineering; dam; life-cycle

Ключевые слова: конструкция; гидротехническое сооружение; плотина; жизненный цикл

Abstract. The level of safety of small earth dams, operating without staff and measurement and control equipment, are considered in this study. Approach enabling the possibility to define the finite lifetime (Tf) of a small earth dam here presented. The proposed approach does not require any variables monitoring. It is based on the definition of Tf by assessing the water impact on the small earth dams by quantitative methods of system analysis. To assess the earth dam Tf, two approaches are offered, which based on the digraph method. They are the classification scale construction and the cluster method. On a quantitative base the Tf of small dam on urban area can be defined as the minimum between the two (75 year for the classification scale and 80 for the clustering), which is however well above the Russian regulations, which indicate a period of 50 years (design life). The estimated value allows defining robustness of earth dam and can be used as a criterion for safety management of earth dams, defining the needs to undertake actions to improve, during the life cycle, earth dam structural features.

Аннотация. Работа посвящена оценке безопасности низконапорных грунтовых плотин, эксплуатирующихся без персонала и контрольно-измерительной аппаратуры на объекте. В статье предложен метод по определению критического срока эксплуатации низконапорных грунтовых плотин, не требующий данных о фактическом состоянии объекта. Предложенный метод основан на количественной оценке различных видов воздействия воды, приводящих к разрушению грунтовой плотины. Для определения критического срока эксплуатации грунтовой плотины, значения полученные методом импульсного процесса, обрабатывались методом построения классификационных шкал и кластерного анализа. Минимальное из полученных значений принято за критический срок эксплуатации грунтовой плотины в пределах урболандшафта. Методом построения классификационных шкал выявлен критический срок эксплуатации грунтовой плотины, равный 75 лет, а методом кластерного анализа – 80 лет. Критическим сроком эксплуатации грунтовой плотины выбрано минимальное из двух полученных, поскольку в соответствии со СНиП 33-01-2003, нормативный срок службы грунтовых плотин IV класса – 50 лет. Полученное значение позволяет определить запас прочности грунтовой плотины и может служить критерием управления безопасностью грунтовых плотин, а именно определяет необходимость проведения мероприятий по увеличению жизненного цикла плотины при обязательном учете особенностей конкретных объектов.

Introduction

Earth dams make about 85 % of all planned and constructed dams all over the world and in most cases they are small dams, in accordance with International commission on large dams (ICOLD), with the height of less than 15 meters [1]. Earth dams are used as a protection against floods and mainly with

Titova T.S., Longobardi A., Akhtyamov R.G., Nasyrova E.S. Lifetime of earth dams. *Magazine of Civil Engineering*. 2017. No. 1. Pp. 34–43. doi: 10.18720/MCE.69.3

drinkable and irrigation water systems supply, such dams now support approximately 30–40 % of the 271 million hectares of irrigated agriculture [2]. The wide use of earth dams as water retaining structures is now determined by the possibility to use local soils, by the emergence of powerful mechanisms and capability to build dams in difficult engineering-geological and seismic conditions. However, not all small dams are designed according to engineering criteria and moreover their maintenance and management criteria are not strictly regulated [3, 4].

The life cycle of any earth dam can be divided into intervals: 1) construction and initial filling; 2) normal operation; 3) a residual life [5]. The cycle construction and initial filling characterized by high failure rate, but at the end of this interval failure rate of the structures is stabilized. During normal operation of dam, failure occurs when excess impacts. The first two intervals are design life (lifetime).

When designing an earth dam, in the technical documentation a design life of dam is determined, before reaching of which dam maintains the normal operational characteristics or operating state. Upon reaching the design life an earth dam is not always taken out of service, because of its durability, which allows exploiting the dam for some time after the end of design life. It is time called residual life and during this time the dam is operational. But at some point the dam from the operating state becomes inoperable, that is a condition in which the object is able to partly perform the required function, that is there comes finite life time (or finite lifespan). At this time the restoration of a working condition is impossible or impractical, and further operation of the earth dam is unacceptable by reason of an emergency [6, 7].

According to the ICOLD, a large number of earth dams nowadays have been operated for more than 50 years, reaching their design life, with an increase in damage occurrences probabilities [8]. For example, today in the Russian Federation there are about 30 thousand dams and their condition of safety level distributed as follows: at normal safety level – 39.4 %, low – 43.4 %, unsatisfactory –12.5 % and the 4.7 % are hazardous. The number of hazardous dams, compared with the previous decade, increased by 2. But the safety conditions are similar worldwide: in China 96% of dam failures, between 1954–2003, involved small dams [9].

Earth dams safety management is directly connected with the possibility to control and monitor the current state and age of the construction, natural and geographical factors, operational planning. Monitoring techniques open the way to forecasting safety level and risk, which can be pursued either in a probabilistic or in a deterministic framework.

Probabilistic models, considering the safety level and risk as random variables and predicting occurrences probabilities, are rather robust methods but need long series of recorded data to perform statistical analysis [10]. Authors in [11] describe a number of different quantitative risk assessments analyses; in [12] consider evaluation of the probabilities of dam safety levels; in [13] prefer the model for service life of dam based on time-varying risk probability and in [14] present rational quantitative optimal approach for the reduction of risk from overtopping of earth-fill dams.

The problem of earth dams durability in the loss of abilities of earth dam to accomplish the assigned functions because of the aging process [15]. This problem is analyzed in a probabilistic approach in [16, 17]. The authors in [18] are proposed probabilistic method which is based on the calculation of two major indexes: a condition index and a condition control index. For stability analysis of dams authors in [19] present new probabilistic method, which is based on First Order Reliability Method and considers some variables as random.

On the other side, deterministic models basically consist of a comparison between monitored variables and the value given to these variables in the current regulations and then they are hindered by the lack of monitored data.

As a result, existing models only allow estimating dam safety risk or critical level of safety for small earth dams, defined as level at which maintenance occurs because of a decreasing dam stability and an excess of maximum allowable safety criteria values, indicating the shift from partially disabled to disabled conditions. In this connection the aim of this article is to present comprehensive approach enabling the possibility to define the finite lifetime (T_f) of a small earth dam. Obtained earth dams T_f value is criteria for monitoring and planning future actions for improving sustainability and ensure safe operation. The lack of statistical and experimental data causes difficulties in assessing dam finite lifetime. Therefore to overcome this problem system analysis method is used, as demonstrated in the following research.

Methods

The proposed approach differs from the probabilistic and deterministic models. It is based on the definition of T_f in the following sequence:

1. Building of directed graph (or just digraph).
2. Calculation of the digraph using the pulse process.
3. Construction of classification scale.
4. Construction of the dendrogram by the results of cluster method.

This approach does not require any variables monitoring, which is rather important for the small earth dams, where usually there are no measurement and control equipment and operating staff.

Digraph method

At construction of a settlement model (digraph) one of the primary procedures is to identify loadings and impacts acting on earth dam at different modes of operation and directly or indirectly leading to the destruction of earth dams, which are in this article divided into:

– climatic (flood, earthquake, karst etc.);

– technogenic (failure of spillway due to insufficient capacity and enginery, substandard work, material defect, staff error etc.);

– water impact (high pressure, filtration, suffusion, cavitation erosion, corrosion processes, wave pressure etc.).

The impacts are selected depending on the physico-geographical conditions of the area, the design features and operating conditions of earth dams. Between the selected impacts directly or indirectly leading to the destruction of earth dams, establishes a correlation and constructs the digraph. In this case an output parameter of a digraph is the damaging effect of impacts.

As rule, a digraph consists of a non-empty finite set of elements called vertices and a finite set of ordered pairs of distinct vertices called arcs [28]. A weighted digraph consists of a digraph and an assignment of a weight on each arc. The weight of the arc can be interpreted as the relative strength of the effect, and can be either positive or negative.

For a quantitative assessment of impacts on earth dams, it is possible to either use observed data or to assign weighting coefficient to each of the arcs. Instrumental measurement is a time consuming process, it requires special equipment and is not generally operated for small earth dam because of the large cost impact.

Due to the lack of data by the each type of impact on earth dams, weights are assigned to each arc. For definition of weight of digraph arcs and signs propose method of expert evaluations (by experts' interviews), further considering that the sum of absolute values of the weight coefficients is equal to unit. For example, authors in their work [16] used expert's judgment.

Pulse process

Modeling of changes in the values of the components included in the digraph (in our case different types of impacts) is made by steps *(S* = 1, 2–12*)* as a pulse process [29]. Each step consist of 10 years, so, in this specific study, the maximum age of an earth dam is made of up to 120 years. The pulse process can be explained as in the following: each vertex *i* refers to a value $V_{i(s)}$ at each step *S*. The succeeding value $V_{i(s+1)}$ introduced at vertex *i* at step *S+1*, and from information about whether other vertices *j* adjacent to *i* went up or down at the last step. If there is an arc from *j* to *i* and *j* goes up by a units at step *S*, then as a result *i* goes up at step *S+1* by an amount equal to steps the sign of arc *(j, i).* For any step *S* value components $V_{i(S)}$ at the vertices *i* is determined by the formula [29]:

$$V_{i(S)} = V_{i(S-1)} + \sum_{i,j=1}^{n} a_{ji} \cdot P_{j(S)} \quad (1)$$

$$P_{j(S)} = V_{j(S)} - V_{j(S-1)}, \quad (2)$$

where $V_{i(S-1)}$, $V_{j(S-1)}$ – the value of components in step *S–1* at vertices *i* and *j*;

i, j – number of vertices;

a_{ji} – weighting coefficient;

n – the number of components included in the calculation component.

Classification scale construction method

Construction of a classification scale is based on cumulative distribution function and is performed according for the formula [30]:

$$V_{c.s.} = \frac{1}{N+1} \cdot \left(\frac{V_{(s)} - a}{b - a} + s - 1\right), \tag{3}$$

where $V_{c.s}$ is the value of damaging effect of impacts, transformed by the method for constructing classification scales;

$V_{(s)}$ – the value of damaging effect of impacts on the step s, calculated by the digraph method;

a – minimum value of $V_{(s)}$;

b – maximum value of $V_{(s)}$;

N – sample length.

The identifier c is calculated by the formula:

$$c = \frac{\sum_{i=1}^{N} V_{(s)}}{\sqrt{\frac{\sum_{i=1}^{N} V_{(s)} - \sum_{i=1}^{N} V_{(s)}^2}{N-1} \cdot N}} \tag{4}$$

Cluster method (dendrogram)

The cluster analysis is an alternative quantitative method for the analysis of the system under investigation. The earth dam T_f will be estimated through the identification of clusters, that are, by definition, groups of elements featured by a high degree of similarity among themselves. Clusters allocation is identified by the construction of the dendrogram.

Inclusion in a particular cluster is defined on the basis of the minimum distance in the Euclidean space. The distance between two damaging effect of impacts corresponding to two different periods of maintenance can be defined as:

$$d_s = \left| \frac{V_{n(si)} - V_{n.av.}}{V_{n.d.}} - \frac{V_{n(si+1)} - V_{n.av.}}{V_{n.d.}} \right|, \tag{5}$$

where d_s – distance in the Euclidean space;

$V_{n(s)}$ – value of damaging effect of impacts on steps i and i+1 derived from the digraph method;

$V_{n.av.}$– average value of damaging effect of impacts;

$V_{n.d.}$ – deviation of value of damaging effect of impacts.

In this article calculated T_f for the small earth dam, forming a pond on urban area, in accordance with the proposed methods and with the following initial conditions:

- there is no operating staff on dams, so technogenic impact – staff error, leading to the destruction of earth dams is excluded;
- failure of spillway due to insufficient capacity is not considered, because the ponds within the urban area, mostly undrained, and the dam is only the pressure front, which does not contain a spillway;
- natural impacts as earthquake and flood are not considered, as they relate to rare events [20]. For example, earthquakes have been the cause of only around 1.5 % of all dam failures and it is considered as less obvious [21, 22];

– urban area with small earth dams located outside of karst fields and is relatively stable;

– the main reasons of the earth dam destructions, according to the ICOLD are overflowing water through the crest and dam basis breakings, which in turn can be caused by a flood [23] and by different types of water impact, for example, high hydrostatic pressure levels, cavitation erosion, filtration, piping, etc. [8, 24–27]. In this regard, settlement model for small dam of urban area includes only different types of water impact. Water exerts intensive physicochemical and biological impacts on earth dams, which are divided into a number of subtypes, increasing variety forms of impact.

Results and Discussion

In accordance with the above initial conditions the digraph is obtained (Fig. 1).

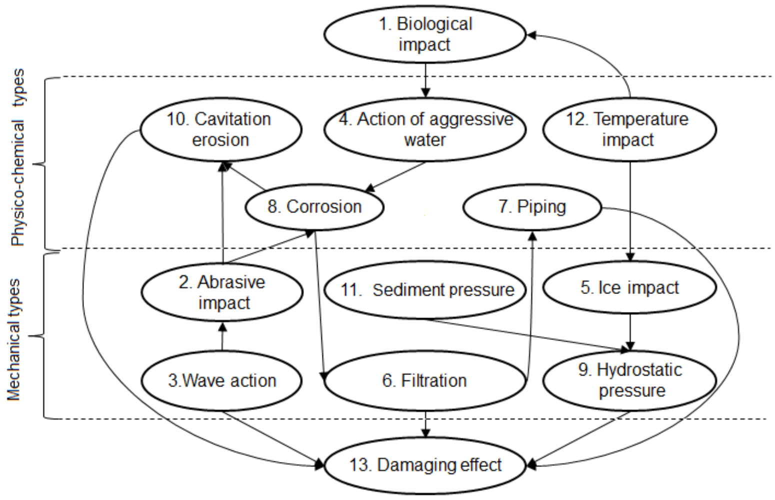

Figure 1. Directed graph, describing the correlation between the forms of water impact

The digraph in Figure 1 illustrates the correlation between different forms of water impact on small earth dams of urban area. It will be used in the following research for further quantitative assessments.

Output digraph parameter is the cumulative impact of all kinds of water impact on earth dam, leading to the destruction of the dam (the damaging effect of water).

To determine the weights of digraph arcs, a survey was conducted of 20 specialists from the following organizations: University of Salerno and Center of laboratory analysis and technical measurements, whose research activities directly or indirectly connected with earth dams. The final result is presented in the work. The expert evaluation assessment in terms of weight coefficients and signs for each arc is graphically represented in Figure 2.

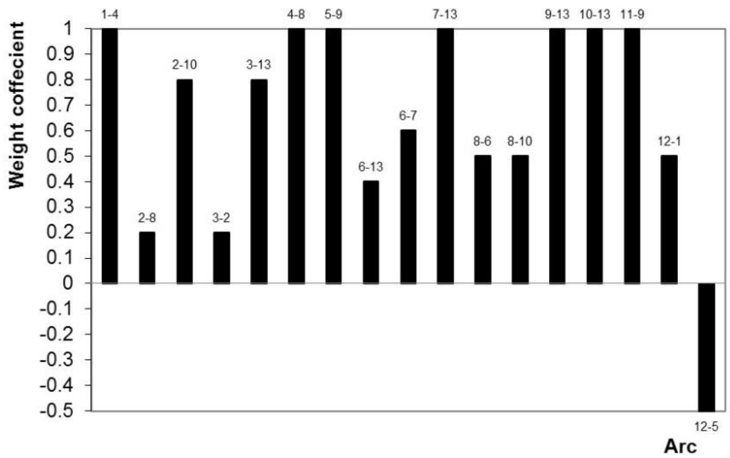

Figure 2. The weights and signs for arcs

Titova T.S., Longobardi A., Akhtyamov R.G., Nasyrova E.S. Lifetime of earth dams. *Magazine of Civil Engineering*. 2017. No. 1. Pp. 34–43. doi: 10.18720/MCE.69.3

As an example, negative value of the weight coefficient appropriated to the arch 12–5 (temperature impact – ice impact) is explained by that at increase in temperature, there is a weakening of ice impact. In other cases coefficients are faced by a positive sign which, by rules, indicates that the increase of one type of water impact leads to the increase of values of a dependent component. For example, the increase of sediment pressure at an earth dam leads to increase in hydrostatic pressure.

As activating the components selected wave action (3), the pressure sediment (11) and temperature impact (12), that is, those components that are do not depend on the other.

On the basis of a digraph (Fig. 1) and formula 1, formulas for calculating the value of components V_i are received:

$V_{1(S)} = V_{1S-1} + a_{12-1} \cdot V_{12(S-1)}$;

$V_{2(S)} = V_{2(S-1)} + a_{3-2} \cdot V_{3(S-1)}$;

$V_{4(S)} = V_{4(S-1)} + a_{1-4} \cdot V_{1(S-1)}$;

$V_{5(S)} = V_{5(S-1)} + a_{12-5} \cdot V_{12(S-1)}$;

$V_{6(S)} = V_{6(S-1)} + a_{8-6} \cdot V_{8(S-1)}$;

$V_{7(S)} = V_{7(S-1)} + a_{6-7} \cdot V_{6(S-1)}$;

$V_{8(S)} = V_{8(S-1)} + a_{1-8} \cdot V_{1(S-1)} + a_{2-8} \cdot V_{2(S-1)} + a_{4-8} \cdot V_{4(S-1)}$;

$V_{9(S)} = V_{9(S-1)} + a_{5-9} \cdot V_{5(S-1)} + a_{11-9} \cdot V_{11(S-1)}$;

$V_{10(S)} = V_{10(S-1)} + a_{2-10} \cdot V_{2(S-1)} + a_{8-10} \cdot V_{8(S-1)}$;

$V_{13(S)} = V_{13(S-1)} + a_{3-13} \cdot V_{3(S-1)} + a_{6-13} \cdot V_{6(S-1)} + a_{7-13} \cdot V_{7(S-1)} + a_{9-13} \cdot V_{9(S-1)} + a_{10-13} \cdot V_{10(S-1)}$.

For example, here is the calculation of the values of components: piping (7), hydrostatic pressure (9), cavitation erosion (10) and damaging effect (13) at $S = 1$.

$V_{6(1)} = 0 + 0.5 \cdot 0 = 0$;

$V_{7(1)} = 0 + 0.6 \cdot 0 = 0$;

$V_{9(1)} = 0 + 1 \cdot 0 + 1 \cdot 1 = 1$;

$V_{10(1)} = 0 + 0.8 \cdot 0 + 0.5 \cdot 0 = 0$;

$V_{13(1)} = 0 + 0.8 \cdot 1 + 0.4 \cdot 0 + 1 \cdot 0 + 1 \cdot 0 + 1 \cdot 0 = 0.8$.

Similarly calculated values of all digraph components (fig. 1) on the steps S = 1, 2–12.

As a result of the modeling of the directed graph components values on the basis of the pulse process, the dependency of the damaging effect of water and earth dam maintenance time is shown in Figure 3.

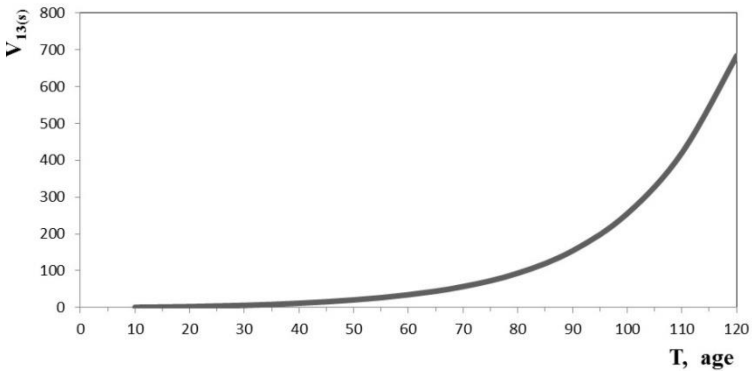

Figure 3. The dependency between the damaging effect of water and the maintenance time of earth dam (T)

As can be seen from Figure 3, it is not possible to determine accurately the finite lifetime T_f of earth dams, because the used modeling approach reproduces a monotonic non-linear increase of damaging effect of water for increasing earth dam maintenance time, without the possibility to identify a value for T_f, as a quantile of the curve.

The obtained values of V_{13} on the steps S = 1, 2–12 were substituted into formula 3. For example, here is the calculation of the damaging effect of water on the steps S = 1 and S = 2:

$$V_{13.c.s.(1)} = \frac{1}{12+1} \cdot \left(\frac{0.8-0.8}{683-0.8} + 1 - 1\right) = 0;$$

$$V_{13.c.s.(2)} = \frac{1}{12+1} \cdot \left(\frac{2.6-0.8}{683-0.8} + 2 - 1\right) = 0.076.$$

Similarly calculated values of the damaging effect of water on the steps S = 3–12.

For the presented report, by construction of a classification scale, the calculated value for c (c = 0.66) and the sample length (N = 12), lead to the number of classes of the maintenance period of earth dams equal to 2.

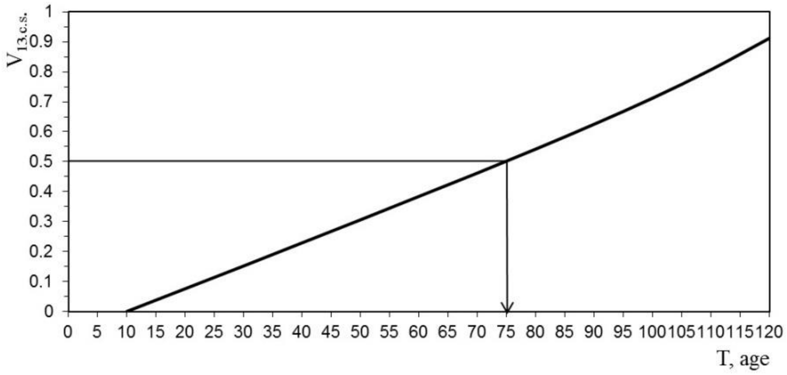

Figure 4. The dependence between the damaging effect of water and the maintenance time of earth dam (classification scales construction method)

Figure 4 illustrates the variation of $V_{13.c.s}$ versus T. Since a number of two classes have been calculated as optimal for the classification scale method, a correspondent estimation of about 75 years for the T_f is reported.

The obtained values of V_{13} on the steps S = 1, 2–12 also were substituted into formula 5. For example, here is the calculation of the minimum distance in the Euclidean space between values of damaging effect of water on the steps S = 1 и S = 2.

$$d_s = \left| \frac{0.8-146.6}{213.5} - \frac{2.6-146.6}{213.5} \right| = 0.01.$$

As a results of cluster method, a matrix containing the minimum distance for each damaging effect of water corresponding to a given maintenance period can be derived (Table 1).

Table 1. Euclidean distance matrix

$V_{n(s)}$	Step	1	2	3	4	5	6	7	8	9	10	11	12
0.80	1		0.01	0.02	0.05	0.10	0.16	0.27	0.44	0.73	1.20	2.03	3.23
2.60	2	0.01		0.02	0.04	0.09	0.15	0.26	0.43	0.72	1.24	2.03	3.23
6.06	3	0.02	0.02		0.03	0.07	0.14	0.24	0.41	0.70	1.23	2.01	3.21
11.90	4	0.05	0.04	0.03		0.04	0.11	0.21	0.39	0.67	1.20	1.98	3.18
20.90	5	0.10	0.09	0.07	0.04		0.07	0.17	0.34	0.63	1.16	1.94	3.14
34.90	6	0.16	0.15	0.14	0.11	0.07		0.11	0.28	0.56	1.09	1.87	3.07
57.10	7	0.27	0.26	0.24	0.21	0.17	0.11		0.17	0.46	0.99	1.77	2.97
93.40	8	0.44	0.43	0.41	0.39	0.34	0.28	0.17		0.29	0.81	1.60	2.80
154	9	0.73	0.72	0.70	0.67	0.63	0.56	0.46	0.29		0.53	1.31	2.51
265	10	1.25	1.24	1.23	1.20	1.16	1.09	0.99	0.81	0.53		0.78	1.98
430	11	2.03	2.03	2.01	1.98	1.94	1.87	1.77	1.60	1.31	0.78		1.20
683	12	3.23	3.23	3.21	3.18	3.14	3.07	2.97	2.80	2.51	2.01	1.20	

The minimum Euclidean distances in each pair in Table 1 are highlighted. Allocation of clusters is then obtained by successive comparisons of the estimated values of the minimum distances (Table 1): according to the hierarchical levels 0.25; 0.50; 0.75; 1.00; 1.25 etc. The results of the cluster analysis are presented in the form of the dendrogram (Fig. 5).

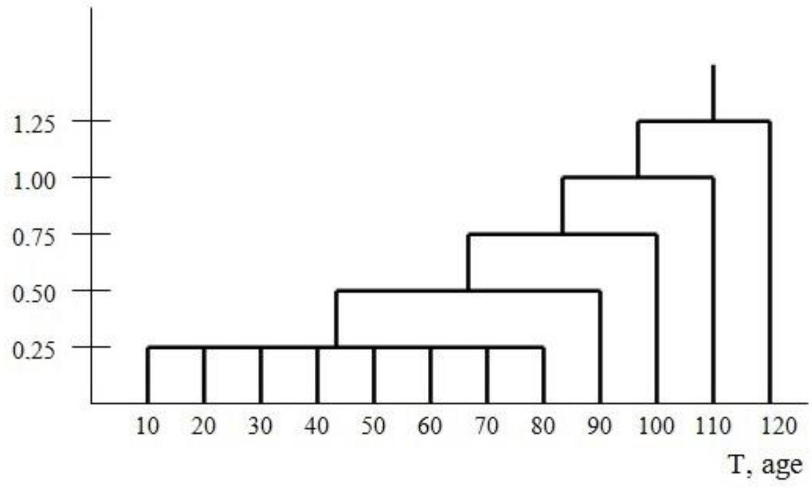

Figure 5. Dendrogram of cluster analysis of maintenance periods of earth dam

According to cluster approach, the dendrogram representation indicates that quantitatively the earth dam T_f is of about 80 years, similar to what found in the case of the classification scales construction approach.

On a quantitative base the T_f can be defined as the minimum between the two (75 year for the classification scale and 80 for the clustering), which is however well above the Russian regulations, which indicate a design life of 50 years.

The resulting value T_f (75 year), comparable with literature data. For example, authors in [31, 32], indicate that earth dams on the territory Moscow city, run for more than 65 years, are in poor condition and need of major repair.

Conclusions

1. Quantitative methods of system analysis (pulse process, method for constructing classification scales, method of cluster analysis) are applied in this report to assess the finite lifetime of small earth dams on urban area. All of the applied methods converged through a value of 75 years for the finite lifetime.

2. The estimated value allows defining robustness of earth dam and can be used as a criterion for safety management of earth dams, defining the needs to undertake actions to improve, during the life cycle, earth dams structural features. In case of excess of design life over T_f is recommended to conduct technical examination of a dam and to make decision on further maintenance. At approach of the real time of maintenance to T_f it is recommended to take additional measures for safety in order to increase stability of a dam to the influence of climatic and technogenic factors. One of such actions is the assessment of stability of a dam to biological, physicochemical and mechanical types of water impact.

3. Like any other method, the approach has its own limitations. Firstly it is the exclusion of natural impacts and other loadings from the settlement model, secondly, the use of expert method for the estimation of weights. On the other hand, considered settlement model can be extended to the excluded loadings and calculated in accordance with the proposed approach. In the settlement model can be used real data of water impact forms on earth dam.

4. Maintenance of earth dams constantly has to adapt for changing conditions during life cycle and must be under strict monitoring of both the operating organization and the state, to ensure public safety. The definition for T_f, and its quantitative assessment, would undoubtedly represent an important step ahead in practical management issues.

References

1. ICOLD Bulletin on Dam Safety Management [Online]. URL: http://www.icold-cigb.org (date of application: 01.10.2016).
2. WCD. Dams and Development. A New Framework for Decision-making. London, 2000. 404 p.
3. Pisaniello J.D., McKay J.M. A farmer-friendly dam safety evaluation procedure as a key part of modern Australian water laws. *Water International.* 2003. No. 28. Pp. 93–102.
4. Stephens T. *Manual on Small Earth Dams: Guide to Siting, Design and Construction.* Rome, 2010. 124 p.
5. *Guidance for Dam Engineering Assessment DOW 3.1.4.* 2011 [Online]. Systems requirements: Adobe Acrobat Reader. URL: http://www.dec.ny.gov/docs/water_pdf/damfengarpt.pdf (date of application: 01.10.2016).
6. Poff N.L., Hart D.D. How dams vary and why it matters for the emerging science of dam removal. *BioScience.* 2002. No. 8(52). Pp. 659–668.
7. Wieland M. *Life-span of Storage Dams* [Online]. URL: http://www.waterpowermagazine.com/features/featurelife-span-of-storage-dams (date of application: 01.10.2016).
8. Sadzeviciusa R., Damuleviciusb V., Skominasa R. The technical state of earth dams in Lithuania. *Journal of Environmental Engineering and Landscape Management.* 2013. No. 3(21). Pp. 180–188.
9. He X.Y., Wang Z.Y., Huang J.C. Temporal and spatial distribution of dam failure events in China. *International Journal of Sediment Research.* 2008. No. 4(23). Pp. 398–405.
10. Sun Y., Chang H., Miao Z., Zhong D. Solution method of overtopping risk model for earth dams. *Safety Science.* 2012. No. 9(50). Pp. 1906–1912.
11. Brown A.J., Gosden J.D. *Defra Interim Guide to Quantitative Risk Assessment for UK Reservoirs.* London, 2004. 161 p.
12. Fan Z.-W., Jiang S.-H., Zhang M. Dynamic probability evaluation of safety levels of earth-rockfill dams using bayesian approach. *Water Science and Engineering*. 2009. No. 2(2). Pp. 61–70.
13. Su H., Wen Z., Hu J., Wu Z. Evaluation model for service life of dam based on time-varying risk probability. Science in China, Series E: Technological Sciences. 2009. No. 7(52). Pp. 1966–1973.
14. Cloete G.C., Retief J.V., Viljoen C. A rational quantitative optimal approach to dam safety risk reduction. Civil Engineering and Environmental Systems. 2016. No. 2(33). Pp. 85–105.
15. Mirtckhulava Tc.E. Podhody k ocenke mery starenija dlitel'no jekspluatiruemyh plotin [Approaches to the measures assessment of the ageing long-term operating dams]. *Gidrotehnicheskoe Stroitel'stvo.* 2008. No. 6. Pp. 41–49. (rus)
16. Peyras L., Royet P., Boissier D. Dam ageing diagnosis and risk analysis: development of methods to support expert judgment. *Canadian Geotechnical Journal.* 2006. No. 2(43). Pp. 169–186.
17. Lin H.C., Hong Y.M., Kan Y.C., Sung W.P. An efficient risk assessment model for structure safety of aged dam. *Disaster Advances.* 2012. No. 4(5). Pp. 410–416.
18. Pimenta L., Caldeira L., Maranha das Neves E. A new qualitative method for the condition assessment of earth and rockfill dams. Structure and Infrastructure Engineering: Maintenance, Management, Life-cycle Design and Performance. 2013. No. 9(11). Pp. 1103–1117.
19. Mafioleti T.R., Neto A.C., Luiz J.P., Júnior A.T. A proposal for probabilistic analysis of stability of earth dams based on first order reliability method. International Journal of Engineering and Applied Sciences. 2016. No. 8(1). Pp. 1–8.
20. Mohan K. J., Kumar R. P. Earthquakes and dams in India: an overview. *International Journal of Civil Engineering and*

Литература

1. ICOLD Bulletin on Dam Safety Management [Электронный ресурс]. URL: http://www.icold-cigb.org (дата обращения: 01.10.2016).
2. WCD. Dams and Development. A New Framework for Decision-making. London, 2000. 404 p.
3. Pisaniello J.D., McKay J.M. A farmer-friendly dam safety evaluation procedure as a key part of modern Australian water laws // Water International. 2003. № 28. Pp. 93–102.
4. Stephens T. Manual on Small Earth Dams: Guide to Siting, Design and Construction. Rome, 2010. 124 p.
5. Guidance for Dam Engineering Assessment DOW 3.1.4. 2011 [Электронный ресурс]. Сист.требования: Adobe Acrobat Reader. URL: http://www.dec.ny.gov/docs/water_pdf/damfengarpt.pdf (дата обращения: 01.10.2016).
6. Poff N.L., Hart D.D. How dams vary and why it matters for the emerging science of dam removal // BioScience. 2002. № 8(52). Pp. 659–668.
7. Wieland M. Life-span of Storage Dams [Электронный ресурс]. URL: http://www.waterpowermagazine.com/features/featurelife-span-of-storage-dams (дата обращения: 01.10.2016).
8. Sadzeviciusa R., Damuleviciusb V., Skominasa R. The technical state of earth dams in Lithuania // Journal of Environmental Engineering and Landscape Management. 2013. № 21(3). Pp.180–188.
9. He X.Y., Wang Z.Y., Huang J.C. Temporal and spatial distribution of dam failure events in China // International Journal of Sediment Research. 2008. № 4(23). Pp. 398–405.
10. Sun Y., Chang H., Miao Z., Zhong D. Solution method of overtopping risk model for earth dams // Safety Science. 2012. № 9(50). Pp. 1906–1912.
11. Brown A.J., Gosden J.D. Defra Interim Guide to Quantitative Risk Assessment for UK Reservoirs. London, 2004. 161 p.
12. Fan Z.-W., Jiang S.-H., Zhang M. Dynamic probability evaluation of safety levels of earth-rockfill dams using bayesian approach // Water Science and Engineering. 2009. № 2(2). Pp. 61–70.
13. Su H., Wen Z., Hu J., Wu Z. Evaluation model for service life of dam based on time-varying risk probability // Science in China, Series E: Technological Sciences. 2009. № 7(52). Pp. 1966–1973.
14. Cloete G.C., Retief J.V., Viljoen C. A rational quantitative optimal approach to dam safety risk reduction // Civil Engineering and Environmental Systems. 2016. № 2(33). Pp. 85–105.
15. Мирцхулава Ц.Е. Подходы к оценке меры старения длительно эксплуатируемых плотин // Гидротехническое строительство. 2008. № 6. С. 41–49.
16. Peyras L., Royet P., Boissier D. Dam ageing diagnosis and risk analysis: development of methods to support expert judgment // Canadian Geotechnical Journal. 2006. № 2(43). Pp. 169–186.
17. Lin H.C., Hong Y.M., Kan Y.C., Sung W.P. An efficient risk assessment model for structure safety of aged dam // Disaster Advances. 2012. № 4(5). Pp.410–416.
18. Pimenta L., Caldeira L., Maranha das Neves E. A new qualitative method for the condition assessment of earth and rockfill dams // Structure and Infrastructure Engineering: Maintenance, Management, Life-cycle Design and Performance. 2013. № 9(11). Pp. 1103–1117.
19. Mafioleti T. R., Neto A. C., Luiz J. P., Júnior A. T. A proposal for probabilistic analysis of stability of earth dams based on first order reliability method // International Journal of Engineering and Applied Sciences. 2016. № 1(8). Pp. 1–8.
20. Mohan K. J., Kumar R. P. Earthquakes and dams in India: an overview // International Journal of Civil Engineering and

Technology. 2013. No. 4(6). Pp. 101–115.

21. Fell R., Bowles D.S., Anderson L.R., Bell G. The status of methods for estimation of the probability of failure of dams for use in quantitative risk assessment. *Conference on Dams.* Jindabyne: Australian national committee on large dams, 1999. Pp. 213–235.
22. De Silva L.I.N., Premkumar S. *Framework for the Estimation of Overall Probability of Dam Failure of Ancient Earth Dams in Sri Lanka* [Online]. Systems requirements: Adobe Acrobat Reader. URL: http://www.civil.mrt.ac.lk/conference/raghu/18.pdf (cited 01.10.2016).
23. *Dam failures – Statistical Analysis.* Bull. No. 99. Paris: ICOLD, 1995. 200 p.
24. Radchenko S.V. Prichiny povrezhdenij i avarij gruntovyh plotin (po dannym SIGB) [The causes of injuries and accidents on soil dams (according to ICOLD)]. *Proceeding of the VNIIG.* 2010. No. 258. Pp. 99–113. (rus)
25. Bellendir E.N., Sol'skij S.V., Nikitina N.Ja. Metodicheskie osnovy, analiz i ocenka avarij gruntovyh plotin v Rossijskoj Federacii [Methodological principles, analysis and risk assessment of accidents on earth dams in the Russian Federation]. *Proceeding of the VNIIG.* 2000. No. 238. Pp. 15–19. (rus)
26. Foster M., Fell R., Spannagle M. The statistics of embankment dam failures and accidents. Canadian Geotechnical Journal. 2000. No. 5(37). Pp. 1000–1024.
27. Zhanga L.M., Xua Y., Jiab J.S. Analysis of earth dam failures: a database approach. *Georisk: Assessment and Management of Risk for Engineered Systems and Geohazards.* 2009. No. 3(3). Pp. 184–189.
28. Bang-Jensen J., Gutin G. *Digraphs Theory, Algorithms and Applications.* Springer-Verlag. 2007. 754 p.
29. De Leon-Calio G., Kuo Y. Signed digraphs and their applications. *Soochow Journal of Mathematics.* 2003. No. 1(29). Pp. 69–81.
30. Gvozdev V.E., Shagiakhmetov A.M. Hazard ranking for industrial areas. *Air Pollution in the Ural Mountains.* 1998. No. 40. Pp. 355–356.
31. Altunin V.I., Volkov V.I., Kaganov G.M., Chernyh O.N. *Rezul'taty monitoringa sostojanija gidrotehnicheskih sooruzhenij g. Moskvy* [The results of monitoring the condition of hydraulic engineering structures Moscow city] [Online]. Systems requirements: Microsoft Word. URL: http://ieek.timacad.ru/science/ht/10/2004/04_2/2.7.doc (date of application: 01.10.2016). (rus)
32. Kaganov G.M., Volkov V.I. Sostojanie beshozjajnyh gidrotehnicheskih sooruzhenij Moskovskoj oblasti [The state of the hydrotechnical structures of the Moscow area which do not have owners]. *Prirodoobustrojstvo.* 2008. No. 2. Pp. 67–74. (rus)

Technology. 2013. № 4(6). Pp. 101–115.

21. Fell R., Bowles D.S., Anderson L.R., Bell G. The status of methods for estimation of the probability of failure of dams for use in quantitative risk assessment // Conference on Dams. Jindabyne, Australia, 1999. Pp. 213–235.
22. De Silva L.I.N., Premkumar S. Framework for the Estimation of Overall Probability of Dam Failure of Ancient Earth Dams in Sri Lanka [Электронный ресурс]. Сист. требования: Adobe Acrobat Reader. URL: http://www.civil.mrt.ac.lk/conference/raghu/18.pdf (дата обращения: 01.10.2016).
23. Dam Failures – Statistical Analysis. Bull. № 99. Paris: ICOLD, 1995. 200 p.
24. Радченко С.В. Причины повреждений и аварий грунтовых плотин (по данным СИГБ) // Известия ВНИИГ им. Б.Е. Веденеева. 2010. № 258. С. 99–113.
25. Беллендир Е.Н., Сольский С.В., Никитина Н.Я. Методические основы, анализ и оценка аварий грунтовых плотин в Российской Федерации // Известия ВНИИГ им. Б.Е. Веденеева. 2000. № 238. С. 15–19.
26. Foster M., Fell R., Spannagle M. The statistics of embankment dam failures and accidents // Canadian Geotechnical Journal. 2000. № 5(37). Pp. 1000–1024.
27. Zhanga L.M., Xua Y., Jiab J.S. Analysis of earth dam failures: a database approach // Georisk: Assessment and Management of Risk for Engineered Systems and Geohazards. 2009. № 3(3). Pp. 184–189.
28. Bang-Jensen J., Gutin G. Digraphs Theory, Algorithms and Applications. Springer-Verlag. 2007. 754 p.
29. De Leon-Calio G., Kuo Y. Signed digraphs and their applications // Soochow Journal of Mathematics. 2003. № 1(29). Pp. 69–81.
30. Gvozdev V.E., Shagiakhmetov A.M. Hazard ranking for industrial areas // Air Pollution in the Ural Mountains.1998. № 40. Pp. 355–356.
31. Алтунин В.И., Волков В.И., Каганов Г.М., Черных О.Н. Результаты мониторинга состояния гидротехнических сооружений г. Москвы [Электронный ресурс]. Систем. требования: Microsoft Word. URL: http://ieek.timacad.ru/science/ht/10/2004/04_2/2.7.doc (дата обращения 01.10.2016).
32. Каганов Г.М., Волков В.И. Состояние бесхозяйных гидротехнических сооружений Московской области // Природообустройство. 2008. № 2. С. 67–74.

Tamila Titova,
+7(812)3102533; titova@pgups.ru

Antonia Longobardi,
+3(908)9963408; alongobardi@unisa.it

Rasul Akhtyamov,
+7(931)5327321; ahtamov_zchs@mail.ru

Elina Nasyrova,
+7(962)5252772; ElinaSagitovna@yandex.ru

Тамила Семеновна Титова,
+7(812)3102533; эл. почта: titova@pgups.ru

Антония Лонгобарди,
+3(908)9963408; эл. почта: alongobardi@unisa.it

Расул Гумерович Ахтямов,
+7(931)5327321;
эл. почта: ahtamov_zchs@mail.ru

Элина Сагитовна Насырова,
+7(962)5252772;
эл. почта: ElinaSagitovna@yandex.ru

Титова Т.С., Лонгобарди А., Ахтямов Р.Г., Насырова Э.С. Срок эксплуатации грунтовых плотин // Инженерно-строительный журнал. 2017. № 1(69). С. 34–43.

doi: 10.18720/MCE.69.4

Stress-strain state and performance of a high rockfill dam with a grout curtain

Напряжённо-деформированное состояние и работоспособность высокой грунтовой плотины с инъекционной завесой

M.P. Sainov,
F.V. Kotov,
National Research Moscow State Civil Engineering University, Moscow, Russia

Канд. техн. наук, доцент М.П. Саинов,
аспирант Ф.В. Котов,
Национальный исследовательский Московский государственный строительный университет, г. Москва, Россия

Key words: cementing; grout curtain; rockfill dam; cemented soil; deformation modulus; stress-strain state

Ключевые слова: цементация; инъекционная завеса; каменно-набросная плотина; зацементированный грунт; модуль деформации; напряжённо-деформированное состояние

Abstract. This paper examines the results of numerical simulation of the stress-strain state (SSS) in a rockfill dam 235 m tall, with a massive three-tier grout curtain used as the impervious element. Calculations were done for multiple scenarios that reflected the wide range of possible changes of the modulus of deformation for the filler rock and cemented soil (200 MPa to 5000 MPa). The author’s original computation program was used in order to consider the elastoplastic behavior of soil. It was discovered that a super-tall dam with a vertical rigid impervious element features an adverse SSS: the hydrostatic pressure in the head reach gives creates a sliding wedge in the upper retaining prism. As the dam has rigid structure, this causes marginal state zones in the filler rock. Only when deforming ability of the filler rock is very low (deformation modulus above 300 MPa), the dam’s SSS may be acceptable. Strength characteristics of the grout curtain were evaluated based on stresses that emerge after it is created. The SSS of the grout curtain is mainly described by bending strains. In case of low deforming ability of the screen material, this can give rise to fissures in the screen material where it contacts the bedrock base. Strength and water impermeability of the grout curtain are secured only after bentonite-cement slurry is injected to make the deforming ability of the screen material and filler rock comparable.

Аннотация. В статье рассматриваются результаты численного моделирования напряжённо-деформированного состояния (НДС) каменно-набросной плотины высотой 235 м, в которой противофильтрационным элементом является массивная инъекционная завеса, выполненная в три яруса. Расчёты проводились для нескольких вариантов, отражавших широкий диапазон возможного изменения модулей деформации каменной наброски и зацементированного грунта (от 200 МПа до 5000 МПа). Использовалась разработанная автором вычислительная программа, что позволило учесть упругопластический характер поведения грунтов. Было получено, что сверхвысокая плотина с вертикальным жёстким противофильтрационным элементом имеет неблагоприятное НДС – гидростатическое давление верхнего бьефа вызывает в верховой упорной призме образование призмы обрушения. Наличие в плотине жёсткой конструкции приводит к образованию в каменной наброске зон предельного состояния. Только при очень низкой деформируемости каменной наброски (модуль деформации свыше 300 МПа), НДС плотины может оказаться приемлемым. Оценка прочностного состояния инъекционной завесы проводилась по тем напряжениям, которые возникают с момента времени её создания. НДС инъекционной завесы в основном определяется деформациями изгиба. При низкой деформируемости материала завесы они могут привести к образованию трещин в материале завесы и на её контакте со скальным основанием. Только при применении для инъекции бентонито-цементных растворов, при которых деформируемость материала завесы и каменной

наброски становятся сопоставимыми друг с другом, прочность и водонепроницаемость инъекционной завесы будут обеспечены.

Introduction

Grout curtains are a widely used type of an impervious device at the dam base. They are built by injecting cement and cement-clayey slurries into the pores and fissures of soil. Most frequently, grout curtains are constructed on bedrock base – virtually each tall dam has a cement-grout screen built at its foot [1-6]. Grout curtains are used less often in earthen dams, because soils tend to have hollows, and much greater quantities of slurry have to be injected of fill in the pores. Nevertheless, building a grout curtain in an earthen base frequently is the only possible dam construction option: when the base is composed of large-grain soils at a considerable depth. Numerous dams with grout curtains built into an earthen base exist around the world. A large grout curtain in an earthen base was first used in France in 1954-56 to build the Serre-Ponçon dam [7].

The grout curtain as impervious element has an advantage that it can be built not only at the base but also inside the body of the earthen dam. Quite frequently, the grout curtain built at the foot continues into the lower section of the dam. Construction Regulation SP 39.13330.2012[1] places such dams into the class of combination impervious element dams. As an illustration of such construction design, one may refer to the dams of Atbashi [8], Maina [9], Aswan [10], and the dam of Kambarata HPP-2 [11]. In one case – the Orto-Tokoy dam in Kyrgyz Republic – a grout curtain was built to the full height of the dam [12].

In the light of those experiences, one can regard the grout curtain as an advanced type of impervious design of an earthen dam. This is particularly relevant for construction of super-tall earthen dams, where selection of reliable design of non-soil impervious element still remains an unsolved issue. This paper examines possible construction of a super-tall earthen dam with an injection-built core. Review of science literature demonstrates that performance of a dam with an injected impervious screen had never been researched before.

Our study considered a dam 235 m tall, standing on a bedrock base (Fig.1). The design of the dam included retaining prisms of rock mass on the sides, while the central part of the dam is filled with sand-gravel mix, then cement and bentonite-cement slurry is injected into the center to form a grout curtain. It was assumed that the top of the bedrock base is cemented to strengthen it. Such a dam could be used to build the Kankun HPP in South Yakutia.

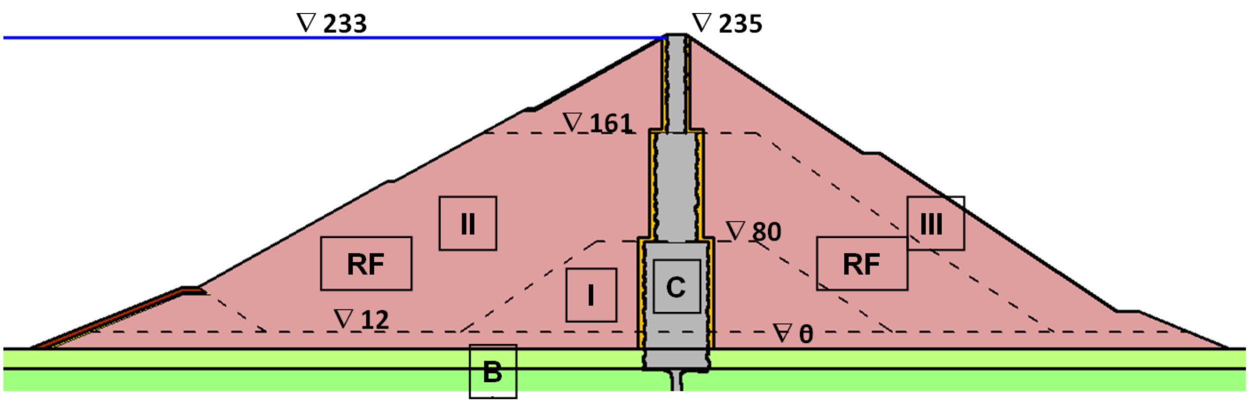

Figure 1. Design of rockfill dam with an anti-seepage element as grout curtain.
C – grout curtain, RF – rock fill, B – bedrock base, I, II, III – construction project phases

Considering the elevation of the dam, the study examined a 3-phase construction project. Each phase had elevations of 80, 161 and 235 m, respectively. It was assumed that the grout curtain was also to be built in three phases (tiers) – injection is done to full height of the construction phase, while soil is being filled in the next phase of the dam at the same time.

Thickness of the grout curtain was assumed different for each construction phase of the dam depending on the head it has to withstand, based on the condition of required filtration strength. This

[1]SP 39.13330.2012.Plotiny iz gruntovyh materialov.Aktualizirovannaj aredakcija SNiP 2.06.05-84* [Dams of soil materials.The updated edition of SNiP 2.06.05-84*].Ministerstvo regional'nogo razvitija.Moskva, 2012. – 86 p.

thickness was taken to be some 20% of the head, because Construction Regulation SP 23.13330.2011[2] regulates that to design grout curtains, the critical gradient of the head should be assumed 7.5 for gravel and shingle, and 6 for large-grain sands. Screen thickness was assumed to be 14 m for the dam at phase one, 31 m for phase two, and 48 m for phase three. Therefore, the grout curtain in question is a massive structure best described as an injection core rather than as a grout curtain – the term adopted in the civil construction regulations.

Research was to address the following assigned tasks:

- identifying the conditions of the grout curtain built inside the earthen dam, to know the zones where its strength can be compromised,
- identifying conditions of the embankment body with a massive rigid structure inside it,
- estimating performance of the design of a tall rockfill dam with a grout curtain, and preparation of recommendations on how to select the design of the earthen dam with an impervious grout curtain to ensure its performance.

Methods

Research was conducted by numerical simulation of stress-strain state (SSS) of the dam using the finite-element method, assisted with Nds_N software application developed by the author [13]. The structure and mass of the bedrock base were divided into a grid of 1,065 finite elements, whereof 121 finite elements were contact elements that modeled possible manifestation of non-linear effects on contacts with different materials (such as detachment, slip, etc.). Contact elements were introduced where the grout curtain contacted the dam body soil, bedrock base, and different phases/tiers of the grout curtain.

All finite elements had quadratic settlements approximation, thus producing more regular distribution of stress and deformation in them. The digital model of the structure featured 5,990 degrees of freedom.

The process of building the grout curtain in the dam was simulated by substituting the properties of the material in its location: the properties of normal soil were substituted with those of injection-strengthened soil. Parameters that described strength characteristics of the area were zeroed out as though this was a newly emerged structure, but the original SSS of the area remained without change.

To address the tasks, we researched how the deforming properties of the filler rock and the grout curtain influenced the dam's SSS.

To simulate performance of the filler rock in the dam, we used two elastoplastic models of soils. One soil model was proposed by Prof. L.N. Rasskazov [14] and modified by M.P. Sainov [15]. It can register plastic, rheological and dilatant properties of soils. The other model was based on the Mohr–Coulomb strength theory, which assumed the soil deformation modulus in the active load area to remain the same regardless the strength condition of the soil.

Both models considered differences in soil deforming ability when actively loads were received and lifted. It was assumed that soil deformation modules off-load were 5 the level registered under active load. In order to delimit the load trajectories, the research used simple conditions based on analysis of changes in the soil condition being loaded. It was assumed that active loading is a fact, if:

- average stress σ is rising,
- greatest shift stresses T are growing,
- as σ and T are decreasing simultaneously, stresses T decrease slower than they grew at the previous loading stages.

This approach generally corresponds to that of the plasticity theory, which calls for location analysis of so-called loading surfaces [12].

We examined three scenarios of deformed properties of the rock fill. Deforming ability parameters of the rock fill in scenario A were found by this author [15] based on processed results of experimental research by Marsal [16] and Gupta [17], and then adjusted to consider field survey data on construction settlement of rockfill dams [18,19]. Converted to the linear-deformation environment model, scenario A

[2]SP 23.13330.2011.Osnovanija gidrotehnicheskih sooruzhenij.Aktualizirovannaja redakcija SNiP 2.02.05-84 [Bases of hydraulic structures. SNiP 2.02.05-84Updated edition]. Ministerstvo regional'nogo razvitija.Moskva, 2011.– 111p.

Sainov M.P., Kotov F.V. Stress-strain state and performance of a high rockfill dam with a grout curtain. *Magazine of Civil Engineering*. 2017. No. 1. Pp. 44–55. doi: 10.18720/MCE.69.4

for the dam in question corresponds to the deformation module of E = 85 MPa (for Poisson's ratio ν = 0.25).

In scenario B, the deforming ability of rock fill was halved (E = 170 MPa), and divided by 4 in scenario C (E = 340 MPa). This interval of rock fill deforming ability corresponds to the dispersion of values observed in real-life dams [20].

The deforming ability of soil in the central zone was assumed permanent in all scenarios: its deformation modulus was approximately 50 MPa.

Material of the grout curtain for computations was assumed to be elastic, with deformation modulus E and Poisson's ratio ν assigned. Computation examined multiple scenarios of deformation behavior of injected sand-gravel, covering a deformation modulus in a very broad range. The reason is that by now, deformation behavior of soils strengthened by injecting cement and cement-clayey slurries is unknown: their properties can only be inferred by the properties of similar materials.

Firstly, there are data from experimental research of the properties of soil-cements – soil mixed with cement or cement slurry [21–25]. In [26], these writers processed the data from traxial tests of sand-cement done by Dr. Amanullah Marri [27]. It was found that if 5÷10% cement is added to sand, its deforming ability is only reduced by 2÷3 times. The modulus of cemented sand was 250 to 1300 MPa depending on content of cement (5÷10 %) and swaging pressure (0 to 10 MPa).

Secondly, data are available about deforming ability of the material known as CSG (cement-sand-gravel), super-lean rolled compacted concrete [28]. Its estimated deformation modulus is 5000-10000 MPa.

However, information on the deforming ability of soil-cements cannot fully qualify as injection-strengthened soils due to differences in the technology used to produce cemented material. To make soil-cements and rolled compacted concretes, cement is mixed with the aggregate before concrete is poured into the dam, and then must also be thoroughly condensed.

Conditions of grouting are rather similar to those used to prepare super-lean rolled compacted concrete – slurry-cemented rock. This is another type of cement-soil mix. The material was researched by A.S. Bestuzheva [29, 30], who discovered its deformation modulus to be around 2,000 MPa.

Thirdly, one can use information about the properties of soils secured by the jet grouting method. Still one must bear in mind that the jet grouting technology of soil strengthening differs from the conventional method. In jet grouting, the jet of slurry or water served at high pressure (35÷45 MPa for cement slurry, and 5÷8 MPa for water) erodes the foundation, then the resulting hollows are filled with the slurry [31]. Information about experimental research of sand samples strengthened in field conditions by the jet grouting method is available in [32]. According to this, compressive resistance of strengthened soil varies from 5 to 22 MPa, with deformation modulus from 1000 to 4500 MPa. However, such excellent performance requires a lot of cement, with needed 500 to 1,100 kg of cement per 1 m^3 of strengthened soil. Less cement is necessary to create grout curtains in large-debris soils. To quote [31], the strength of sand-gravel soil after jet grouting was approximately 5 MPa with cement consumption rate of 150 kg per 1 m^3. No data is available on deformation modulus of such soil.

The above research data on the properties of cemented soil are mere approximations, because injection-strengthened soils differ. The fundamental difference of the latter is that the composition of injected slurries typically contains bentonite or other similar clayey material in addition to pure cement. Cement-bentonite or bentonite-cement slurries are used for injection. Presence of bentonite reduces the deforming ability and strength of processed soils.

In Table 1, we quote the composition of the slurries that were used to build the grout curtains for the dams of Atbashinskaya and Mainaskaya HPP [8, 9]. Analysis demonstrated that bentonite-cement slurry could contain between 15 and 60 % of bentonite.

Table 1. Information on materials consumption to build grout curtains

Dams	Injection slurry structure			Slurry density, ton/m³	Consumption per 1 m³ of soil		
	Cement, kg	Bentonite, kg	Water, kg		slurry, m³	solid matter, kg	cement, kg
Atbashinskaya	350–475	82–59	826–852	1.29–1.36	0.26	181	110–160
Mainskaya	100	140–110	920–930	1.16–1.14	0.42–0.60	200–240	85–110
	400	120–100	826–830	1.33			150–190
	600–500	160–120	750–800	1.5–1.42			140–220

Calculations demonstrated that to build 1 m³ of strengthened soil, one needs 80 to 220 kg of cement, and 25 to 140 kg of bentonite.

Apparently, injection-strengthened soil is closer to clay-cement concrete rather than soil-cement or rolled compacted concrete, but it is weaker and more prone to deformations due to insufficient stirring. As properties of clay-cement concretes can vary over a broad range of values depending on cement content ratio [33], we examined a broad range of soil properties in a grout curtain. The three scenarios for properties of grout curtain material were:

- scenario 1 – E=5000 MPa, ν=0.22,
- scenario 2 – E=1000 MPa, ν=0.25,
- scenario 3 – E=200 MPa, ν=0.30.

It can be said that in scenario 1 soil pores are filled with cement slurry (by jet grouting), while scenario 2 uses injection of cement-bentonite slurry, and scenario 3 uses bentonite-cement slurry. According to [32] and [33], strength of cement (cement-clayey) rock resisting single-action compression was assumed to be around 20 MPa, 5 MPa and 2 MPa respectively for scenarios 1, 2 and 3.

We have examined 9 computing scenarios, each with different deformation properties of filler rock and the grout curtain material. The numeration for the scenarios was dual (e.g., scenario 1A, 2C, etc.).

Calculations addressed own-weight loads of soil and hydrostatic pressure on impervious elements.

It was found that SSS for a tall earthen dam with a massive and rigid impervious element was rather complex and adverse, featuring marginal state zones that develop in the dam soil. Among the causes underlying the adverse SSS of the dam is the abrupt difference in the deforming ability between the soil of retaining prisms and the cemented material of the grout curtain. As the dam carries its own weight, retaining prisms are suspended on the rigid grout curtain, while substantial tangential stress arises at their contact point. In the top and middle tiers of the dam, where such tangential stress is not too high, calculations showed that shear strength of soil was compromised, and as a result the retaining prisms tended to slip relative to the grout curtain.

Adverse SSS of the dam body particularly emerges on the borderlines of construction phases, where there are changes in thickness of the grout curtain. Failure zones emerge here, but not on the boundary of prisms and the screen, but inside the body of the soil embankment proper. They are caused by irregular deformations: one part of the embankment can settle freely; while settlement of the other in the bottom tier of the screen is limited. This compromises strength of the soil resisting shear and strain. It can be concluded that use of a staggered profile in the multi-tier grout curtain is undesirable, and one should seek smooth outlines of the impervious element.

As the reservoir is filled, processes of strength failures emerging in the body of the earthen embankment get more intense. Driven by hydrostatic pressure, the earthen embankment shifts towards the tail reach (Fig. 2, 3). Because the dam is very tall, settlements are considerable. In Series A scenarios, greatest core settlements amount to 238÷268 cm respectively. Such settlements in the top prism creates a sliding wedge, even as the top prism slides along the vertical pressure face of the impervious element, because lack of compressive stress σ_x reduces soil resistance to shear dramatically. Due to the resulting sliding wedge, the top of the dam's ridge settles by more than 1 meter in Series A scenarios.

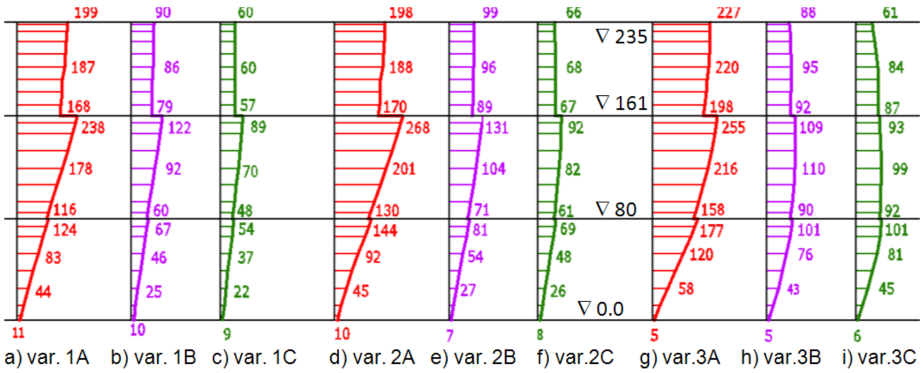

Figure 2. Grout curtain settlements (cm) in various scenarios (estimated using the soil model by prof. L.N. Rasskazov)

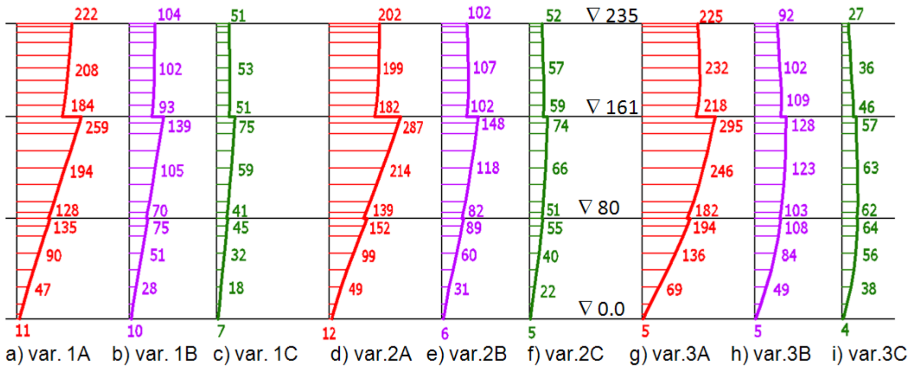

Figure 3. Grout curtain settlements (cm) in various scenarios (estimated using the Coulomb-Mohr soil model)

A sliding wedge also emerges in Series C scenarios, where greatest settlements of the grout curtain amount to some 100 cm (Figs. 2, 3); however, settlement of the top prism becomes less manifest. One can conclude that to ensure performance of a super-tall rockfill dam, very high consolidation of the filler rock is needed so that its modulus of deformation is at least 300 MPa.

Now let us consider SSS (stress-strain state) of the impervious element: the grout curtain. As we examine SSS of the grout curtain, we need to consider an important factor: stress in the cement rock, i.e. hardened mortar can develop stress only after injection is completed. Therefore, material of the grout curtain evidently should be correctly regarded as a compound of two components: rock skeleton and cement rock located in the hollows of the skeleton. Each component carries loads of different levels. Strength of the grout curtain should be evaluated based on stresses that exist only in the cement rock. To measure such stresses, we need to take total stresses borne by the grout curtain's material, and subtract from the figure the stresses borne by the soil before it is filled with injected slurry.

As an illustration, Figure 4 compares SSS of the grout curtain in scenario 1B for the case of total stress, and stresses existing in the cement rock. Obviously, differences are material in terms of strength analysis of the grout curtain. If we evaluate strength by stresses borne by injection-filled soil as a whole, then existence of stretching stresses registers only in the bottom tiers of the screen (Fig. 4a). And when we evaluate stresses borne only by the cement rock, we can find crack formation in all three tiers of the screen (Fig. 4b).

Figures 2, 3, 5, and 6 show stresses and settlements that emerge in the cement rock of the grout curtain, disregarding the stresses and settlements that existed in different tiers before the grout curtains are built. The settlements curves in Figures 2 and 3 have staggered shapes because each tier appeared at different points of time.

Analysis of SSS demonstrates that working conditions differ for each tier of the grout curtain. The top tier – the last one built – does not carry the dam's own weight, mainly having to withstand just hydrostatic pressure of water. This tear resists the bending force. The bottom and middle tiers, in addition to hydrostatic pressure, have to bear the dam's own weight, created by settling soil and then transferred with friction to the screen. Consequently, the bottom tier and the middle tier not only have to resist the bending force, but also the longitudinal compressing forces.

Bending deformations of the grout curtain are rather complex by nature. This work can be described as that of a console restrained in the rock base. The top and middle tiers bend towards the tail reach, and the lower tiers work towards the head reach. Thus, stretching vertical stress σ_y emerges in the lowest facet of the top tier, while the top tier has to resist compressing forces (Figs. 5, 6). In the middle tiers, the bend is faint, as possible stretching stresses are overcome by compressing longitudinal forces.

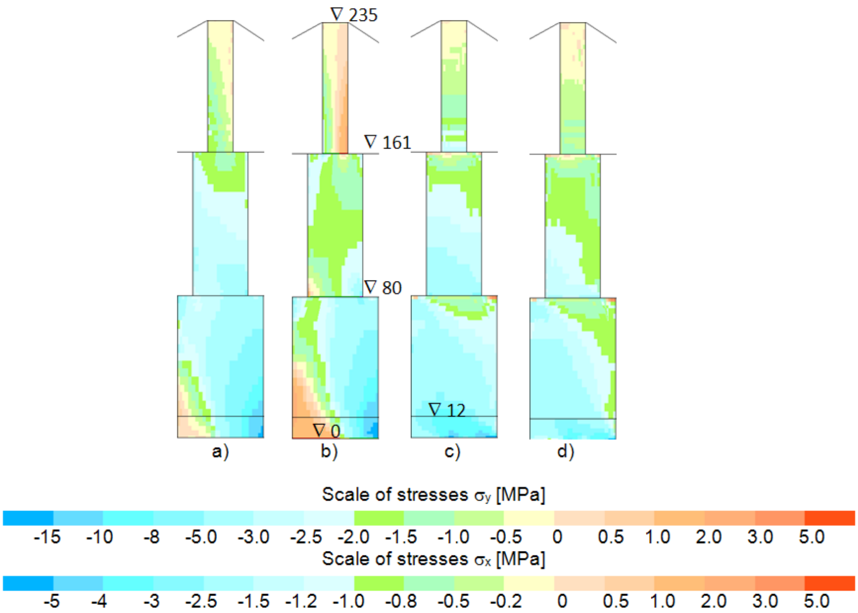

Figure 4. Comparing stresses (MPa) in the grout curtain for scenario 2C: a, b – σ_y, c, d – σ_x, a, c – total stresses borne by grout curtain material; b, d – stresses borne by cement rock.

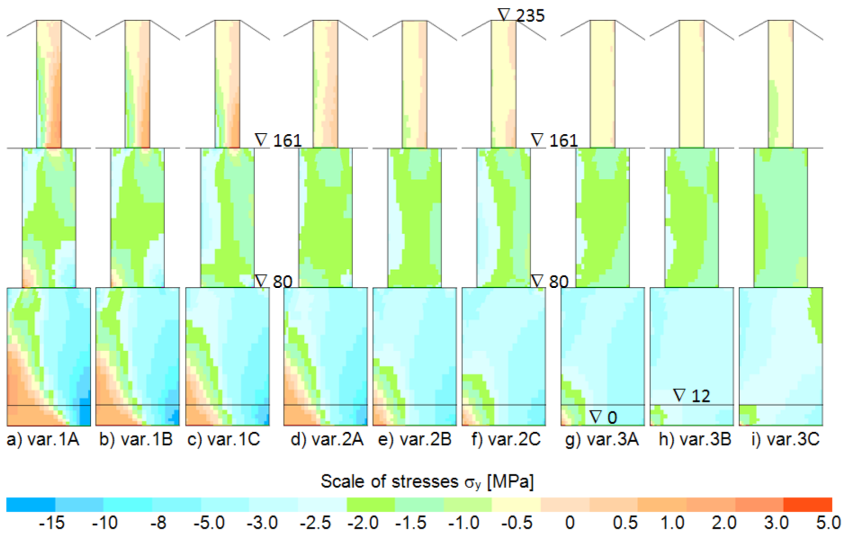

Fig. 5. Vertical stresses σy in the grout curtain, building up after construction and until the reservoir is filled with water (estimate based on soil model by Prof. L.N. Rasskazov)

The strongest bend deformations bear on the bottom tier of the screen. This occurs because its deformations are limited by the rigid bedrock that underlies it. Despite serious longitudinal compressing forces existing in the bottom tier, its top facet has a zone of stretching stresses σ_y.

Bend deformations are especially notable in the contact section, where the injection core contacts the bedrock. On the side, on the bottom facet in the contact section, there is a zone of concentrated compressing stresses σ_y, while at the top the contact seeks to open due to straining strength failure.

The above quality image of SSS of the grout curtain is typical for all estimation scenarios, and for any of the two soil models. Differences in the SSS for estimated scenarios are merely quantitative. The grout curtain has a more favorable SSS in the event of low deforming ability of filler rock and high deforming ability of the grout curtain material.

For scenarios, where the grout curtain is made of rigid material (Series 1 scenarios with high cement content), its SSS is extremely adverse under any option of deforming ability of filler rock (Fig. 5a–c, 6a–c). In the top and middle tiers, stretching stresses σ_y can be up to 2÷3 MPa, greater than the straining force in the cement rock. This force opens up the seam between the upper and middle tier from below. The middle tier is in better strained condition, it also may develop stretching stresses yet. In the lower tier, the material is prone to both compression and tension. In each Series 1 scenario, the contact seam opens to considerable length that can compromise the dam's reliable operation.

In scenarios that have the grout curtain made of a more pliant material (Series 2 scenarios with cement-bentonite slurry injected), SSS is much better, but still adverse (Fig. 5d–f, 5d–f). In many zones of the impervious element, the material is not strong enough to resist strength either compression or tension, and the contact seam opens rather wide. Only scenario 2C with failure zones of local sizes (Fig. 5f, 6f) can be considered as relatively robust.

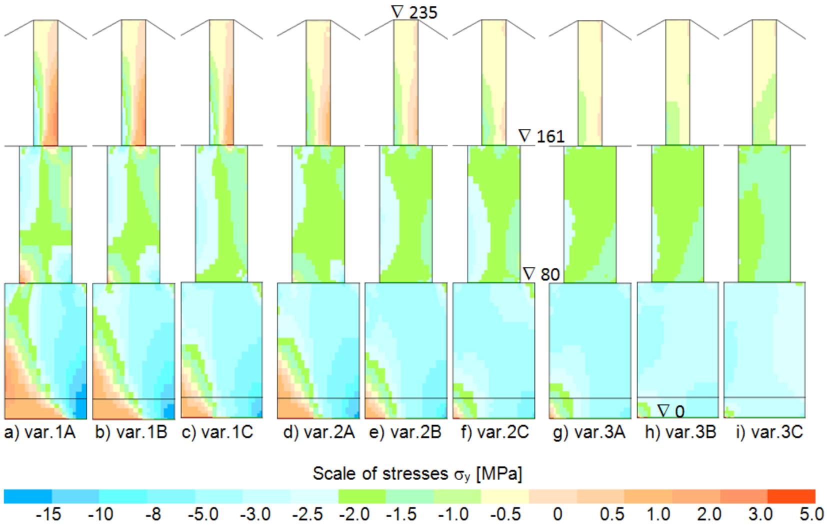

Figure 6. Vertical stresses σ_y in the grout curtain, building up after construction and until the reservoir is filled with water (estimate based on the Coulomb-Mohr soil model)

SSS of the grout curtain can be regarded favorable only when bentonite-cement slurry is injected (Series scenarios 3) (Fig. 5g–i, 6g–i). In these scenarios, no stretching stress emerges in the top and middle tiers, and compressing stresses roughly match the adopted material strength for single-axis compression. Given that strength of plastic materials rises along with lateral reduction, one may expect that compression strength is assured, because the screen's material withstands compression on every side all around. In most of the screen's bottom tier, compression and straining strength is in fact assured, yet singular zones exist where failures are possible. Scenarios 3B and 3C (Fig. 5h–i, 6h–i) can be regarded as usable, since their failure zones are local by size and cannot jeopardize the structure's integrity, and their contact seam only opens over an insignificant length. In these scenarios, the deforming ability of the grout curtain material roughly matches that of the filler rock.

Scenario 3A can be regarded as conditionally usable. In it, compressing stress σ_y of 2÷3 MPa embraces virtually the entire bottom tier of the core, and this level of stress is approximately equal to or greater than the strength of clay-cement rock withstanding single-axis compression (Fig. 5g, 6g). At the same time, strength can be assured, if the compression stress is considered.

Table 2. SSS of the grout curtain for estimated scenarios (based on Prof. L.N. Rasskazov soil model)

tier	value	scenarios								
		1A	1B	1C	2A	2B	2C	3A	3B	3C
top	max σ_y, MPa	3.3	2.4	2.6	1.0	0.7	0.9	0.1	0.02	0.0
	min σ_y, MPa	-3.7	-2.4	-3.5	-0.9	-0.9	-0.8	-0.4	-0.5	-1.0
middle	max σ_y, MPa	2.3	1.4	-0.5	-0.1	-1.1	-1.1	-1.2	-1.3	-0.8
	min σ_y, MPa	-8.1	-7.0	-5.1	-4.1	-2.5	-3.3	-2.3	-2.3	-1.9
bottom	max σ_y, MPa	3.3	2.3	2.1	2.1	1.4	1.3	1.7	0.8	0.7
	min σ_y, MPa	-54.4	-34.9	-29.4	-21.5	-14	-12.2	-6.0	-4.2	-4.0
contact	L, m	36	26.5	18	21	8	6	2,5	1	1
	P, mm	365	106	52	172	18	7.0	11.6	0.9	3.3

Note: L – opening length over contact between grout curtain and base,

P – greatest opening at contact between grout curtain and base.

Table 3. SSS of the grout curtain for estimated scenarios (based on Coulomb-Mohr soil model)

tier	value	scenarios								
		1A	1B	1C	2A	2B	2C	3A	3B	3C
top	max σ_y, MPa	4.4	3.3	2.5	1.7	1.1	0.5	0.2	0.06	0.04
	min σ_y, MPa	-6.5	-4.6	-3.6	-1.8	-1.5	-1.7	-1	-1.2	-1.2
middle	max σ_y, MPa	2.3	1.3	-0.9	0.3	-1.1	-0.9	-1.2	-1.2	-1.1
	min σ_y, MPa	-8.7	-6.9	-3.1	-5	-2.7	-2.9	-2.4	-2.4	-2.0
bottom	max σ_y, MPa	3.2	2.2	1.8	2.2	1.5	1.1	1.5	1.1	0.3
	min σ_y, MPa	-61.7	-41	-28.1	-24.9	-16.6	-12.1	-7.6	-5.3	-4.1
contact	L, m	38	29.5	18.5	21	12	4	2.5	2	1
	P, mm	424	151	43	194	42	9	24	3.3	1.0

Therefore, slurries with high bentonite content should be used to build grout curtains as this helps to bring the properties of manmade material's deforming ability close to soil in the dam body, thus resulting in better SSS. In addition, banked soil in the dam body needs to be better compacted to reduce its deforming ability. According to calculations, SSS of the grout curtain is favorable only where its material's deformation modulus is below or nearly the same as that of the soil in the dam body.

The study has also revealed the danger of fissures emerging in the grout curtain material as the dam is built, even before it is exposed to any hydrostatic force. The upper part of the screen's tier were discovered to develop stretching stresses σ_x that may cause vertical fissures in it. Such fissures can subsequently compromise water tightness of the impervious element. Stretching stresses σ_x in the upper part of the tier may emerge when the next phase of the dam is added on top of it. Under its own weight, the earthen embankment works to expand on both sides, but this is prevented by the rigid grout curtain. This however causes the upper part of the grout curtain's tier to stretch.

Greatest stretching stresses σ_x were observed on the tier edges, where they can exceed 2 MPa (Table 4). The zone in which the two tiers of the core are subsequently going to close have weaker stretching stresses σ_x at around 1 MPa. Such stresses are the same or greater than the stretching strength of cement rock, and so vertical fissures are quite probable. Stretching stress σ_x does not appear in scenarios 3A and 3B that use bentonite-cement slurry to build the grout curtain.

Table 4. Highest stretching stress σ_x (MPa) in bottom tier of the core being built

value	scenarios								
	1A	1B	1C	2A	2B	2C	3A	3B	3C
total maximum	2.3	2.4	2.0	2.1	2.0	1.4	0.5	0.1	-
maximum at contact with tier No. 2	1.1	1.2	1.0	1.0	0.9	0.7	0.9	-	-

Conclusions

1. Adverse SSS is typical for super-tall earthen dams with central impervious elements (vertical screens or cores). Hydrostatic pressure causes horizontal settlements in such dams, and they can be strong enough to create a collapsing soils in the upstream retaining prism. To ensure reliable operation of such dams, filler rock must be compacted very dense to achieve the deformation module of at least 300 MPa.

2. Working conditions for a massive impervious element such as a grout curtain are similar to those required for thin-wall impervious cores built using the diaphragm wall method. Its SSS is mainly the result of bending deformations, but also longitudinal compressing forces created by settling surrounding soil. Yet, unlike a thin-wall core, massive injection cores themselves can bear most of the hydrostatic load that acts on the dam. Besides, exposed to bending deformation, massive injection cores may develop serious stretching stresses that bring the risk of fissures with loss of water tightness in the impervious element.

3. Strength analysis of the grout curtain material is necessary for the part of stress that is applied to hardened mortar in pores of the injection-processed soil. These stressing forces emerge as soon as the grout curtain is built; they include the compressing stresses created in the injection-processed soil under its own weight. This is important because SSS of cement rock is more adverse than that of integral material of the grout curtain.

4. According to the estimate, SSS of the grout curtain will be favorable only when its material's deformation modulus is under 5 times that of the soil in the dam body, which in turn should be at least 200 MPa. To ensure reliable performance of the impervious screen, one needs, on the one hand to inject clayey-cement slurries that increase the deforming ability of the screen material, and on the other hand to try and reduce the deforming ability of filler rock by making it more dense.

5. While selecting the profile of the impervious element as a multi-tier grout curtain, one should not use the staggered or stepwise profile (with screen width changing abruptly), because this will cause irregular deformation of the dam body and may create strength failure zones in it.

6. The results of SSS estimated for earthen dams, produced using two soil models, are fairly close, particularly in terms of grout curtain SSS evaluation. First of all, this suggests accuracy of the results; and secondly, it demonstrates that in terms of SSS of manmade structures, the non-linear nature of soil deformation is not too critical to consider as the structure bears loads. To estimate SSS for earth structures, it is most important to correctly discriminate the deforming ability of soil actively loaded and unloaded.

References

1. Rasskazov L.N., Orekhov V.G., Aniskin N.A., Malakhanov V.V., Bestuzheva A.S., Sainov M.P., Soldatov P.V., Tolstikov V.V. *Gidrotekhnicheskiye sooruzheniya (rechnyye)* [Hydraulic Structures (River)]. Part 1. Moskva: ASV, 2008. 576p. (rus)
2. Argal E.S., Tuzhikhin G.G. Protivofiltratsionnyye ustroystva v osnovanii plotiny Bureyskogo gidrouzla (opyt proyektirovaniya i pervyye rezultaty proizvodstva rabot) [Counterseepage devices (CD) in the dam foundation of the Bureya hydraulic power system (HPS) (designing experience and first results of its realization)]. *Gidrotekhnicheskoye stroitelstvo.* 2001. No. 8. Pp. 14–21. (rus)
3. Argal E.S., Kudrin K.P., Tuzhikhin G.G. Opyt proizvodstva tsementatsionnykh rabot v osnovanii plotiny Bureyskoy GES [Experience of production of cement grouting (CG) into the dam foundation of the Bureya HPP]. *Gidrotekhnicheskoye stroitelstvo.* 2006. No. 9. Pp. 37–42. (rus)
4. Tuzhikhin G.G., Kolichko A.V. Tsementatsionnyye raboty na stroitelstve plotiny Kousar (Iran) [Grouting works during construction of the Kousar dam (Iran)].

Литература

1. Рассказов Л.Н., Орехов В.Г., Анискин Н.А., Малаханов В.В., Бестужева А.С., Саинов М.П., Солдатов П.В., Толстиков В.В. Гидротехнические сооружения (речные). Часть 1. Москва: АСВ, 576 с.
2. Аргал Э.С., Тужихин Г.Г. Противофильтрационные устройства в основании плотины Бурейского гидроузла (опыт проектирования и первые результаты производства работ) // Гидротехническое строительство. 2001. № 8. С.14–21.
3. Аргал Э.С., Кудрин К.П., Тужихин Г.Г. Опыт производства цементационных работ в основании плотины Бурейской ГЭС // Гидротехническое строительство. 2006. № 9. С. 37–42.
4. Тужихин Г.Г., Количко А.В. Цементационные работы на строительстве плотины Коусар (Иран) // Гидротехническое строительство. 2001. № 8. С. 22–25.
5. Aalianvari A. Optimum depth of grout curtain in accordance with seepage conditions (Sangtuda2- Dam&Hpp-Tajikistan) // 23rd International Mining Congress and Exhibition of Turkey, IMCET. 2013. № 3. Pp. 2029–2034.
6. Belicevic V., Knezevic D. Antifiltration grout curtain of hydro power plant Piva-Mratinje dam // Dam Maintenance and

Gidrotekhnicheskoye stroitelstvo. 2001. No. 8. Pp. 22–25. (rus)

5. Aalianvari A. Optimum depth of grout curtain in accordance with seepage conditions (Sangtuda2- Dam&Hpp-Tajikistan). *23rd International Mining Congress and Exhibition of Turkey, IMCET.* 2013. No. 3. Pp. 2029–2034.
6. Belicevic V., Knezevic D. Antifiltration grout curtain of hydro power plant Piva-Mratinje dam. *Dam Maintenance and Rehabilitation II – Proceedings of the 2nd International Congress on Dam Maintenance and Rehabilitation.* 2011. Pp. 415–424.
7. Bobrov R.I. Inyektsionnyye zavesy v neskalnykh porodakh [Grout Curtains in Petroglyphic Rock]. *Gidrotekhnicheskoye stroitelstvo*. 1963. No. 7. Pp. 47–56. (rus)
8. Loginov K.A., Kuznetsov V.V. Vozvedeniye inyektsionnogo yadra plotiny Atbashinskoy GES (Kirgizskaya SSR) [Erection of Atbashinsk Grout Dam Core in Kyrgyzstan]. *Gidrotekhnicheskoye stroitelstvo.* 1972. No. 12. Pp. 25–27. (rus)
9. Zhurkina N.N. Inyektsionnaya zavesa v osnovanii gruntovoy plotiny Maynskoy GES [Grout Curtains in Soil Dam Base of Mainskaya HPP]. *Gidrotekhnicheskoye stroitelstvo.* 1987. No. 11. Pp. 39–42.
10. Moiseyev S.N., Moiseyev I.S. *Kamenno-zemlyanyye plotiny. Osnovy proyektirovaniya i stroitelstvo* [Earth-rockfill dam. Basis of design and construction]. Moscow: Energiya. 1977. 281p. (rus)
11. Korchevskiy V.F., Obopol A.Yu. O proyektirovanii i stroitelstve Kambaratinskikh gidroelektrostantsiy na r.Naryne v Kirgizskoy Respublike [On the design and construction of the Kambarata hydropower stations on the Naryn river in Kyrgyzstan]. *Gidrotekhnicheskoye stroitelstvo*. 2012. No. 2. Pp. 2–12. (rus)
12. Goldin A.L., Rasskazov L.N. *Proyektirovaniye gruntovykh plotin* [Design of Soil Dams]. Moscow: Izd-vo ASV, 2001. 384p. (rus)
13. Sainov M.P. Vychislitelnaya programma po raschetu napryazhenno-deformirovannogo sostoyaniya gruntovykh plotin: opyt sozdaniya, metodiki i algoritmy [Computer Program for the Calculation of the Stress-strain State of Soil Dams: the Experience of Creation, Techniques and Algorithms]. *International Journal for Computational Civil and Structural Engineering*. 2013. No. 9(4). Pp. 208–225. (rus)
14. Rasskazov L.N., Dzhkha Dzh. Deformiruyemost i prochnost grunta pri raschete vysokikh gruntovykh plotin [Deformability and Strength of Soils in High Soil Dam Calculation]. *Gidrotekhnicheskoye stroitelstvo.* 1987. No. 7. Pp. 31–36. (rus)
15. Sainov M.P. Poluempiricheskaya formula dlya otsenki osadok odnorodnykh gruntovykh plotin [Semiempirical Formula for Assessment of homogeneous Earthfill Dams]. *Privolzhskiy nauchnyy zhurnal*. 2014. No. 4(32). Pp. 108–115
16. Marsal R.J. Large scale testing of rockfill materials. *Journal of the Soil Mechanics and Foundations Division, ASCE.* 1967. No. 93(2). Pp. 27–43.
17. Gupta A.K. Triaxial behaviour of rockfill materials. *Electronic Journal of Geotechnical Engineering.* 2009. Vol. 14. Pp. 1–18.
18. Park H.G., Kim Y.-S., Seo M.-W., Lim H.-D. Settlement behavior characteristics of CFRD in construction period. Case of Daegok Dam. *Journal of the KGS*. 2005. Vol. 21. No. 7. Pp. 91–105.
19. Sainov M.P. Otsenka deformiruemosti i prochnosti gruntov, zakreplennykh putem tsementatsii [Assessment of Deformation and Strength of Soils strengthened by Cementing]. Stroitel'stvo: nauka i obrazovanie. 2014. No. 3. Paper 1. (rus)
20. Marques Filho P., De Pinto N.L.S. CFRD dam characteristics learned from experience. *International Journal on Hydropower and Dams.* 2005. No. 12(1). Pp. 72–76
21. Abdulla A.A., Kiousis P.D. Behavior of cemented sands .1. Testing. *International Journal for Numerical and Analytical methods in Geomechanics*. 1997. No. 21(8). Pp. 533–547.

Rehabilitation II – Proceedings of the 2nd International Congress on Dam Maintenance and Rehabilitation. 2011. Pp. 415–424.

7. Бобров Р.И. Инъекционные завесы в нескальных породах // Гидротехническое строительство. 1963. № 7. С. 47–56.
8. Логинов К.А., Кузнецов В.В. Возведение инъекционного ядра плотины Атбашинской ГЭС (Киргизская ССР) // Гидротехническое строительство. 1972. № 12. С. 25–27.
9. Журкина Н.Н. Инъекционная завеса в основании грунтовой плотины Майнской ГЭС // Гидротехническое строительство. 1987. № 11. С. 39–42.
10. Моисеев С.Н., Моисеев И.С. Каменно-земляные плотины. Основы проектирования и строительство. М.: Энергия, 1977. 281 с.
11. Корчевский В.Ф., Обополь А.Ю. О проектировании и строительстве Камбаратинских гидроэлектростанций на р. Нарыне в Киргизской Республике // Гидротехническое строительство. 2012. № 2. С. 2–12.
12. Гольдин А.Л., Рассказов Л.Н. Проектирование грунтовых плотин. М.: Изд-во АСВ, 2001. 384 с.
13. Саинов М.П. Вычислительная программа по расчёту напряжённо-деформированного состояния грунтовых плотин: опыт создания, методики и алгоритмы // International Journal for Computational Civil and Structural Engineering. 2013. № 9(4). Pp. 208–225.
14. Рассказов Л.Н., Джха Дж. Деформируемость и прочность грунта при расчете высоких грунтовых плотин // Гидротехническое строительство. 1987. № 7. С. 31–36.
15. Саинов М.П. Полуэмпирическая формула для оценки осадок однородных грунтовых плотин // Приволжский научный журнал. 2014. № 4(32). С. 108–115.
16. Marsal, R.J. Large scale testing of rockfill materials // Journal of the Soil Mechanics and Foundations Division, ASCE. 1967. № 93(2). Pp. 27–43.
17. Gupta A.K. Triaxial behaviour of rockfill materials // Electronic Journal of Geotechnical Engineering. 2009. Vol. 14. Pp. 1–18.
18. Park H.G., Kim Y.-S., Seo M.-W., Lim H.-D. Settlement Behavior Characteristics of CFRD in Construction Period. Case of Daegok Dam // Journal of the KGS. 2005. Vol. 21. № 7. Pp. 91–105.
19. Саинов М.П. Параметры деформируемости крупнообломочных грунтов в теле грунтовых плотин // Строительство: наука и образование. 2014. № 2. Статья 2.
20. Marques Filho P., De Pinto N.L.S. CFRD dam characteristics learned from experience // International Journal on Hydropower and Dams. 2005. № 12(1). Pp. 72–76
21. Abdulla A.A., Kiousis P.D. Behaviour of cemented sands .1. Testing // International Journal for Numerical and Analytical methods in Geomechanics. 1997. № 21(8). Pp. 533–547.
22. Asghari E., Toll D.G., Haeri S.M. Triaxial behaviour of a cemented gravely sand, Tehran alluvium // Geotechnical and Geological Engineering. 2003. № 21(1). Pp. 1–28.
23. Haeri S.M., Hamidi A., Hosseini S.M., Asghari E., Toll D.G. Effect of cement type on the mechanical behaviour of a gravely sand // Geotechnical and Geological Engineering. 2006. № 24(2). Pp.335-360.
24. Ismael N.F. Influence of artificial cement content on the properties of Kuwaiti sands // Kuwait Journal of Science & Engineering. 2000. № 27(1). Pp. 59–76.
25. Schnaid F., Prietto, P.D.M., Consoli N.C. Characterization of cemented sand in triaxial compression // Journal of Geotechnical and Geoenvironmental Engineering. 2001.

Journal on Hydropower and Dams. 2005. No. 12(1). Pp. 72–76.

21. Abdulla A.A., Kiousis P.D. Behaviour of cemented sands .1. Testing. International Journal for Numerical and Analytical methods in Geomechanics. 1997. No. 21(8). Pp. 533–547.
22. Asghari E., Toll D.G., Haeri S.M. Triaxial behaviour of a cemented gravely sand, Tehran alluvium. *Geotechnical and Geological Engineering*. 2003. No. 21(1). Pp. 1–28.
23. Haeri S.M., Hamidi A., Hosseini S.M., Asghari E., Toll D.G. Effect of cement type on the mechanical behaviour of a gravely sand. *Geotechnical and Geological Engineering*. 2006. No. 24(2). Pp. 335–360.
24. Ismael N.F. Influence of artificial cement content on the properties of Kuwaiti sands. *Kuwait Journal of Science & Engineering.* 2000. No. 27(1). Pp. 59–76.
25. Schnaid F., Prietto P.D.M., Consoli N.C. Characterization of cemented sand in triaxial compression. *Journal of Geotechnical and Geoenvironmental Engineering.* 2001. No. 127(10). Pp. 857–868.
26. Sainov M.P. Parametry deformiruemosti krupnooblomochnykh gruntov v tele gruntovykh plotin [Deformation Parameters of Macrofragment Soils in Soil Dams]. Stroitel'stvo: nauka i obrazovanie. 2014. No. 2. Paper 2. (rus)
27. Marri A. The mechanical behavior of cemented granular materials at high pressures. *Thesis submitted to The University of Nottingham for the degree of Doctor of Philosophy.* 2010.
28. Glagovskiy V.B., Radchenko V.G. Novyye tendentsii v stroitelstve gruntovykh plotin [New trends in the construction of embankment dams]. *Gidrotekhnicheskoye stroitelstvo*. 2013. No. 1. Pp. 2–8. (rus)
29. Bestuzheva A.S. Kamnebeton kak material dlya podekranovoy zony plotiny s zhelezobetonnym ekranom [Rock-cement as material for bedding layer Concrete Faced Rockfill Dams]. *Nauchnoye obozreniye.* 2015. No. 23. Pp. 75–79. (rus)
30. Bestuzheva A.S., Bukanov G.N. Kamnebeton v stroitelstve plotin [Rock-cement in the construction of dams]. *Gidrotekhnicheskoye stroitelstvo.* 2016. No. 10. Pp. 34–38. (rus)
31. Yurkevich O.P. Italyanskiy opyt ispolzovaniya struynoy tsementatsii [Italian Experience of jet-grouting using]. *Metro i tonneli*. 2004. No. 1. Pp. 11–13. (rus)
32. Malinin A.G., Zhemchugov A.A., Gladkov I.L. Opredeleniye fiziko-mekhanicheskikh svoystv gruntotsementa v khode naturnykh issledovaniy [Determination of physical and mechanical properties soil-cement a field study]. *Izvestiya Tulskogo gosudarstvennogo universiteta. Nauki o Zemle.* 2011. No. 1. Pp. 325–330. (rus)
33. Rasskazov L.N., Radzinskiy A.V., Sainov M.P. Vybor sostava glinotsementobetona pri sozdanii “steny v grunte” [Selection of composition of clay-cement concrete for of cutoff wall construction]. *Gidrotekhnicheskoye stroitelstvo.* 2014. No. 3. Pp. 16–23. (rus)

№ 127(10). Pp. 857–868.

26. Саинов М.П. Оценка деформируемости и прочности грунтов, закрепленных путем цементации // Строительство: наука и образование. 2014. № 3. Статья 1.
27. Marri A. The mechanical behavior of cemented granular materials at high pressures // Thesis submitted to The University of Nottingham for the degree of Doctor of Philosophy. 2010.
28. Глаговский В.Б., Радченко В.Г. Новые тенденции в строительстве грунтовых плотин // Гидротехническое строительство. 2013. № 1. С. 2–8.
29. Бестужева А.С. Камнебетон как материал для подэкрановой зоны плотины с железобетонным экраном // Научное обозрение. 2015. № 23. С. 75–79.
30. Бестужева А.С., Буканов Г.Н. Камнебетон в строительстве плотин // Гидротехническое строительство. 2016. № 10. С. 34–38.
31. Юркевич О.П. Итальянский опыт использования струйной цементации // Метро и тоннели. 2004. № 1. С. 11–13.
32. Малинин А.Г., Жемчугов А.А., Гладков И.Л. Определение физико-механических свойств грунтоцемента в ходе натурных исследований // Известия Тульского государственного университета. Науки о Земле. 2011. № 1. С. 325–330.
33. Рассказов Л.Н., Радзинский А.В., Саинов М.П. Выбор состава глиноцементобетона при создании “стены в грунте” // Гидротехническое строительство. 2014. № 3. С. 16–23.

Mikhail Sainov,
+7(926)6078931; mp_sainov@mail.ru

Filipp Kotov,
+7(926)6525881; filipp_net@mail.ru

Михаил Петрович Саинов,
+7(926)6078931; эл. почта: mp_sainov@mail.ru

Филипп Викторович Котов,
+7(926)6525881; эл. почта: filipp_net@mail.ru

doi: 10.18720/MCE.69.5

Deformation of concrete creep in the thermal stress state calculation of massive concrete and reinforced concrete structures

Деформации ползучести бетона в расчетах термонапряженного состояния массивных бетонных и железобетонных конструкций

I.A. Korotchenko,
E.N. Ivanov,
S.S. Manovitsky,
V.A. Borisova,
K.V. Semenov,
Yu.G. Barabanshchikov,
Peter the Great St. Petersburg Polytechnic University, St. Petersburg, Russia

студент И.А. Коротченко,
студент Э.Н. Иванов,
студент С.С. Мановицкий,
студент В.А. Борисова,
канд. техн. наук, доцент К.В. Семенов,
д-р техн. наук, профессор Ю.Г. Барабанщиков,
Санкт-Петербургский политехнический университет Петра Великого, г. Санкт-Петербург, Россия

Key words: massive concrete structures; reinforced concrete; cement setting temperature; thermal stressed state; thermal cracking resistance

Ключевые слова: массивные железобетонные конструкции; железобетон; нарастание температуры смеси; термонапряженное состояние; трещиностойкость

Abstract. In the article the thermal stress state of the reinforced concrete foundation of a nuclear power plant during the building period are analyzed. The calculation results of thermal stressed state in massive foundation slabs with and without concrete creep is given. The article also provides a comparative selection of insulation to ensure crack resistance of the foundation plate with and without creep. Authors found that calculation of the problem at elastic definition leads to substantial over the tensile stresses and the elongation deformations on the surface of the slab for the point of time to create maximum of heat dissipation. Not taking into account concrete creep deformation in the problems of crack control for concrete and reinforced concrete massive structures in the building period leads to substantial increasing of required thickness of heat insulation.

Аннотация. В статье проведен анализ термонапряженного состояния железобетонного фундамента атомной электростанции в период строительства. Представлены результаты расчета теплового напряженного состояния в массивных фундаментных плитах с учетом и без ползучести бетона. Проведен сравнительный выбор изоляции для обеспечения трещиностойкости фундаментной плиты с учетом ползучести и без. Авторами было установлено, что расчет задачи в упругой постановке приводит к существенным переоценкам растягивающих напряжений и деформаций удлинения на поверхности плиты в момент для создания максимального тепловыделения. Показано, что не учет деформаций ползучести бетона в задачах обеспечения трещиностойкости бетонных и железобетонных массивов в строительный период приводит к значительному увеличению требуемой толщины необходимой теплоизоляции.

Introduction

The point of over research is the calculation of thermal fields which based on the heat equation solution as well as thermal stresses definition [1–13], linked with calculation of cracking resistance of NPP reactor base slab in construction period. A change in the thermal state of such structures occurs due to the heat liberation from cement hydration during the concrete hardening process, as well as outside temperature fluctuations, solar exposure, various technological factors, etc. Emerging thermal stresses may cause damage to the structural integrity [14–33].

Korotchenko I.A., Ivanov E.N., Manovitsky S.S., Borisova V.A., Semenov K.V., Barabanshchikov Yu.G. Deformation of concrete creep in the thermal stress state calculation of massive concrete and reinforced concrete structures. *Magazine of Civil Engineering*. 2017. No. 1. Pp. 56–63. doi: 10.18720/MCE.69.5

Due to a number of technological and manufacturing reasons, it is preferable to concrete massive foundation mats and other massive structures as a single block of equal height. However, it causes a considerable heat rise in the mass concrete as the result of an exothermic reaction during the concrete hardening. Consequently, the irregular temperature distribution arises along with the block height, which leads to the dangerous tensile strain first on the surface of the foundation slab and then in its central zones. In this regard, the winter period is especially unfavorable for construction [1, 3, 28].

Lowering the thermal field irregularity inside the block by raising its surface temperature prevents high tensile strain in the winter period. Both heat enclosure and an insulation layer on the concrete block are used in order to prevent high tensile strain [1, 3, 21, 26]. A peripheral concrete electric cable with or without minimum thermal protection is usually used as a more efficient and expensive measure.

The regulation process of the hardening concrete thermal effect requires preliminary thermal protection calculations or the electric heating management depending on the environmental conditions, thermal field inside the block and other factors. The papers [1, 29–31] deal with issues of safe replacement of passive thermal protection and lists the calculation results of electric-mode heating of massive concrete structures in the strict formulation (taking into account the influence of the hardening temperature on the thermal and deformation characteristics of concrete).

Calculation of thermal stressed state of massive concrete structures in the building period and value of cracking resistance are hard enough with a practice and engineering point of view. Some researchers close to solution of these problems in a simplified variant. In on nearly every methods, used in a practice calculations at the present time not be taken account hardening temperature influence on the heat dissipation process.[20, 24, 26] and its deformation characteristics.[14, 15, 19]. The research papers [19, 20, 24] have not taken account deformation of concrete creep, but solve to thermoelastic problem.

The purpose of this article is rationale for allowance deformation of concrete creep in the calculation of the NPP reactor base slab thermal stressed state. Calculations of thermal stressed state and cracking resistance taken account the temperature influence on a concrete characteristic.

This paper demonstrates calculation of the foundation mat thermal stressed state with the help of TERM software developed by the staff of the Structural Mechanics and Building Structures department of the Institute of Civil Engineering at the Peter the Great St.Petersburg Polytechnic University [18, 21].Considering horizontal mats sizes significantly exceed their height, we can study a one-dimensional structural model for the mat central part with the reasonable degree of accuracy. In this model, stress and temperature are functions of the vertical coordinate space. In order to estimate the cracking resistance of the foundation mat, we would use the deformation criterion suggested by P.I. Vasiliev [24]. According to this criterion, concrete elongation deformations, determined in view of the concrete creep factor and variable deformation modulus, should not exceed the ultimate concrete elongation.

Methods

Consider B35 foundation slab 2 m high with the cement consumption of 340 kg/m^3 constructed in winter (Fig.1). The foundation slab is supported by the concrete bedding layer B12.5 with the grade foundation. Thermal and physical characteristics of the concrete B40 are defined by the concrete thermal conductivity λ = 2.67 W/(m·^{0}C) and thermal capacity c = 1.0 kJ/(kg·^{0}C).

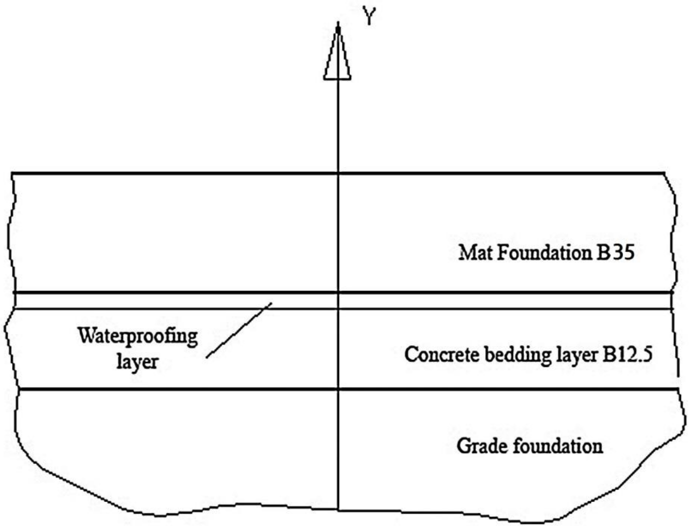

Figure 1. The structural model of the foundation slab

As demonstrated in [14], the instantaneous elastic deformation modulus of concrete is:

$$E(t) = E_{max}\left(1 - e^{\alpha t^{\gamma}}\right), \tag{1}$$

where E_{max} = 34500 MPa is the limit value of deformation of concrete B35 [15, 16];

α = – 0.37, γ = 0.72 – are functional dependency parameters;

t – the current time.

Consideration of creep deformation in the paper is based on straight line inherited theory of aging. The equation between stress and deformation are defined by the P.I. Vasiliev recommendation [24]:

$$\sigma(y,t) = \frac{1}{1-\nu}\int_0^t \frac{\partial \varepsilon_n(\gamma,t,\tau)}{\partial \tau} E(\gamma,\tau) \times R(\gamma,t,\tau) d\tau\,, \tag{2}$$

where σ(y,t) – normal stresses in concrete ;

ε_n(y,t,τ) – deformation induced normal stresses;

E(y,τ) – elastic deformation modulus of concrete;

R(y,t,τ) – function of relaxation;

t – the current time;

τ – applied force moment.

The relaxation function in the fixed value is of the form:

$$R(t,\tau) = A\left(1 - e^{-\beta\tau^{\alpha}}\right) + \left(B_1 + D_1 e^{-\beta\tau^{\alpha}}\right)e^{-\gamma_1(t-\tau)} + \left(B_2 + D_2 e^{-\beta\tau^{\alpha}}\right)e^{-\gamma_2(t-\tau)}, \tag{3}$$

where functional dependency parameters are as follows:

A = 0.7; B_1 = 0.2; D_1 = 0.4; B_2 = 0.1; D_2 = 0.3; α = 0.67; β = 3.61×10^{-6} c^{-1}; γ_1 = 1.17×10^{-5} c^{-1}; γ_2 = 2.33×10^{-7} c^{-1}.

The heat dissipation process follows the I.D. Zaporozhets equation [19]. The equation parameters I.D. Zaporozhets gets from experimental evidence on concrete heat dissipation.

The heat dissipation process and deformation characteristics depend on the concrete hardening temperature. Registration of such influence goes by adjustment time hypothesis in which a real time is exchanged to adjustment time, which is a function of hardening temperature. The temperature function is of the form:

$$f_T = 2^{\frac{(T_1 - T_2)}{\varepsilon}}, \tag{4}$$

where ε is the characteristic temperature difference.

The following technological specifications of concrete pouring were taken into account: inside the heat enclosure, the concrete mix is poured as a single 2.0 m high block with the inside heat enclosure temperature is 5 °C and surface concrete temperature is 15 °C. After concreting the surface is covered with insulation, which thickness is determined by the cracking prevention condition.

Results

Evaluation of thermal stressed state with a fixed thickness of thermal insulation

Calculations of this paragraph provide for the same thickness of thermal insulation layer for concrete creep and without concrete creep. Fig. 2 shows graphs of variation in time the thermal stresses in the control points of the base slab. Dash line on the graph is response a thermal stresses determined with concrete creep. Solid line is the thermal stresses in the elastic problem definition.

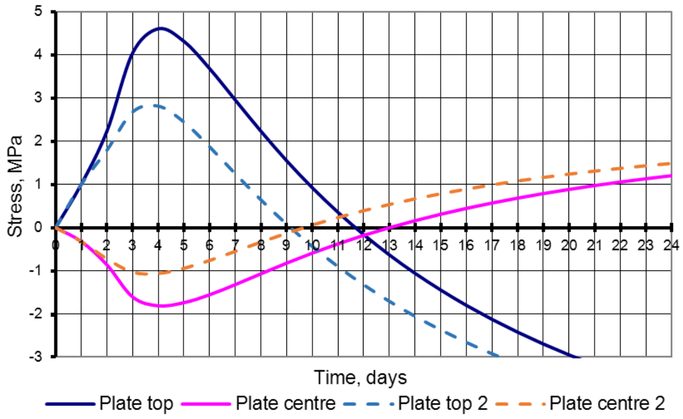

Fig 2. Dependency graph of stresses in the center and on the upper surface of the slab depends on time without concrete creep (solid line) and with concrete creep (dash line)

Analyze of a results show us the following:

1. Character of changing thermal stresses with time is the same in a both cases.
2. The maximum stresses in the elastic problem definition for exothermal heating moment (4 days) is: tensile on the surface of the slab is 4.6 MPa, compressive in the center of the slab is 1.8 MPa;
3. Similarly in the case of concrete creep: tensile stresses on the surface is 2.8 MPa, compressive in the center is 1.1 MPa.

In such a way, problem solution in the thermoelastic definition leads to increase of tensile stresses on the surface to 1.8 MPa (or to 40 %), but compressive tensile to 0.7 MPa (or to 39 %).

Figure 3 shows graphs of changing of stretching deformation on the surface slab in the time for the thermoelastic problem and problem in the strict definition.

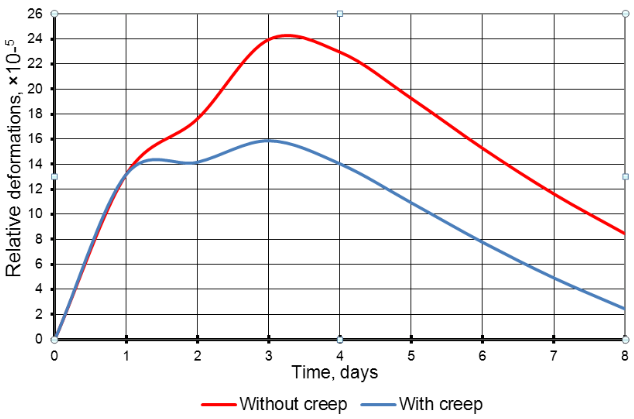

Figure 3. Dependency the relative elongation stresses on the surface of the slab in the time without concrete creep and with concrete creep

Analyze of a results show us:

1. Character of the relative elongation deformation is the same in a both cases.
2. The maximum of the relative elongation deformations in the elastic problem definition for exothermal heating moment (4 days) is 24×10^{-5};
3. Similarly in the case of concrete creep is 16×10^{-5};

In such a way, problem solution in the thermoelastic definition leads to increase of the relative elongation deformation on the surface of the slab to 8×10^{-5} (or to 33 %).

Selection of the required insulation thickness

Calculation is performed for the thermal insulation of foam polystyrene density 40 kg/m^3, with a coefficient of heat conductivity: λ = 0.030 W/m×ºC.

For the problem in thermoelastic definition the required thickness of insulation layer is 13 cm. The maximum tensile stresses on the surface of the slab occur on the 4-th day and being 2.1 MPa with modulus of deformation is 33317 MPa. The corresponding relative elongation deformation is 6.3×10^{-5} with their limit value is 6.5×10^{-5}.

For the problem in the strict definition the required thickness of insulation layer is 3 cm. The maximum tensile stresses on the surface of the slab occur on the 4-th day and being 1.7 MPa with modulus of deformation is 32366 MPa. The corresponding relative elongation deformation is 5.3×10^{-5} with their limit value is 6.5×10^{-5}.

In such a way, the concrete creep accounting in the thermal stress stated of massive concrete structures leads to substantial saving of the thermal insulating material: in this case an economy is 70 %.

Discussion

According to studies, the calculation of the problem in an elastic formulation leads to a significant overestimation of stresses. And in the neglect of creep strain there are problems with the definition of rational thickness of heat insulation from the technical and economic points of view.

According to the work [5–10, 12, 14] energy efficiency and the economic benefit from the application of technical solutions is crucial in modern construction. Therefore, we can recommend using in the calculation of the inelastic formulation of the problem, which turns out to be more advantageous and profitable. And also take into account creep deformation, which give more accurate results [1, 2, 4, 21, 23, 27].

Conclusions

1. Calculation of the problem thermal stressed state of massive concrete and reinforced concrete structures in the building period at elastic definition leads to substantial over the tensile stresses (to 40 %) and the elongation deformations (to 33 %) on the surface of the slab for the point of time to create maximum of heat dissipation.

2. Not accounting concrete creep deformation in the problem of crack control for concrete and reinforced concrete massive structures in the building period leads to substantial increasing of required thickness of heat insulation (to 70 %).

References

1. Korotchenko I., Ivanov E., Semenov K., Barabanschikov Yu. Thermal stressed state in Mmssive concrete structures in the winter building period. *MATEC Web of Conferences*. 2016. No. 53.
2. Tarasova D., Staritcyna A., Nemova D., Andreev K. The using feasibility Russian and Europe software products at thermal calculations. *MATEC Web of Conferences*. 2016. No. 53.
3. Gnam P.A., Kiviharju R.K. Tehnologii zimnego betonirovania v Rossii [Technologies of winter concreting in Russia]. *Construction of Unique Buildings and Structures*. 2016. No. 9. Pp. 7–25. (rus)
4. Semenov, K.V., Konstantinov V.A., Savchenko A.V., Kokoreva K.A., Nesterov A.A. Effect temperaturnogo vozdeystvia v raschetah termonapryazhennogo sostoyania

Литература

1. Korotchenko I., Ivanov E., Semenov K., Barabanschikov Yu. Thermal stressed state in Mmssive concrete structures in the winter building period // MATEC Web of Conferences. 2016. № 53.
2. Tarasova D., Staritcyna A., Nemova D., Andreev K. The using feasibility Russian and Europe software products at thermal calculations // MATEC Web of Conferences. 2016. № 53.
3. Гнам П.А., Кивихарью Р.К. Технологии зимнего бетонирования в России // Строительство уникальных зданий и сооружений. 2016. № 9. С. 7–25.
4. Семенов К.В., Константинов В.А., Савченко А.В., Кокорева К.А., Нестеров А.А. Эффект температурного воздействия в расчетах термонапряженного состояния дискретно наращиваемых бетонных тел //

diskretno narashivaemih betonnih tel [The effect of temperature influence in calculations of a thermostressed state of discretely increased concrete bodies]. *Construction of Unique Buildings and Structures*. 2016. No. 5(32). Pp. 18–28. (rus)

5. Vatin N.I., Nemova D.V., Rymkevich P.P., Gorshkov A.S. Vliyanie urovnya teplovoy zashchity ograzhdayushchikh konstruktsiy na velichinu poter' teplovoy energii v zdanii [Influence of building envelope thermal protection on heat loss value in the building]. *Magazine of Civil Engineering.* 2012. No. 8. Pp. 1–13. (rus)
6. Petrosova D.V., Kuzmenko N.M., Petrosov D.V. Eksperimental'noe issledovanie teplovogo rezhima legkoy ograzhdayushchey konstruktsii v naturnykh usloviyakh [A field experimental investigation of the thermal regime of lightweight building envelope construction]. *Magazine of Civil Engineering*. 2013. No. 8. Pp. 31–37. (rus)
7. Vatin N.I., Gorshkov A.S., Nemova D.V. Energoeffektivnost' ograzhdayushchikh konstruktsiy pri kapital'nom remonte [Energy efficiency of envelopes at major repairs]. *Construction of Unique Buildings and Structures.* 2013. No. 3. Pp. 1–11. (rus)
8. Nemova D.V., Vatin N.I., Gorshkov A.S., Kashabin A.V., Rymkevich P.P., Tseytin D.N. Tekhniko-ekonomicheskoe obosnovanie meropriyatiy po utepleniyuograzhdayushchikh konstruktsiy individual'nogo zhilogo doma [Technical and economic assessment on actions for heat insulation of external envelops of an individual house]. *Construction of Unique Buildings and Structures*. 2014. No. 8. Pp. 93–115. (rus)
9. Vatin N.I., Nemova D.V. Povyshenie energoeffektivnosti zdaniy detskikh sadov [Increase of power efficiency of buildings of kindergartens]. *Construction of Unique Buildings and Structures.* 2012. No. 3. Pp. 1–11. (rus)
10. Gorshkov A.S., Rymkevich P.P., Vatin N.I. Modelirovanie protsessov nestatsionarnogo perenosa tepla v stenovykh konstruktsiyakh iz gazobetonnykh blokov [Simulation of non-stationary heat transfer processesin autoclaved aerated concrete-walls]. *Magazine of Civil Engineering*. 2014. No. 8. Pp. 38–48. (rus)
11. Platonova M.A., Vatin N.I., Nemova D.V., Matoshkina S.A., Iotti D., Togo I. Vliyanie vozdukhoizolyatsionnogo sostava na teplotekhnicheskie kharakteristiki ograzhdayushchikh konstruktsiy [The influence of the airproof composition on the thermo technical characteristics of the enclosing structures]. *Construction of Unique Buildings and Structures*. 2014. No. 4. Pp. 83–95. (rus)
12. Teplova Z.S., Solovyeva K.I., Nemova D.V., Trubina D.A., Petrosova D.V. Teplotekhnicheskiy raschet ograzhdayushchey konstruktsii obshcheobrazovatel'noy shkoly [Thermo technical calculation of enclosure structure of comprehensive school]. *Construction of Unique Buildings and Structures*. 2014. No. 4. Pp. 96–108. (rus)
13. Gorshkov A., Vatin N., Nemova D., Tarasova D. The brickwork joints effect on the thermotechnical uniformity of the exterior walls from gas – concrete blocks. *Applied Mechanics and Materials*. 2015. Vols. 725–726. Pp. 3–8.
14. Vatin N., Petrichenko M., Nemova D., Staritcyna A., Tarasova D. Renovation of educational buildings to increase energy efficiency. *Applied Mechanics and Materials.* 2014. Vols. 633–634. Pp. 1023–1028.
15. Korsun V., Korsun A. The influence of precompression on strength and strain properties of concrete under the effect of elevated temperatures. *Applied Mechanics and Materials*. 2015. Vols. 725–726. Pp. 469–474.
16. Korsun V., Vatin N., Korsun A., Nemova D. Physical-mechanical properties of the modified fine-grained concrete subjected to thermal effects up to 200°C. *Applied Mechanics and Materials*. 2014. Vols. 633–634. Pp. 1013–1017.

Строительство уникальных зданий и сооружений. 2015. № 5(32). Pp. 18–28.

5. Ватин Н.И., Немова Д.В., Рымкевич П.П.,Горшков А.С. Влияние уровня тепловой защиты ограждающих конструкций на величину потерь тепловой энергии в здании // Инженерно-строительный журнал. 2012 № 8. С. 1–13.
6. Петросова Д.В., Кузьменко Н.М., Петросов Д.В. Экспериментальное исследование теплового режима легкой ограждающей конструкции в натурных условиях // Инженерно-строительный журнал. 2013. № 8. С. 31–37.
7. Ватин Н.И., Горшков А.С., Немова Д.В. Энергоэффективность ограждающих конструкций при капитальном ремонте // Строительство уникальных зданий и сооружений. 2013. № 3. С. 1–11.
8. Немова Д.В., Ватин Н.И., Горшков А.С., Кашабин А.В., Рымкевич П.П., Цейтин Д.Н. Технико-экономическое обоснование мероприятий по утеплению ограждающих конструкций индивидуального жилого дома // Строительство уникальных зданий и сооружений. 2014. № 8. С. 93–115.
9. Ватин Н.И., Немова Д.В. Повышение энергоэффективности зданий детских садов // Строительство уникальных зданий и сооружений. 2012. № 3. С. 1–11.
10. Горшков А.С., Рымкевич П.П., Ватин Н.И. Моделирование процессов нестанционарного переноса тепла в стеновых конструкциях из газобетонных блоков // Инженерно-строительный журнал. 2014. № 8. С. 38–48.
11. Платонова М.А., Ватин Н.И., Немова Д.В., Матошкина С.А., Иотти Д., Того И. Влияние воздухоизоляционного состава на теплотехнические характеристики ограждающих конструкций // Строительство уникальных зданий и сооружений. 2014. № 4. С. 83–95.
12. Теплова Ж.С., Соловьева К.И., Немова Д.В., Трубина Д.А., Петросова Д.В. Теплотехнический расчет ограждающей конструкции общеобразовательной школы [Thermo technical calculation of enclosure structure of comprehensive school] // Строительство уникальных зданий и сооружений. 2014. № 4. С. 96–108.
13. Gorshkov A., Vatin N., Nemova D., Tarasova D. The brickwork joints effect on the thermotechnical uniformity of the exterior walls from gas – concrete blocks // Applied Mechanics and Materials. 2015. Vols. 725–726. Pp. 3–8.
14. Vatin N., Petrichenko M., Nemova D., Staritcyna A., Tarasova D. Renovation of educational buildings to increase energy efficiency // Applied Mechanics and Materials. 2014. Vols. 633–634. Pp. 1023–1028.
15. Korsun V., Korsun A. The influence of precompression on strength and strain properties of concrete under the effect of elevated temperatures // Applied Mechanics and Materials. 2015. Vol. 725–726. Pp. 469–474.
16. Korsun V., Vatin N., Korsun A., Nemova D. Physical-mechanical properties of the modified fine-grained concrete subjected to thermal effects up to 200°C // Applied Mechanics and Materials. 2014. Vol. 633–634. Pp. 1013–1017.
17. Барабанщиков Ю.Г., Соколов В.А., Васильев А.С., Шевелев М.В. Регулирование сркоов схватывание цемента химическими добавками. Regulirovanie srokov skhvatyvaniya tsementa khimicheskimi dobavkami [Adjustment of cement setup time with chemical admixtures] // ALITINFORM: Цемент, бетон, сухие смеси. 2012. № 3. С. 32–41.
18. Александровский С.В. Расчет бетонных и железобетонных конструкций на измерения температуры и влажности с учетом ползучести. М.,

17. Barabanshchikov Y.G., Sokolov V.A., Vasiliev A.S., Shevelev M.V. Regulirovanie srokov skhvatyvaniya tsementa khimicheskimi dobavkami [Adjustment of cement setup time with chemical admixtures]. *ALITINFORM: Tsement, Beton, Sukhie smesi*. 2012. No. 3. Pp. 32–41. (rus)
18. Aleksandrovskiy S.V. *Raschet betonnykh i zhelezobetonnykh konstruktsiy na izmeneniya temperatury i vlazhnosti s uchetom polzuchesti* [Calculation of temperature change and humidity in terms of concerete creep in concrete and reinforced concrete structures]. Moscow, 1973. 444 p. (rus)
19. Zaporozhets I.D., Okorokov S.D., Pariyskiy A.A. *Teplovydeleniye betona* [Heat Liberation by Concrete]. Leningrad-Moscow: Stroyizdat, 1966. 316 p. (rus)
20. Malinin N.A. *Issledovaniye termonapryazhennogo sostoyaniya massivnykh betonnykh konstruktsiy s peremennymi deformativnymi kharakteristikami.* Diss. na soisk. uchen. step. kan. teh. nauk: Spets 05.23.01 [Research of thermal stressed state of mass concrete structures with changing deformations characteristics.PhD Thesis]. Leningrad, 1977. 186 p. (rus)
21. Semenov K.V. *Temperaturnoye i termonapryazhennoye sostoyaniye blokov betonirovaniya korpusa vysokogo davleniya v stroitelnyy period.* Dis. na soisk. uchen. step. kan. teh. nauk: Spets 05.23.01 [Temperature and thermal stressed state of concreting blocks in a high pressure shell during the building period. PhD Thesis]. Leningrad, 1990. 156 p. (rus)
22. Barabanshchikov Y.G., Semenov K.V. Increasing the plasticity of concrete mixes in hydrotechnical construction. *Power Technology and Engineering.* 2007. No. 41. Pp. 197–200.
23. Barabanshchikov Y.G., Semenov K.V., Shevelev M.V. Termicheskaya treshchinostoykost betona fundamentnykh plit [Thermal cracking resistance of concrete foundation mats]. *Populyarnoye betonovedeniye.* 2009. No. 1. Pp. 70–76. (rus)
24. Vasilyev P.I., Ivanov D.A., Kononov Yu.I., Semenov K.V., Starikov O.P. Raschetnoye obosnovaniye razmerov blokov i posledovatelnosti betonirovaniya korpusa reaktora VG - 400 s proverkoy na modeli 1/5 naturalnoy velichiny [Calculation analysis of concreting blocks and VG -400 reactor shell concreting sequence using a 1/5 scale model]. *Problems of Atomic Science and Technology*. 1988. No. 1. Pp. 62–68. (rus)
25. Trapeznikov, L.P. *Temperaturnaya treshchinostoykost massivnykh betonnykh sooruzheniy* [Thermal cracking resistance of mass concrete structures]. Moscow, 1986. 272 p. (rus)
26. Semenov K.V., Barabanshchikov Y.G. Termicheskaya treshchinostoykost massivnykh betonnykh fundamentnykh plit i yeye obespecheniye v stroitelnyy period zimoy [Maintenance of thermal cracking resistance in massive concrete base slabs during winter concreting]. *Construction of Unique Buildings and Structures.* 2014. No. 2. Pp. 125–135. (rus)
27. Semenov K., Barabanshchikov Y. Thermal cracking resistance in massive concrete structures in the winter building period. *Applied Mechanics and Materials*. 2015. Vols. 725–726. Pp. 431–441.
28. Russian Set of Rules SP 41.13330.2012. Betonnye i zhelezobetonnye konstrukcii gidrotehnicheskih sooruzhenij [Concrete and reinforced concrete structures of hydroengineering facilities]. (rus)
29. Larson M. Thermal crack estimation in early age concrete - models and methods for practical application. Doctoral Thesis. Lulea University of Technology. 2003. 190 p.
30. Miyazawa S., Koibuchi K., Hiroshima A., Ohtomo T., Usui T. Control of thermal cracking in mass concrete with blast

1973. 444 с.

19. Запорожец И.Д., Окороков С.Д., Парийский А.А. Тепловыделение бетона. Л.–М.: Стройиздат, 1966. 316 с.
20. Малинин Н.А.. Исследование термонапряженного состояния массивыных бетонных конструкций с переменными деформативными характеристиками. Дисс. на соиск. учен. степ. к.т.н.: Спец. 05.23.01. Ленинград, 1977. 186 с.
21. Семенов К.В. Температурное и термонапряженное состояние блоков бетонирвоания корпуса выского давления в строительный период. Дисс. на соиск. учен. степ. к.т.н.: Спец. 05.23.01. Ленинград, 1990. 156 с.
22. Barabanshchikov Yu.G., Semenov K.V. Increasing the plasticity of concrete mixes in hydrotechnical construction // Power Technology and Engineering. 2007. № 41. Pp. 197–200.
23. Барабанщиков Ю.Г., Семенов К.В., Шевелев М.В. Термическая трещиностойкость бетона фундаментных плит // Популярное бетоноведение. 2009. № 1. С. 70–76.
24. Васильев П.И., Иванов Д.А., Кононов Ю.И., Семенов К.В., Стариков О.П. Расчетное обоснование размеров блоков и последовтаельности бетонирования корпуса реатора ВГ-400 с проверкой на модели 1/5 натуральной величины // Problems of Atomic Science and Technology. 1988. № 1. Pp. 62–68.
25. Трапезников Л.П. Температурная трещиностойкость массивных бетонных сооружений. М.: Энегоатом издат, 1987. 272 с.
26. Семенов К.В., Барабанщиков Ю.Г Термическая трещиностойкость массивных бетонных фундаментальных плит и ее обеспечение в стоительный период зимой // Строительство уникальных зданий и сооружений. 2014. № 2. С. 125–135.
27. Semenov K., Barabanshchikov Y. Thermal cracking resistance in massive concrete structures in the winter building period // Applied Mechanics and Materials. 2015. Vol. 725–726. Pp. 431–441.
28. СП 41.13330.2012. Бетонные и железобетонные конструкции гидротехнических сооружений.
29. Larson M. Thermal crack estimation in early age concrete - models and methods for practical application. Doctoral Thesis. Lulea: Lulea University of Technology, 2003. 190 p.
30. Miyazawa S., Koibuchi K., Hiroshima A., Ohtomo T., Usui T. Control of thermal cracking in mass concrete with blast–furnace slag cement // Concrete Under Severe Conditions (CONCEC'10). 2010. Pp. 1487–1495.
31. Shengxing W., Donghui H. Estimation of cracking risk of concrete at early age based on thermal stress analysis // Journal of Thermal Analysis and Calorimetry. 2011. Vol. 105. № 1. Pp. 171–186.
32. Zhang Z., Zhang X., Wang X., Zhang T., Zhang X. Merge concreting and crack control analysis of mass–concrete base slab of nuclear power plant // Applied Mechanics and Materials. 2011. Vol.94–96. Pp. 2107–2110.
33. Barabanshchikov Yu.G., Semenov K.V. Increasing the plasticity of concrete mixes in hydrotechnical construction // Power Technology and Engineering. 2007. № 41. С. 197–200.

– furnace slag cement. *Concrete Under Severe Conditions (CONCEC'10).* 2010. Pp. 1487–1495.

31. Shengxing W., Donghui H. Estimation of cracking risk of concrete at early age based on thermal stress analysis. *Journal of Thermal Analysis and Calorimetry*. 2011. Vol. 105. No. 1. Pp. 171–186.
32. Zhang Z., Zhang X., Wang X., Zhang T., Zhang X. Merge concreting and crack control analysis of mass -concrete base slab of nuclear power plant. *Applied Mechanics and Materials*. 2011. Vol. 94–96. Pp. 2107–2110.
33. Barabanshchikov Yu.G., Semenov K.V. Increasing the plasticity of concrete mixes in hydrotechnical construction. *Power Technology and Engineering.* 2007. No. 41. Pp. 197–200.

Ivan Korotchenko,
+7(911)7537423; saenko84@yandex.ru

Ernest Ivanov,
+7(960)2615868; ivanov-efimov.e@yandex.ru

Sergey Manovitsky,
+7(981)9803734; sergeimanovitsky@mail.ru

Victoria Borisova,
+7(921)7718791; vi4ko93@mail.ru

Kirill Semenov,
+7(921)7811957; kvsemenov@bk.ru

Yuriy Barabanshchikov,
+7(812)5341286; ugb@mail.ru

Иван Алексеевич Коротченко,
+7(911)7537423;
эл. почта: saenko84@yandex.ru

Эрнест Николаевич Иванов,
+7(960)2615868;
эл. почта: ivanov-efimov.e@yandex.ru

Сергей Сергеевич Мановицкий,
+7(981)9803734;
эл. почта: sergeimanovitsky@mail.ru

Виктория Александровна Борисова,
+7(921)7718791;
эл. почта: vi4ko93@mail.ru

Кирилл Владимирович Семенов,
+7(921)7811957; эл. почта: kvsemenov@bk.ru

Юрий Германович Барабанщиков,
+7(812)5341286; эл. почта: ugb@mail.ru

doi: 10.18720/MCE.69.6

Design features of facade cassettes from thin ceramics

Особенности проектирования фасадных кассет из тонких керамических панелей

A.V. Galyamichev,
A.I. Alkhimenko,
Peter the Great St. Petersburg Polytechnic University, St. Petersburg, Russia

Старший преподаватель А.В. Галямичев,
д-р техн. наук, профессор А.И. Альхименко,
Санкт-Петербургский политехнический университет Петра Великого, г. Санкт-Петербург, Россия

Key words: facade structures; cassette cladding; thin ceramics; adhesive-sealant connection; aluminum structures; ventilated facade

Ключевые слова: фасадные конструкции; кассетная облицовка; тонкая керамика; клеевое соединение; алюминиевые конструкции; вентилируемый фасад

Abstract. Thin ceramic plates are a promising material for architectural use which has significant potential for the realization of different interior and exterior solutions. The use of thin ceramics as facade cladding requires increased attention to the stress-strain state and the nature of its destruction. The main feature of this construction type is the ability to use facade panels with dimensions reaching 3000 x 1000 mm with a small weight and small thickness (3–5 mm). This research studies stress-strain state parameters of thin ceramic panels by testing on uniformly distributed load, simulating the wind effect on the cassette in conditions of the facade exploitation. As a result of laboratory tests obtained the dependence of the plate deflection on the action of a uniformly distributed load and identified convergence with the results of similar experimental work and theoretical studies. Also in this research was studied the work of facade structural sealants as part of facade structures: evaluated the effect of profile color, reinforcing mesh of plate and preliminary surface preparation with a primer on the adhesion to the cassette elements.

Аннотация. Тонкие керамические панели – перспективный материал для архитектурного использования, имеющий значительный потенциал для реализации различных интерьерных и экстерьерных решений. Применение тонкой керамики в качестве фасадной облицовки требует повышенного внимания к напряженно-деформируемому состоянию и характеру её разрушения. Основной особенностью конструкций данного типа является возможность использования на фасаде панелей с размерами, достигающими 3000x1000 мм, обладающими небольшим весом и малой толщиной (3-5 мм). Данное исследование посвящено изучению работы тонких керамических панелей под воздействием равномерно распределённой нагрузки, имитирующей ветровое воздействие на кассету в условиях эксплуатации на фасаде здания. В результате лабораторных экспериментальных исследований была получена зависимость величины прогиба пластины от действия равномерно распределённой нагрузки, получена сходимость с результатами аналогичных экспериментальных работ и теоретических изысканий. Также изучена работа фасадных структурных герметиков в составе фасадных конструкций. Исследованием оценено влияние окраски, усиляющей сетки и предварительной подготовки поверхности праймером на адгезионное соединение элементов кассеты.

Introduction

Exterior view of the building, which formed by facade elements, has a great importance not only for residents, but also for a large group of specialists, including architects, engineers and operating companies. In the design process, they need to provide compliance of aesthetic component and functional purpose of walling. Nowadays, to this list of tasks is increasingly added need for further research into new materials, used as facade cladding.

Today we have big variety of cladding materials: natural stone, brick, aluminum composite panels, different types of ceramic products and others. However, often from these types of materials we cannot make large details. For example, we can look on a residential complex, located on the Optikov Street in St. Petersburg, (Fig. 1). Here, designs chosen large-format elements, which based on the ventilated facade system. For such tasks and static conditions, we can apply only glass and thin ceramic panels, which have big original size, low thickness, lightweight and high strength to resist wind loading.

Figure 1. Project visualization (left)[3] and photo from the object (right) with thin ceramic cladding

Glass plates are widely used in building process as transparent elements of glass walls. It`s applying on opaque surfaces complicated by the high degree of reflection and high probability of scratching.

Thin ceramics (thickness is 3–6 mm, in some cases 10 mm), have many similar options with glass, like thickness and strength, except reflection, but this material researched not so widely as glazing. In particular, engineers do not have any information about static work of this material.

Also for this type of structures, big question is fixing to the supporting base. Constructions of this type usually have mechanical type of fastening – via clamp. Adhesive fixing is common rare [1]. In particular, it is possible to abandon the external aluminum frame, having carried out only on the adhesive bonding. Structures of this type is widely researched in [2, 3, 4] In addition, for large size panels is permissible to use combined systems of mechanical and adhesive type. This mechanical work panel for different system variants will be similar: a thin slab with hinged at the place of installation clamps or glue joints.

To perform detailed engineering, in the absence of full information about static properties of used material, there is a need for a study of thin ceramic plates to solve a group of questions, including:

1. Determine the influence of color on the adhesion of the sealant
2. Determine the influence of the reinforcing mesh on the adhesion of the sealant
3. Determine the influence of surface preparation of profiles on the adhesion of the sealant
4. Identify the influence of the thickness of the adhesive sealant on the bearing capacity of the joint
5. Indicate the actual type of plate fixing to the aluminum sub-structure
6. Determine the convergence of the results of the experiment on the uniform loading of the ceramic plate with similar tests and theoretical data
7. Investigate the mechanism of work and destruction of the panel construction

Materials and Methods

For the research the thin ceramic plate was used. Its distinguishing feature – is the slab size, which can reach up to 3000 mm in length, width has a maximum dimension – 1000 mm, with a relatively small thickness – 3 and 5 mm in unreinforced execution and 3.5 mm with reinforcement fiberglass (Fig.2). The panel made from a mixture of clay, feldspar, silica sand and mineral dyes and then pressed in a facility that does not restrict the acceptance form, to avoid creating stresses in the edge zones. Obtained sheet tempered in special furnaces at temperatures above 1220 °C, which ensures uniformity of the finished ceramic product. Follow cutting ensures exact compliance of panel dimensions for cassette elements.

[3] - Photo link: https://optikov.legenda-dom.ru

Figure 2. Example of the front surface (left)[4] and reverse side of the reinforced ceramic panel (right)

Detailed specifications of the material shown in Table 1. Here presented comparison of technical characteristics for thin ceramic panels and untempered glass.

Table 1. Characteristics of ceramic panels Laminam

№	Physical and chemical properties	Test method	Requirements EN14411-G/ISO13006-G	Units	3.5 mm (with mesh)	5 mm (without mesh)	Glass (5 mm)
1	Weight			kg/sq.m.	8.2	14	12.5
2	Water absorption	ISO 10545-3	<0.5	%	0.1 (<0.3)	0.1 (<0.3)	0.1
3	Dimensions of a slab			м	3x1	3x1	6x4
4	Bending strength in N/mm²	ISO 10545-4	≥ 35	N/sq.mm	90	50	45
5	Mohs scale hardness	UNI EN 101	-	-	≥ 6	≥ 6	≥ 6
6	Coefficient of linear thermal expansion / 10¯6/°C	ISO 10545-8	-	-	6.6	6.6	9
7	Elastic Modulus			MPa	55600	55600	70000

To carry out tests for determination of the bearing capacity and deformability of thin ceramic panels necessary to make loading by uniformly distributed load. As the test sample allowed using constructive scheme of facade cassettes. To form the facade element (cassette), which will be ready for testing, cladding panel installed in the aluminum profile. Fixation in the cassette is achieved by using of facade adhesive sealant. Constructive scheme of a cassette is shown on Figure 3 [5].

Taking into account work specifics of the thin plate elements, which applying leads to big deformation of panel surface – this fact determined chosen research methodology, based on the control of deflection value in the system.

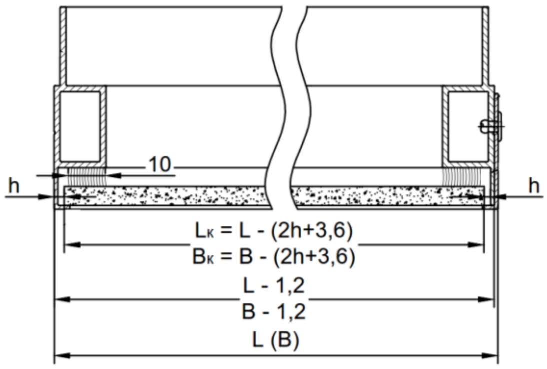

Figure 3. Constructive scheme of facade cassette

[4] - Photo link: http://www.laminam.it/ru/collections/1000x3000

Galyamichev A.V., Alkhimenko A.I. Design features of facade cassettes from thin ceramics. *Magazine of Civil Engineering*. 2017. No. 1. Pp. 64–76. doi: 10.18720/MCE.69.6

The numerical and experimental research methods are used during the study of the structure static work.

In the numerical calculations was applied software, which uses finite element method in the embodiment of the displacement [6, 7, 8]. Structure modeling determines the theoretical values of the stress and displacement of system. As a calculative scheme was designated hinge plate, which is fixed by the four sides to cassette profiles. Based on a constructive solution, the cassette profile hinged fastened to the vertical mullions.

Stiffness of the vertical mullions and bearing brackets in the calculation not been evaluated. Bearing aluminum corners, which is situated at the top of cassette, is appointed as fixed supports. Hooks, which do not take the weight load, modeled as a vertical hinge (Fig.4).

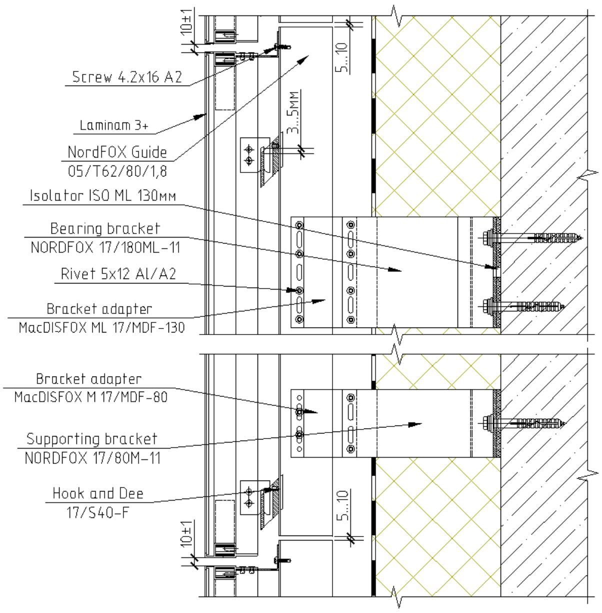

Figure 4. Section of facade system

The experimental method of investigation included several characteristic steps:

1. Test the adhesive joint on the bonding strength and compatibility

2. Testing the full-size cassette sample to the action of a uniformly distributed load

The first stage of experimental research was to test the strength of adhesive joints bonded materials (ceramic materials and aluminum frame) to determine the bearing capacity of the connection and purpose necessary and sufficient width of the sealant layer. At the same time, we determined the parameters for the compatibility of bonding surfaces: take into account paint coating on the profile (including a variety of colors), appointment of priming and cleaning the surface of profile and influence of deleting reinforcing grid in glue zones, as well as its influence on the load-bearing capacity of adhesive layer.

As the test samples were used fragments of the cassette profile with 100 mm length and standard width (16.5 mm) (Fig.5). A tensile testing machine with fixing the maximum value of the applied longitudinal force reached determination of the bearing capacity. The samples were prepared with different thickness of the sealant to determine the possible influence of this parameter.

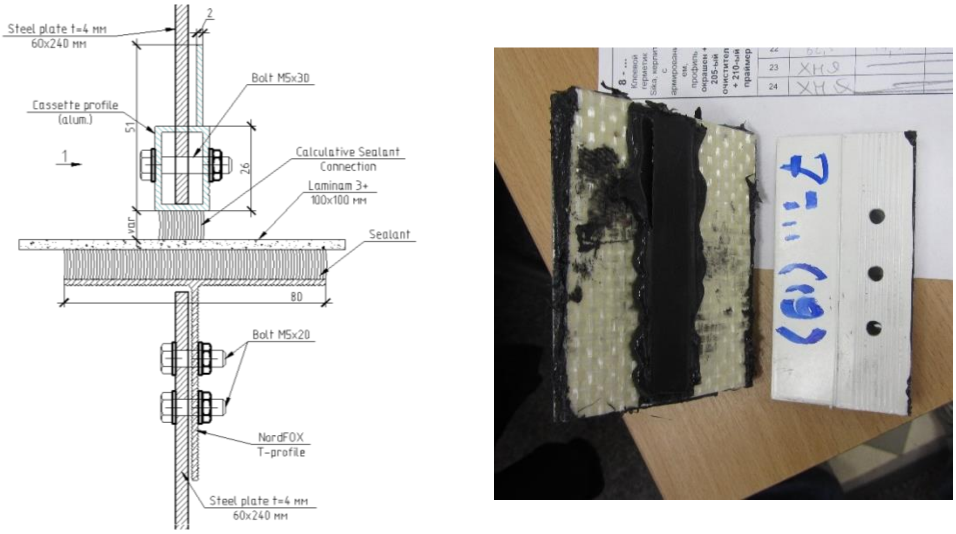

Figure 5. Testing scheme (left) and breaking results (right)

Research of compatibility and quality adhesive sealant adhesion to aluminum alloy 6060 made by CQP 033-1 – definition of adhesion and CQP 034-1 – the testing conditions in the determination of adhesion.

The tests of full-size samples carried out to determine the actual deflections of different cassette types (vertical, angular, horizontal with or without supporting beams) and compare it with the results obtained by analytical method [9, 10, 11], to identify the maximum bearing capacity and the nature of structural failure. During the test, was made an assumption about the possibility of loading the samples in a horizontal plane because of the small own weight cladding elements and aluminum profiles (Fig.6).

Figure 6. Testing stand (left) and deflectometer 6PAO (right)

On the test installation was mounted fragment of subsystem, which shown on Figure 4. Instead of concrete base, laboratory used traverses from I-beams (Fig.6). Uniformly distributed load on thin ceramic slab realized by gravel in measured package. Value of deformation was measure by several deflectometers (model 6PAO), fixed in the center of panel. Loading corresponded to a peak (gust) wind load at different height marks. Testing algorithm includes loading the sample to estimated maximum load (126 kg/sq.m for ordinary and 228 kg/sq.m. for corner zone of a building), then complete unloading and repeated loading until appearance of signs of the sample destruction.

In a laboratory were tested ordinary cassettes with sizes: 2700 x 1050 mm, 1100 x 1910 mm, corner type of cassettes with dimensions: 1100 x 1050 mm, 1050 x 1910 mm.

Comparison of the results proposed to carry out with a test of not tempered glass, which been loaded by uniformly distributed load with the help of the compression camera [12].

Results and Discussion

Results of test on bonding strength of the adhesive joint and compatibility

During tensile tests of samples obtained graphics of sealant deformation from applied longitudinal force under different conditions of applying sealant (Fig.7). Also, research determined influence of reinforcement grid on the load-bearing capacity in order to identify the need for its deletion in the field of gluing. In addition to this option, on the basis of value of the ultimate load, lab tests determines the minimum term for one or two-component sealant to reduce the time to start the mounting of cladding structures. Significant influence on the economics of the facade has adopted adhesive sealant thickness. According to [13], recommended minimum thickness is 6 mm. According to [14] – 3.6 mm value obtained by calculations (but minimal thickness by this document is – 5 mm for factory produced elements). During experiment was checked influence of the sealant thickness on bearing capacity of connection. Result values were summarized in the two tables (Tables 2 and 3), separated by production brand. Also test showed that unpainted profile had sufficient adhesion even without surface preparation. Primer pre-treatment applied to profile samples with powder painting. At the same time, be aware that a variety of colors and paint show different degrees of adhesion (as a result of the test was found a difference in the degree of adhesion of red (high) and white (low) color).

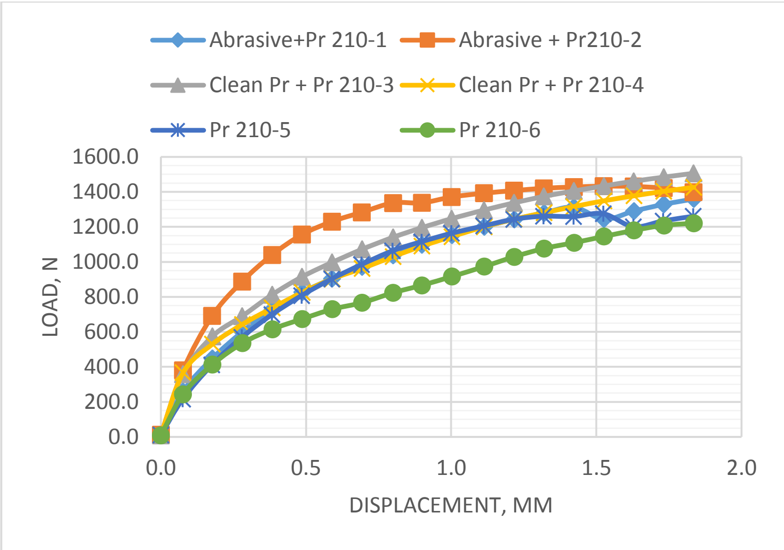

Figure 7. Testing stand (left) and deflectometer 6PAO (right)

Table 2. Characteristics of "Sika" adhesive sealant

Type of example	№	Joint parameters, mm			Breaking load, kg	Avg. Value, N	Avg. area, mm²	Calc. stresses, N/mm²
		Length	Width	Thick.				
Date of producing: 18/06/2014; Date of test: 23/06/2014								
Sika sealant (2 component), LAM3+, unpainted profile	1	87	18	6	152	1386	1392	0.996
	2	86	14	6	120			
	3	87	16	6	152			
Sika sealant (2 component), LAM3, unpainted profile	1	87	15	6	120	1439	1392	1.034
	2	86	14	6	144			
	3	87	18	6	176			
Date of producing: 18/06/2014; Date of test: 08/07/2014								
Sika sealant (2 component), LAM3+, painted profile	1	88	16	6	168	1099	1408	0.780
	2	88	11	6	72			
	3	86	13	6	112			
	4	88	13	6	96			
Date of producing: 03/03/2015; Date of test: 07/04/2015								
Sika sealant (1 component), LAM3+, painted profile	1	91	17	4	61	581	1424	0.408
	2	89	16	4	58			
	3	93	17	4	59			

Table 3. Characteristics of "Dow Corning" adhesive sealant

Type of example	№	Joint parameters, mm			Breaking load, kg	Avg. Value, N	Avg. area, mm²	Calc. stresses, N/mm²
		Length	Width	Thick.				
Date of producing: 23/06/2014; Date of test: 08/07/2014								
DC sealant (1 component), LAM3+, unpainted profile	1	88	15	6	184	1753	1305	1.343
	2	85	15	6	176			
	3	87	15	6	176			
DC sealant (1 component), LAM3, unpainted profile	1	87	15	6	176	1596	1305	1.223
	2	87	15	6	144			
	3	87	15	6	168			
Date of producing: 18/06/2014; Date of test: 08/07/2014								
DC sealant (1 component), LAM3+, unpainted profile	1	100	16	4	120	1046	1600	0.713
	2	95	16	4	128			
	3	100	16	4	101			
DC sealant (1 component), LAM3, unpainted profile	1	95	16	4	168	1465	1520	0.964
	2	94	16	4	120			
	3	91	16	4	160			
DC sealant (1 component), LAM3+, painted profile	1	81	16	6	72	810	1408	0.576
	2	88	16	6	80			
	3	93	16	6	96			
Date of producing: 03/03/2015; Date of test: 07/04/2015								
DC sealant (1 component), LAM3+, painted profile	1	89	16	4	72	526	1376	0.383
	2	88	16	4	40			
	3	86	16	4	49			

Results of numerical and experimental tests for full-size cassette samples

Research results are the values of displacements (Fig. 9), obtained by applied impact of uniformly distributed load on a full-size sample design (Fig. 8), and the maximum value of the wind pressure, which led to destruction of the sample (Table 4).

Analytical results have been obtained as a result of the static calculation of displacements (Fig. 9), which used as the basis for assigning a necessary step of strengthening cassettes by transverse or longitudinal (depending on the orientation of the cassette) supporting beams

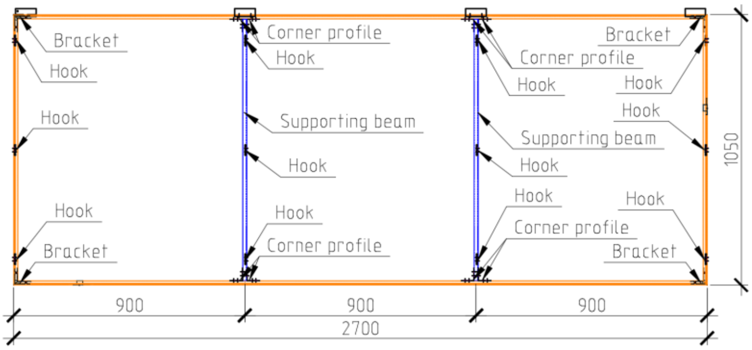

Figure 8. Example of cassette with dimensions 2700x1050 mm

The graph (Fig. 9) shows deflections of the center of panel with dimensions 2.7 x 1.05 m divided on 3 cell and 1.91 x 1.05 m, divided on 2 cell, obtained by the formula, reached in research of thin plates, was made in Samara University of Civil Engineering for glass panels, and during the experimental test [15]. In case these panels we have good repeatability of results.

Galyamichev A.V., Alkhimenko A.I. Design features of facade cassettes from thin ceramics. *Magazine of Civil Engineering*. 2017. No. 1. Pp. 64–76. doi: 10.18720/MCE.69.6

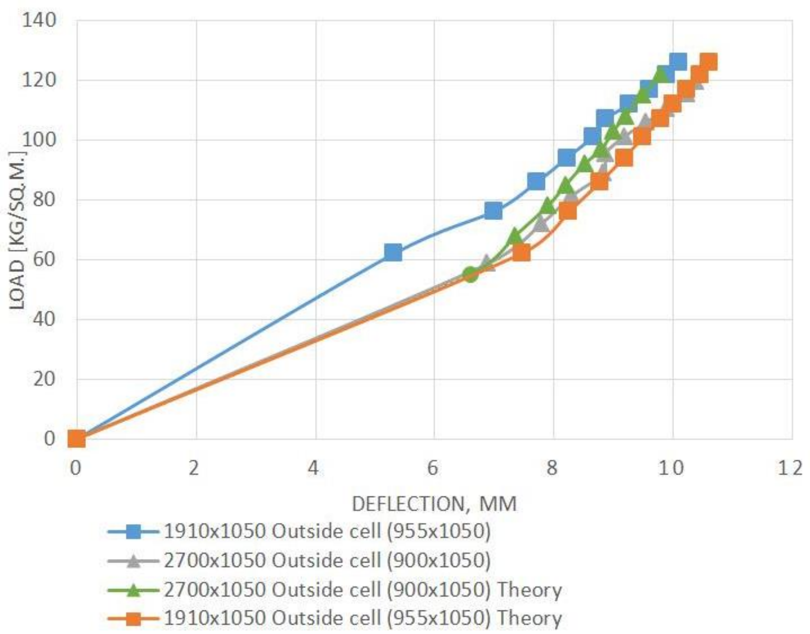

Figure 9. Test and theoretical calculation result

Table 4 summarizes test results of several types of cassettes used on the object:

Table 4. Results of full-sized breaking test for cassettes

№	Dimensions and characteristic of cassette	Sketch	Ultimate load, kg/m2	Max. deflection, mm	Theoretical deflection, mm
1	2700 x 1050, RAL 9016, normal	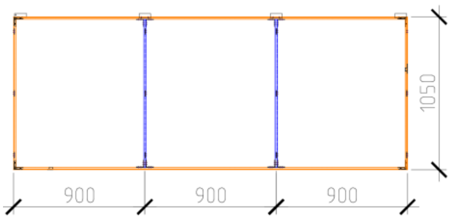	433.86	16.87	17.9
2	1100 x 1050, RAL 9016, corner	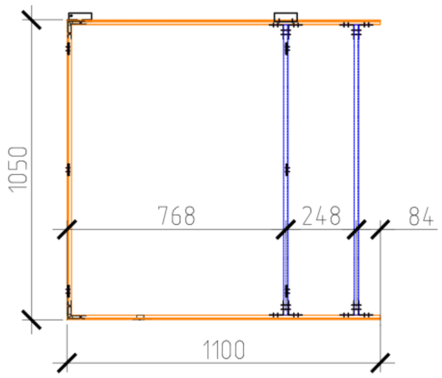	486.35	20	19.08
	1100 x 1050, RAL 9016, corner		463.47	19.46	18.65

<table>
<tr><th>№</th><th>Dimensions and characteristic of cassette</th><th>Sketch</th><th>Ultimate load, kg/m2</th><th>Max. deflection, mm</th><th>Theoretical deflection, mm</th></tr>
<tr><td>3</td><td>1050 x 1910, RAL 2002, normal</td><td>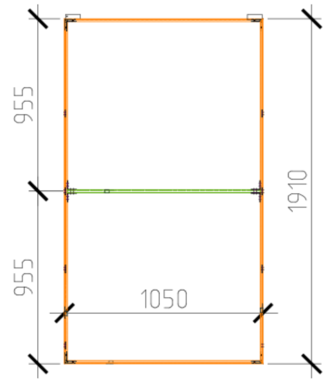
</td><td>192.36</td><td>13.32</td><td>12.15</td></tr>
<tr><td rowspan="2">4</td><td>1050 x 1910, RAL 9016, normal</td><td rowspan="2">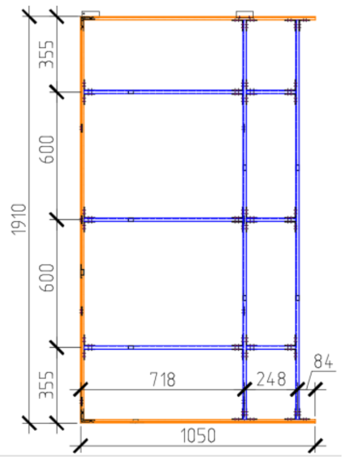
</td><td>445.65</td><td>13.92</td><td>13.8</td></tr>
<tr><td>1050 x 1910, RAL 2002, normal</td><td>613.04</td><td>14.15</td><td>16.65</td></tr>
</table>

Analysis of the results shows that the design of the facade cladding, especially with adhesive sealants, it is necessary to take into account a number of factors that have a significant influence over the technical solutions.

Gluing of thin ceramics to the aluminum profile surfaces must be resolved by the tests for each object individually, as the color profile, the preparation of the slab or profile, and the presence or absence of reinforcing mesh, adjusts the bearing capacity of the connection

Based on performed research, can be made a conclusion that the greatest influence on the adhesive bond has a painting of the profile (reduction of load bearing capacity is 22 % for a two-component adhesive and 56 % for a single-component sealant). As a result, unpainted profile recommended using for facade constructions in places with hidden adhesive fixing and implementing mount directly to the pre-skim profile.

The inclusion of reinforcing mesh also has an effect on the connection: its presence reduces the carrying capacity by 4 % and 26 % for different types of sealants. Need to say, that work to remove this coating is rather hard and consuming a lot of time, that is why we expect, that version with not deleted mesh will be main in design calculation.

Reduced sealant thickness not directly affected on the load capacity under the action of tensile forces, but in this particular case of use in the cassette was performed departing from ETAG 002 recommendations regarding the minimum of sealant thickness (4 mm instead of the recommended 6 mm) and part of aspect ratio (4:1, instead of the recommended 3:1). A minimal thickness recommended by the manufacturers to make sure that a shear stress coming a differential thermal (temperature difference between the sealing and the installing of the panel) or structural movement that sealant can transfer. Moreover, the manufacturing process (pouring of the sealant) might require a minimum gap to assure that the silicone spreads correctly over the whole bite (width) of the joint [16, 17].

As a result, during the test, it has been identified reduction of bearing capacity, the average for the two producers up to 46 %. Specimens with a thickness of 4 mm in 10 % of cases showed break by adhesion failure, also inside the joint located cavity with the sealant having a viscous structure, it is indicating an incomplete set of strength including the twenty-day exposure. This phenomenon directly related to non-compliance with the proportions of sealant joint. However, the load-bearing capacity, demonstrated by adhesive is sufficient for the perception of wind loads, which used in the test bench.

Test results have shown good agreement with theoretical data of Volmir theory for thin plates and with the same tests carried out in Samara University of Civil Engineering for glass panels (Fig.10) [15, 18, 19]. Differences in the final test data for ceramic plates obtained because of the presence of backlash in the bearing brackets with rivet connections, crumple effect in aluminum because of tight contact with stainless steel fasteners and deformation of the aluminum cassette profiles between the fixing points.

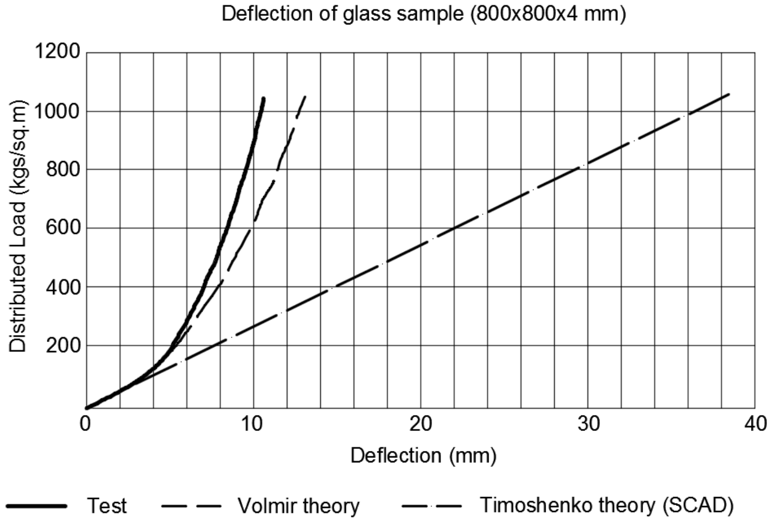

Figure 10. Results of glass plate test

As the result, formula for deformation of thin ceramics plates is:

$$f = a \cdot 10^{-4} \cdot (p)^{\gamma} \cdot 12 \cdot (1 - \mu^2) \qquad (1)$$

where f – deflection of the middle of plate, mm

a, b – Long and short side of plate, mm

$$p = \frac{q}{E} 10^{-1} (\frac{b}{h})^3 \qquad (2)$$

q – Uniformly distributed load, N/mm^2

E – Elastic modulus, MPa

h – Plate thickness, mm

μ – Shear deformation coefficient,

γ – Coefficient, depends on plate stiffness during loading.

Samples of the full-size cassettes that are involved in the tests, today approved on the real facades. Ordinary vertical cassette with sizes 1050 x 1910 tested to assess the possibility of increasing step of supporting beams up to 955 mm to economy the profile in production of cassettes of thin ceramic slabs.

Important note, that the destruction of the panel under the influence of uniformly distributed load carried safety in terms of the impact on pedestrians and vehicles: under the critical load, ceramics crack, but at the expense of reinforcement mesh action, cladding retains its shape and stay in place (Fig.11).

Figure 11. Destruction of cassette under the influence of distributed load

In this case, it may indicate the possibility of the timely replacement of the damaged panel without causing threats to human security. According to the results of research for full-sized cassettes was appointed a step of applying supporting beams in ordinary zone wind zone (850 mm) and in corner wind zone (680 mm) for conditions of Saint-Petersburg [20, 21].

The test results showed that bearing capacity of slabs from thin ceramics in 4.5 times more than the load, resulting in a maximum permissible deflection. In connection with this phenomenon appears the question of the rationality check of cladding structures from thin ceramic panels, glass or aluminum composite sheets on the critical deformations on the action of the peak wind load [22, 23]. This action has the effect of an emergency nature (hurricane, storm), does not lead to permanent deformations in the material of the panel and the frame and does not lead to technological malfunctions of the structure. Aesthetic psychological impact on the around people, during a hurricane, is limited by deflection designs which do not lead to the destruction, and this situation will not have influence on people.

In this connection, the authors offer to consider the possibility of making adjustments to existing regulations regarding check structures for deformations, based on foreign experience [24], which is the example of the German technical document divides the lining (in particular, glazing) on the vertical (Vertikalverglasung) less than 10° and horizontal (Überkopfverglasung) more than 10° deviation from vertical. For vertical glazing fixed on four sides, the deflection is not standardized, and for the horizontal is 1/100. For the horizontal glazing, fixed on three or two sides, the limit is 1/200 of the free edge length. This will allow produce more economical and at the same time reliable facade construction, because in Russian Federation for all types of structures on the aluminum frame, maximal deflection is 1/150 [20] for opaque surfaces and 1/250 for glass [25]. In addition, in this regard, it looks promising research at the Technical University of Darmstadt, regarding significant increase of the sealant hardness with the short-time loading, but loses this property with long-term action of load [26].

Conclusions

1. Unpainted profile has good adhesion even without surface preparation. Profile with powder painting needs primer pre-treatment. Different colors and paint methods has different degrees of adhesion.

2. In the course of the study, we determined influence of the reinforcing mesh on reducing the bearing capacity of the adhesive sealant by 4–26 % (depending on the manufacturer of adhesive sealant).

3. To ensure the adhesion of the adhesive sealant to the surface it is recommended to use a primer with an easy surface treatment with abrasive materials.

4. Reducing of sealant thickness has influence on bearing capacity and quality of adhesion. However, small adhesive thicknesses recommended using for two-component adhesive sealant (where aspect ratio of joint does not have influence). In other cases, recommended to use 5 mm minimal thickness.

5. In accordance with the test results, the hinge character of the fixing detected for the ceramic panel.

6. Test results have shown good agreement with theoretical data of Volmir theory for thin plates and with the same tests carried out in Samara University of Civil Engineering for glass panels.

7. The destruction of the panel under the action of a uniformly distributed load occurs because of the safe destruction of the ceramic plate (the expense of reinforcement mesh action, cladding retains its shape and stay in place).

Acknowledgement

The authors wish to express their gratitude to the NordFOX, Archskin, Sika and Dow Corning Company for the provision of the specimens.

References

1. Dow Corning Corporation: Case study. *Forum Hochhaus Frankfurt am Main.* Germany, 2010.
2. Staudt Y., Odenbreit C., Schneider J. Investigation of bonded connections with silicone under shear loading. *Challenging Glass 5 – Conference on architectural and structural applications of glass.* Ghen: Ghent University, 2016.
3. Staudt Y., Schneider J., Odenbreit C. Investigation of the material behavior of bonded connections with silicone. *Engineered transparency. International Conference at glasstec.* Düsseldorf, Germany, 2014
4. Dias V. *Development of adhesives constitutive material laws for the assessment of bonded steel to glass partial composite beams.* Doctorial thesis. Luxembourg: University of Luxembourg, 2013.
5. *Tekhnologicheskaya karta na sborku kassetnykh paneley s litsevoy poverkhnostyu iz krupnoformatnogo keramogranita v sisteme "NordFOX MLK-v-300"* [The technological map for the assembly of cassette panels with the front surface of large-format ceramic slabs in the system "NordFOX MLK-v-300"]. Moscow: OOO "Studio-Keramika", 2014. 4 p. (rus)
6. Karpilovskiy V.S., Kriksunov E.Z., Malyarenko A.A., Perelmuter A.V., Perelmuter M.A. *SCAD Office. Vychislitelnyy kompleks SCAD* [SCAD Office. Calculation complex SCAD]. Moscow: Izdatelstvo SKAD SOFT, 2011: Pp. 75–82. (rus)
7. Nakamura T., Lopez-Pamies O. A finite element approach to study cavitation instabilities in non-linear elastic solids under general loading conditions. *International Journal of Non-Linear Mechanics.* 2012. No. 47(2). Pp. 331–340.
8. Weißgraeber P., Becker W. Finite fracture mechanics model for mixed mode fracture in adhesive joints. *International Journal of Solids and Structures.* 2013. No. 50. Pp. 2383–2394.
9. Volmir A.S. *Gibkiye plastiny i obolochki* [Flexible plates and shells] Moscow: Gosudarstvennoye izdatelstvo tekhniko-teoreticheskoy literatury, 1956. 419 p. (rus)
10. Timoshenko S.P., Voynovskiy-Kriger S. *Plastinki i obolochki* [Plates and shells]. Moscow: Fizmatgiz, 1963. 636 p. (rus)
11. Vaynberg D.V., Vaynberg Ye.D. *Raschet plastin*. [Calculation of plates]. Kiyev: Budivelnik, 1970. 436 p. (rus)
12. Kondratyeva N.V. Eksperimentalnyye issledovaniya prochnosti listovogo stekla pri poperechnom izgibe [Experimental study of the sheet glass strength upon lateral bending]. *Steklo i keramika.* 2006. No. 2. Pp. 5–7. (rus)
13. *ETAG 002. Guideline for European Technical Approval for Structural Sealant Glazing Kits.* European Organisation for Technical Approvals, 2012. 91 p.
14. *ASTM C1401-14. Standard Guide for Structural Sealant Glazing.* ASTM International, West Conshohocken, PA, 2014. 23 p.
15. Kondratyeva N.V. *Prochnost i deformativnost konstruktsiy iz listovogo stekla pri poperechnom izgibe ravnomerno raspredelennoy nagruzkoy* [Strength and deformability of structures made of sheet glass under transverse bending by a uniformly distributed load]. PhD Thesis. Samara: Samarskiy gosudarstvennyy arkhitekturno-stroitelnyy

Литература

1. Dow Corning Corporation: Case study // Forum Hochhaus Frankfurt am Main. Germany, 2010.
2. Staudt Y., Odenbreit C., Schneider J. Investigation of bonded connections with silicone under shear loading // Challenging Glass 5 – Conference on architectural and structural applications of glass. Ghen: Ghent University, 2016.
3. Staudt Y., Schneider J., Odenbreit C. Investigation of the material behavior of bonded connections with silicone // Engineered transparency. International Conference at glasstec. Düsseldorf, Germany, 2014
4. Dias V. Development of adhesives constitutive material laws for the assessment of bonded steel to glass partial composite beams. Doctorial thesis. Luxembourg: University of Luxembourg, 2013.
5. Технологическая карта на сборку кассетных панелей с лицевой поверхностью из крупноформатного керамогранита в системе "NordFOX MLK-v-300". М.: ООО "Студио-Керамика", 2014. 4 с.
6. Карпиловский В.С., Криксунов Э.З., Маляренко А.А., Перельмутер А.В., Перельмутер М.А. SCAD Office. Вычислительный комплекс SCAD М.: Издательство СКАД СОФТ, 2011. С. 75–82.
7. Nakamura T., Lopez-Pamies O. A finite element approach to study cavitation instabilities in non-linear elastic solids under general loading conditions // International Journal of Non-Linear Mechanics. 2012. № 47(2). Pp. 331–340.
8. Weißgraeber P., Becker W. Finite fracture mechanics model for mixed mode fracture in adhesive joints // International Journal of Solids and Structures. 2013. № 50. Pp. 2383–2394.
9. Вольмир А.С. Гибкие пластины и оболочки. Москва: Государственное издательство технико-теоретической литературы. 1956. 419 с.
10. Тимошенко С.П., Войновский-Кригер С. Пластинки и оболочки. М.:Физматгиз, 1963. 636 с.
11. Вайнберг Д.В., Вайнберг Е.Д. Расчёт пластин. Киев: Будивельник, 1970. 436 с.
12. Кондратьева Н.В. Экспериментальные исследования прочности листового стекла при поперечном изгибе // Стекло и керамика. 2006. № 2. С. 5–7.
13. ETAG 002. Guideline for European Technical Approval for Structural Sealant Glazing Kits. European Organisation for Technical Approvals, 2012. 91 p.
14. ASTM C1401-14. Standard Guide for Structural Sealant Glazing. ASTM International, West Conshohocken, PA, 2014. 23 p.
15. Кондратьева Н.В. Прочность и деформативность конструкций из листового стекла при поперечном изгибе равномерно распределенной нагрузкой. Дисс на соиск. учен. степ. к. т. н. Самара: Самарский государственный архитектурно-строительный университет, 2010. С. 72–75
16. Marlow R.S. A general first-invariant hyperelastic constitutive model // Constitutive Models for Rubber III. 2003. Pp. 157–160.
17. Santarsiero M., Louter C., Lebet J. Parametric numerical investigation of adhesive laminated point connections //

universitet, 2010. Pp. 72–75. (rus)

16. Marlow R.S. A general first-invariant hyperelastic constitutive model. *Constitutive Models for Rubber III.* 2003. Pp. 157–160.
17. Santarsiero M., Louter C., Lebet J. Parametric numerical investigation of adhesive laminated point connections. *COST Action TU0905, Mid-term Conference on Structural Glass.* Taylor & Francis Group, 2013.
18. Zubkov V.A., Kondratyeva N.V. Raschet prochnosti listovogo stekla pri poperechnom izgibe [Calculation of the strength of flat glass in transverse bending]. *Steklo i keramika.* 2009. No. 5. Pp. 14–16. (rus)
19. Kurenkova A.Yu., Kuzmenko A.V., Kurenkova O.M. Uchet vetrovykh nagruzok pri raschete tolshchiny stekla v svetoprozrachnykh konstruktsiyakh [Allowance for wind loads when calculating the thickness of glass in translucent structures]. *Svetoprozrachnyye konstruktsii*. 2012. No. 2(82). Pp. 5–15. (rus)
20. *SP 20.13330.2011. Nagruzki i vozdeystviya. Aktualizirovannaya redaktsiya SNiP 2.01.07-85** [Russian Set of Rulles SP 20.13330.2011. Loads and impacts. Actualized version] Moscow, 2011. 23 p. (rus)
21. *SNiP 2.01.07-85. Nagruzki i vozdeystviya* [Construction Norms and Regulations SNiP 2.01.07-85. Loads and impacts]. Moscow, 2003. 18 p. (rus)
22. Galyamichev A.V. Spetsifika opredeleniya nagruzok na ograzhdayushchiye konstruktsii i yeye vliyaniye na rezultaty ikh staticheskogo rascheta [Specificity of determining loads on enclosing structures and its effect on the results of their static calculation]. *Scientific open access journal Naukovedeniye.* 2015. Vol. 7. No. 2(27). 54TVN215. (rus)
23. Galyamichev A.V. Konstruktivnaya i raschetnaya skhema svetoprozrachnykh konstruktsiy [Constructive and design scheme of translucent structures]. *Svetoprozrachnyye konstruktsii.* 2013. No. 5(91). Pp. 40–42. (rus)
24. TechnischeRegelnfür die Verwendung von linienförmiggelagerten Verglasungen (TRLV). Schlussfassung. August, 2006. 5 p.
25. *GOST 30698-2014. Steklo zakalennoye. Tekhnicheskiye usloviya* [Russian State Standard GOST 30698-2014. Tempered Glass. Technical conditions]. Moscow: Standartinform, 2015. 13 p. (rus)
26. Drass M., Schneider J. On the mechanical behavior of transparent structural silicone adhesive – TSSA // *SEMC 2016 – Sixth International Conference on Structural Engineering, Mechanics and Computation.* Captown, South Africa: Elsevier B.V., 2016.

COST Action TU0905, Mid-term Conference on Structural Glass. Taylor & Francis Group, 2013.

18. Зубков В.А., Кондратьева Н.В. Расчет прочности листового стекла при поперечном изгибе // Стекло и керамика. 2009. № 5. С. 14–16.
19. Куренкова А.Ю., Кузьменко А.В., Куренкова О.М. Учёт ветровых нагрузок при расчёте толщины стекла в светопрозрачных конструкциях // Светопрозрачные конструкции. 2012. № 2(82). С. 5–15.
20. СП 20.13330.2011. Нагрузки и воздействия. Актуализированная редакция СНиП 2.01.07-85*. М., 2011. 23 с.
21. СНиП 2.01.07-85. Нагрузки и воздействия. М., 2003. 18 с.
22. Галямичев А.В. Специфика определения нагрузок на ограждающие конструкции и её влияние на результаты их статического расчёта // Интернет-журнал Науковедение. 2015. Т. 7. № 2(27). 54TVN215.
23. Галямичев А.В. Конструктивная и расчетная схема светопрозрачных конструкций // Светопрозрачные конструкции. 2013. № 5(91). С. 40–42.
24. TechnischeRegelnfür die Verwendung von linienförmiggelagerten Verglasungen (TRLV). Schlussfassung. August, 2006. 5 p.
25. ГОСТ 30698-2014. Стекло закалённое. Технические условия. М.: Стандартинформ, 2015. 13 с.
26. Drass M., Schneider J. On the mechanical behavior of transparent structural silicone adhesive – TSSA // SEMC 2016 – Sixth International Conference on Structural Engineering, Mechanics and Computation. Captown, South Africa: Elsevier B.V., 2016.

Alexander Galyamichev,
+7(911)8110719; galyamichev@yandex.ru

Alexander Alkhimenko,
+7(812)5354610; vils@cef.spbstu.ru

Александр Викторович Галямичев,
+7(911)8110719;
эл. почта: galyamichev@yandex.ru

Александр Иванович Альхименко,
+7(812)5354610; эл. почта: vils@cef.spbstu.ru

Galyamichev A.V., Alkhimenko A.I. Design features of facade cassettes from thin ceramics. *Magazine of Civil Engineering*. 2017. No. 1. Pp. 64–76. doi: 10.18720/MCE.69.6

doi: 10.18720/MCE.69.7

BIM in the assessment of labor protection

BIM технологии в оценке уровня охраны труда

V.V. Sharmanov,
Scientific–technical center "Etalon",
St. Petersburg, Russia
T.L. Simankina,
A.E. Mamaev,
Peter the Great St. Petersburg Polytechnic University, St. Petersburg, Russia

Инженер В.В. Шарманов,
ООО «Научно – технический центр «Эталон»,
г. Санкт-Петербург, Россия
канд. техн. наук, доцент Т.Л. Симанкина,
магистрант А.Е. Мамаев,
Санкт-Петербургский политехнический университет Петра Великого,
г. Санкт-Петербург, Россия

Key words: BIM; 3D-model; construction production; building information modeling; security index; barometer security; plugin; occupational safety; insurance

Ключевые слова: BIM; 3D; индекс безопасности; информационное моделирование зданий; барометр безопасности; плагин; охрана труда; страхование

Abstract. The article presents methodology of monitoring and control of safety and labor protection on the basis of modern innovative technologies and the digital model of the construction site. Monitoring based on the BIM technology enables a qualitatively new approach to monitoring safety and occupational safety on the construction site. The result of control by the offered method in the form of a security index, reflects the actual situation in the checked object and gives the chance to estimate influence of dangerous production factors. This approach to assessment will allow reacting quickly to the processes taking place in the territory of the checked object and also to prevent emergence of a dangerous situation.

Аннотация. В статье представлена методика мониторинга и контроля техники безопасности и охраны труда на основе современных инновационных технологий и цифровой модели строительной площадки. Мониторинг на основе BIM технологии позволяет качественно по-новому подойти к контролю техники безопасности и охраны труда на строительном объекте. Показано, что результат контроля предложенным методом в виде индекса безопасности отражает фактическую ситуацию на проверяемом объекте и даёт возможность оценить влияние опасных производственных факторов. Выявлено, что данный подход к оценке позволит оперативно реагировать на процессы, проходящие на территории проверяемого объекта, а также предупредить возникновение опасных ситуаций.

Introduction

Modern competitive struggle of industrial manufactures forces producers to give special influence to innovations both in the field of enhancement of the production technology, and in the field of enhancement of labor protection. Not high quality of labor conditions has negative impact on the labor market in general that is expressed in the high fluidity and labor shortage, harmful and dangerous working conditions, etc.

Even today it is possible to notice that the measures for improvement of working conditions and safety at the entities undertaken by the government bring results. Financing of the preventive measures directed to decrease in an injury rate at the entities grows, the total quantity of victims on production and the number of patients with occupational diseases decreases. So, in 2014 the Social Insurance Fund of the Russian Federation (Social Insurance Fund of the Russian Federation) fixed 47 453 insured events, linked with an injury rate at the entity that is below similar indicator of 2013 for 5.0 % (for 2486 cases) [1]. According to Federal Service for Labor and Employment (Rostrud) in 2014 as a result of occupational accidents in all organizations in all types of economic activity 2344 persons died that is for 413 people or 15 % less than in 2013 (2757 persons).

Шарманов В.В., Симанкина Т.Л., Мамаев А.Е. BIM технологии в оценке уровня охраны труда // Инженерно-строительный журнал. 2017. № 1(69). С. 77–88.

According to the international labour organization annually, 2.3 million people die in accidents at workplace and occupational diseases. The average mortality rate is about 6,000 people daily. Registered in the world around 340 million accidents at production and about 160 million victims of occupational diseases. With regard to the construction industry, there is a disproportionately high level of accidents considered, it should be noted that unrecorded data at times overlap counted several times, which can be associated with minor injuries that have not led to deaths. Also, pay attention to the lack of proper level of control and enforcement of regulatory literature production sites.

Director for political Affairs of the International labor organization Sandra Polaski noted that "the problem of ensuring workplace safety is relevant to all countries, and a major role in improving the safety of the work belongs not only to the state but also employers and the workers themselves". In addition, Polaski noted that the state's challenge of "PREVENTIVE CULTURE" – a culture of accident prevention. Thus, for the protection of labour needs to follow all the links of the chain involved in the production of a product, whether we build a house, or manufactured item at the factory. There is a need to develop strategies to improve occupational health and safety in the workplace, which would help to monitor the current situation and signal the presence of vulnerabilities in the system of labor protection at the facility.

The Government of the Russian Federation continues work on transition of work management from compensational, costly model to the modern, oriented to the risk management, allowing realizing preventive methods to preserving life and health of workers on production, and also attempts to reduce all types of costs linked with adverse conditions of work are performed.

The presidential decree of the Russian Federation of 07.05.2012 No. 596–606 on the main activities of the Government of the Russian Federation is directed to the activization of work on creation of modern model of the organization of labor protection. Work in this direction, according to the decree, shall consist in implementation and ensuring functioning of institute of assessment of working conditions, enhancements of the legislation in the field of labor protection, updating of the specifications and technical documentation, carrying out comprehensive supervision by all concerned parties of state conditions and labor protection.

BIM technologies, including three-dimensional modeling are recognized as the most perspective way of modern modeling. So, on December 29, 2014 the Ministry of a construction and housing-and-municipal and civil engineering (Ministry of Construction of Russia) signed the order No. 926/pr "On approval of the Plan of step-by-step implementation of information modeling in the field of industrial and civil engineering" [2] which approved the plan of step-by-step implementation of BIM in the field of industrial and civil engineering.

At the turn of XX century and XXI century the rapid growth of information technologies in a construction which qualitatively changed design approaches of architectural objects is observed, at the same time the approach to work on designing has changed too, as well as the subsequent operation of objects designed in BIM technology is affected. In other words, BIM (Building Information Modeling) is the information modeling of buildings, it is a process of collective creation and the use of project information (model) of future construction, at the same time in creation of a model all related departments of project agency take part [3].

For many years scientists and public Figures were engaged in a research of questions of operational injuries and labor protection. So at the beginning of the 20th century in Russia the big contribution to the solution of a question about social protections of wage workers and a risks assessment was made by V.V. Bervi-Flerovsky, E.M. Dementiev, G.V. Hlopin was engaged in questions of hygiene, N.A. Vigdorchik was engaged in questions of occupational diseases and social insurance.

The Russian scientists and public Figures who were engaged in studying of problems of work at the beginning of the XX century can be divided conditionally into four groups: the first should include the Figures pursuing the academic science and also public Figures to the first; to the second group is factory inspectors; the third includes the representatives of employers; and the fourth includes statesmen and officials. If we talk about the second, third and fourth groups, then their interest had something common with their job responsibilities, but the representatives of the first group made the significant contribution to studying of problems of work and they were pioneers of labor researches. These are the famous scientists: R.A. Disterlo, L.S. Tal, M.I. Tugan-Baranovsky, V.V. Svyatlovsky, V.G. Yarotsky, I.S. Voytinsky, M.G. Lunts, I.A. Trakhtenberg, V.M. Dogadov, etc.

In the research of V.D. Royk [4] the economic and legal mechanisms of workers protection against industrial hazards are considered. The work experience of the mechanism of compensation of disability on production is considered in details. Bases of the theory and methodology of the organization of system of compulsory social insurance from occupational accidents are lit.

In the paper [5] theoretical bases and practical recommendations of insurance underwriting are stated. The underwrating role in activities of an insurance company as well as how this activity begins to play a key role in insurance is shown. Levels of underwriting and their types are considered.

We would like to notice the research [6] in which situations on labor protections and industrial safety are considered. Statistical data on an injury rate are given in production depending on a type of economic activity, as well as expenses on providing the correct working conditions.

In his research S.P. Levashov [7] provided the analytical review of system of monitoring and a risks assessment to the Russian Federation and abroad; considered a number of consecutive actions of detection of potential dangers of working conditions; provided the analysis of criteria for evaluation of the risks arising in the course of professional activity of the worker.

In the article of O.S. Gamayunova [8] the statistics of an industrial injuries in St. Petersburg is provided, education options in the sphere of safety in a construction are considered, foreign experience in the solution of questions of increase in level of safe engineering and labor protection is given.

In the articles of T.F. Morozova [9, 10] various evaluation methods of risks when implementing the investment and construction projects are considered. In particular, the example of a risks assessment by an expert method and method of statistical modeling is given.

Today the international practice in development of labor protection moves on the way of preventive measures in assessment of professional risks and creation of an effective control system. Positive experience of Great Britain in decrease in level of an industrial traumatism helped with it and it was adopted by the International Labour Organization (ILO) [11] in 1999. In the developed document OHSAS 18001:1999 "System of management of professional health and safety. The specification" new approach to a control system of labor protection is considered. Specifics of the document consist in the mechanism of continuous control of actions for improvement of working conditions.

Addressing sources of BIM technologies it should be noted that the foundation is laid by Chuck Istman professor of Technology Institute of Georgia in 1975 in the magazine of the American Institute of Architects (AIA) under the working name "Building Description System" (System of the description of the building). In 1986, for the first time Englishman Robert Ashe in his article used the term "Building Modeling" in its present understanding as information modeling of buildings. Robert Ashe showed qualitatively new approach in designing, and 3rd terminal of the London Heathrow airport became an example of successful project implementation. It was the first case of use of BIM technology in world project and construction practice.

Today in the Russian Federation quite great interest in development of BIM-of technologies is noted. More and more companies realize benefits of this technology. Many domestic authors deal with problems of implementation and development of BIM technologies. For example, V.V. Talapov [12] gives the detailed characteristic of BIM technology, he considers practical benefits of its application for all participants of the investment and construction project, he designates the main stages of creation of information model of a construction.

Analyzing works [13–15], it is possible to note that rather much attention is paid to safety issues. Authors [16, 17] emphasize the need of assessment of safety of working conditions at the level of designing of a construction object, in particular suggesting to be protected from such factor as fall from height at the level of a project portrayal. Also the possibility of an algorithm creation analyzed by a 3D model is considered and it finds threats for safety of works. The author [18] suggests to systematize and integrate all knowledge gained in course of construction in one model, beginning from designing through all stages of a construction and finishing with exploitation. Authors [19] consider construction safety issues by creation of the base guided to accurate coordination of questions of labor protection. At the same time the security system consists of the principles, both enhancement of culture of production, and general corporate safety.

In researches [20–27] the application of BIM in construction practice as the instrument of designing is considered. The author [28] made functional assessment of BIM technology in implementation in Real Estate Development Company. In researches [29–41] the authors specify that BIM is the tool which allows not only to estimate projects, but to analyze safety of future structures, as well as it gives the chance to apply alternative systems to a possibility of evacuation of people from buildings.

In Russian literature there are a large number of sources on training with the BIM tools but, unfortunately, there are not enough publications on use of these technologies for the purpose of increase in safe engineering and labor protection [3, 42].

Transition to BIM technologies in assessment of a condition of labor protection and safe engineering on the building site is the perspective and effective direction development of all construction production.

The purpose of this article is to show a possibility of digitization of the major dangerous and harmful production factors by types of installation and construction works according to MDS 12-28.2006 "A methodical management on carrying out an expert evaluation of safety of non-stationary workplaces on construction places" [43] using BIM technology for assessment of a condition of labor protection and safe engineering.

Methods

BIM is the cornerstone three-dimensional information model of future project in which the major characteristics (material) and physical parameters (the geometrical sizes) of the materials used in case of a construction and future operation of an object are laid. BIM-technology is the information platform on which additional technologies and opportunities are imposed.

BIM technologies are made on the basis of three-dimensional modeling of an object. Three-dimensional modeling of the object or the analyzed site, such as, the building site allows to divide it into separate parts and to allocate borders for assessment of the situation on safe engineering and labor protection. The valuation principle is linked with splitting of the researched object into elementary sites up to 100 m^2. At this stage it is important to research the most dangerous production factors which will be exposed to the analysis.

As the software product, the Autodesk Navisworks Simulate which supports these technologies is applied, however it isn't capable to make the analysis of labor protection and safe engineering independently therefore it is required to supplement its functionality with the program superstructure called the PLUGIN.

Developing the new program module (PLUGIN), we set in it the key parameters, namely: name of dangerous production factors and algorithm of calculation of these factors. The PLUGIN with the set algorithm helps to digitize the researched object and to receive a resulting effect.

All dangerous production factors are collected in a 3D model and tied to a certain site as it was noted above, up to 100 m^2. In turn supervisory authorities when bypassing the checked object by means of Tablet computers on which this software supporting 3D is installed will be able visually to estimate each checked elementary site and to enter data into the program module PLUGIN. In case of a bypass of the building site, the inspector gives marks opposite of each dangerous production factor in columns "Right" and "Wrong". After entering the data, the program module processes each of the checked dangerous production factors and shows the final number expressed as a percentage or in unit fractions. Conclusion of results is made in the Excel format in the form of the Table where numbers of the checked sites shall be specified, as well as the quantity of marks "right", "wrong" and the most important general security index.

It can be presented in the form of reporting Tables and schedules (Tab. 1, Fig. 1, 2)..

Table 1. The security index for each hazardous production factor

	1	3	2	9	6	8	11	5	10	4	7	Total
Actual Index, %	43	56	57	66	27	42	56	33	67	28	33	51
Current threshold, %	95	95	95	95	95	95	95	95	95	95	95	95

where Figure from 1 to 11 mean the following dangerous factors:

1 – workplace location near the height drop of 1.3 m or more;

2 – moving machines, their working parts, moved objects;

3 – high voltage electrical circuit, which short circuit can happen through a body of the person;

4 – the collapsing rocks;

5 – spontaneous collapse of building constructions, scaffolding;

6 – fall of materials and constructions;

7 – tipping machines, means of paving;

8 – sharp angles, edges;

9 – the increased content in air of dust and hazardous substances;

10 – noise and vibration;

11 – the increased temperature of the equipment, materials.

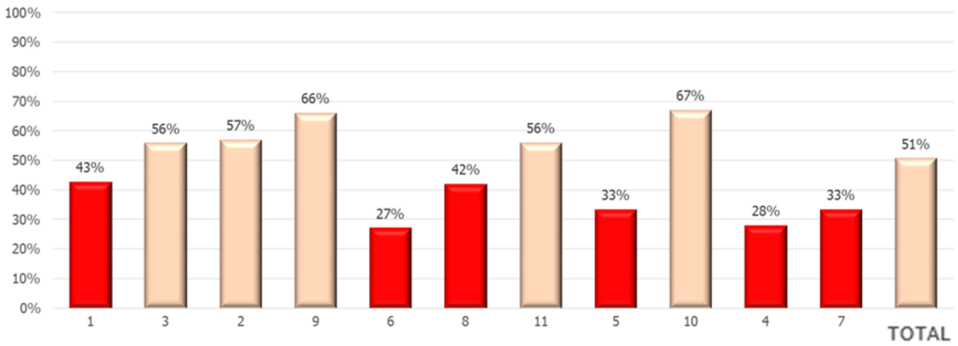

Figure 1. A security index on dangerous and harmful production factors

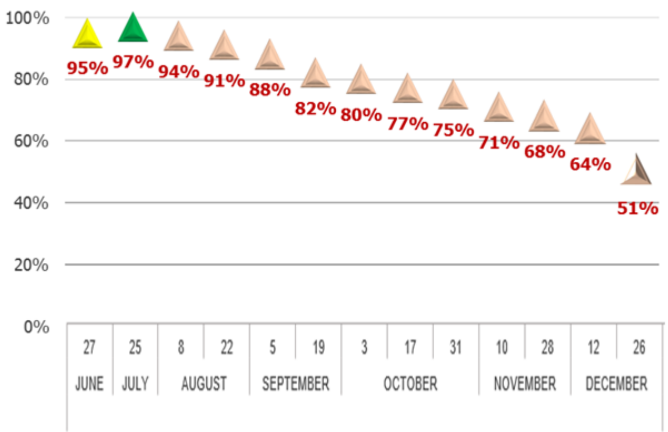

Figure 2. A security index in dynamics

The following step is determination of a stage of monitoring procedure where as the most suitable it is possible to choose a production phase of works, that is to take active part directly in forming of the standard of work and observance of safe engineering and labor protection when working.

The system of monitoring (control) of level of labor protection and safe engineering was applied on the object, representing the site allocated under a construction of the apartment house with the built-in attached rooms and the attached car park located at the address: St. Petersburg, Obukhovskoy Oborony Avenue, house 110, Lit. B, in borders of the territorial zone TD1-2.

When implementing this monitoring the software products of the Autodesk company are used. The implementation of a technique on a specific example is shown in the Figure 3.

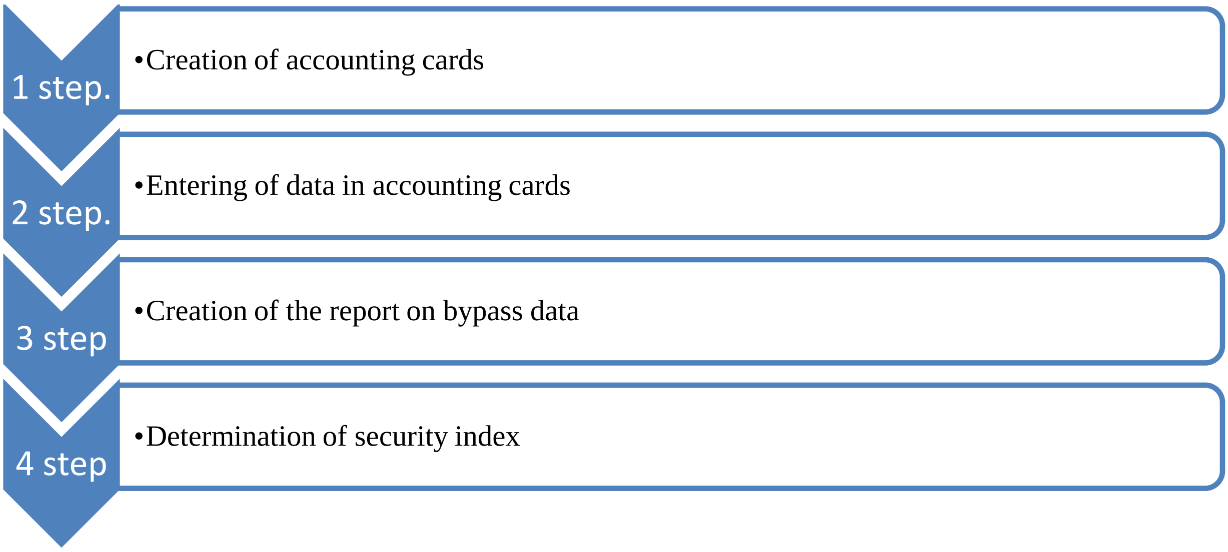

Figure 3. The integrated scheme of implementation of a technique

Results and Discussion

First step. The PLUGIN built in program complexes of the Autodesk Company is developed for implementation of control. At the same time the accounting cards for entering of bypass data are created. This program allows to calculate the security index of the object. The model of a general view of a bypass on occupational health and safety is provided in the Figure 4.

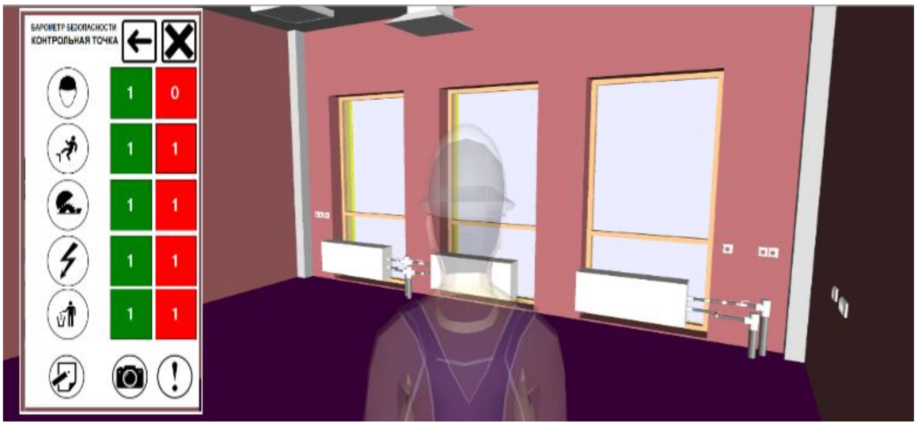

Figure 4.The bypass model of occupational health and safety

Second step. Bypass Information is entered in accounting cards. At the same time the program complex determines itself the inspector's arrangement in space by GPS navigation. In the accounting card necessary parameters of control are programmed. These parameters will be controlled throughout all construction. Each sphere has its identification number or ID-code. The following parameters of control were considered:

1. the engineering processes of construction and installation works;
2. the unprotected sites influencing injury risk on the object;
3. the processing equipment used in work;
4. electrical engineering;
5. garbage.

Sharmanov V.V., Simankina T.L., Mamaev A.E. BIM in the assessment of labor protection. *Magazine of Civil Engineering*. 2017. No. 1. Pp. 77–88. doi: 10.18720/MCE.69.7

All parameters of control are checked according to the regulating documentation.

In the PLUGIN there is also an opportunity to take pictures of the revealed violation and to attach them to the accounting card on which filming (Fig. 5) was made. At the same time the photo receives the same ID code, as the accounting card.

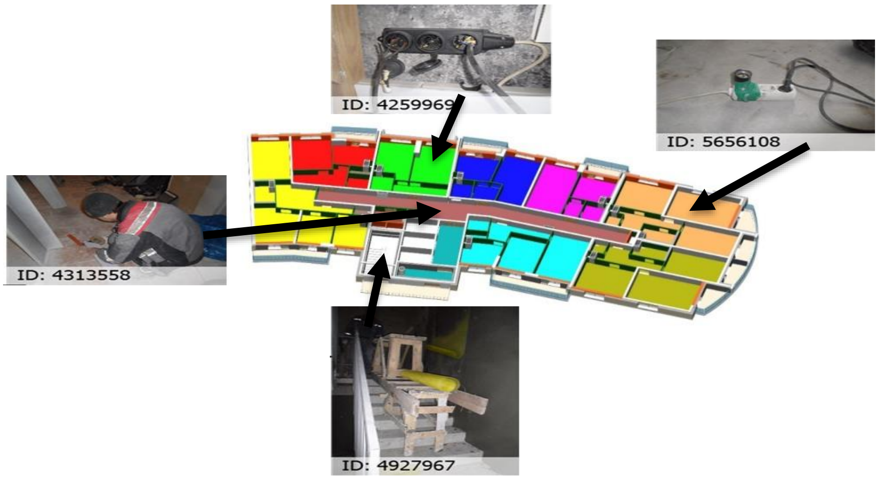

Figure 5. The accounting card with the photo attached to it

The number of accounting cards is appointed from accounting of at most 100 m^2 of the checked area (the elementary site), however in the reviewed example one card was appointed to one room. Each accounting card creates control data on all criteria according to which the assessment of actual state of the checked elementary site is carried out. The assessment of actual state of the checked site is noted as "right" and "wrong". To assess an objective situation on the checked site, it is necessary to expose both marks. Each of the checked parameters shall conform to requirements of the regulating documentation, Construction Rules and Regulations, Design and Construction Specifications, otherwise the mark "Wrong" is given.

To form the security index the borders of danger areas are determined:

– 70 – 100% – safe level of occupational health and safety;

– 50 – 70% – satisfactory level;

– - 0 – 50% – unsatisfactory level.

In the reviewed example 2711 accounting cards are processed, at the same time 3206 measurements are performed (in one bypass of the engineer). The accounting cards which aren't participating for any reasons in measurements and entering of data weren't taken into consideration respectively. From 3206 measurements: 1359 yielded positive result, 1847 were negative - that shows the availability of dangerous actions when implementing installation and construction works which can lead to an injury rate.

Third step. For handling and calculation of the security index the PLUGIN can unload the bypass data in a text format. In the reviewed example results of a bypass were unloaded in the MicrosoftExcel program as it is shown in the Table 2.

Table 2. A report form after unloading of the entered data on a bypass

Date			**Report**		
Project:	Project name				
Security index:	90%				
ID of the accounting card	**Evaluation criteria**				
	criterion 1	**criterion 2**	**criterion 3**	**criterion 4**	**criterion 5**
3659807	0	0	0	0	0
3659957	0	0	0	0	0
3660423	0	0	1	0	0
3660539	0	1	0	2	1
3661000	0	0	0	0	0
3591626	0	0	1	0	0
3591958	0	0	1	0	0
3654682	0	0	0	5	0

Numbers of each accounting card and indicators are reflected in the unloaded Table 6. The quantity of marks is determined proceeding from that how many compliance or discrepancies according to the regulating documentation were revealed.

Fourth step. As a result of unloading of the data PLUGIN calculates the security index expressed as a percentage. The report on the level of the security index is created automatically by the program and directly goes to the server to a management of the company. It should be noted that by results of a bypass and depending on what positions there is weakening, the program gives particular recommendations for rising of general level of the security index. Calculation of the security index is made only according to accounting cards according to which the measurements were made, i.e. data were entered.

The security index represents the generalized indicator characterizing a general condition on the building site, being the effective tool capable to determine the level of safe engineering and labor protection on a construction object. It is at the same time possible to track each of controlled parameters and all situation in dynamics. Table 3 shows dynamics (Dynamics of the security index) of change of a situation on the building site for five months.

Table 3. Dynamics of the security index

Year/month	**July**	**August**		**September**		**October**			**November**	
Date	25	8	22	5	19	3	17	31	10	28
Index	68%	68%	70%	71%	69%	73%	75%	76%	79%	79%

Dynamics of change of level of the security index can be synchronized with the works schedule, analyzing which, it is possible to reveal in case of what work types there is a decrease in the security index, and thus the occupational health and safety.

Dynamics of the key indicators creating a general security index is shown in Table 4.

Table 4. Dynamics of the key indicators creating a general security index

	Engineering procedures of construction and installation work implementation	**The unprotected sites influencing injury risk on an object the**	**Processing equipment used in work**	**Electrical engineering**	**Garbage**	**Total**
Actual Index, %	71	64	50	67	75	79
Current threshold, %	70	70	70	70	70	70

Table 4 shows the ways in which there is a weakening of the positions. Using this approach it is possible to work for the prevention.

Conclusion

As the monitoring of safe engineering and labor protection was carried out before commissioning of the object, the substantial increase of discipline of workers, and also increase in culture of production became result of its implementation. Thus, the result of control by the offered method reflects the actual situation in the checked object, gives the chance to receive specific Figures on each of dangerous production factors, and allows carrying out the analysis of the dangerous production factors weakening positions. This approach to the assessment will allow reacting quickly to the processes which are taking place in the territory of the checked object, preventing emergence of a dangerous situation. In view of dynamics of change of the security it is possible to consider seasonality of the organization of works as the practice shows, seasonality of works is also a key indicator on the organization of such works as excavations, concrete, stone, roofing, etc.

Monitoring on the basis of BIM technology allows to approach qualitatively in a new way to control of safe engineering and labor protection on the object.

Thus, it is possible to measure the level of labor protection at the enterprise.

The presented method allows not only to estimate the level of labor protection in the enterprise, but also to analyze its weaknesses. This approach to the analysis of labor protection has a wide application range, can meet the needs and interests of any customer, when you select and enter criteria that meet the requirements of the state or particular enterprise. When considering the future application of the final numbers, it should be noted that it is possible to set a target (lower) limit (level) for which it is impossible to escape, and to associate it with the bonus the bonus system of remuneration as a motivational component.

References

1. *Doklad o realizatsii gosudarstvennoy politiki v oblasti usloviy i okhrany truda v Rossiyskoy Federatsii v 2014 godu* / Ministerstvo truda i sotsialnoy zashchity Rossiyskoy Federatsii [The report on implementation of state policy in the field of conditions and labor protection in the Russian Federation in 2014 / the Ministry of Labour and Social Protection of the Russian Federation] [Online] URL:http://www.rosmintrud.ru/docs/mintrud/salary/24 (date of application: 17.02.2016). (rus)
2. *3D-proektirovanie budet ispol'zovat'sja v oblasti promyshlennogo i grazhdanskogo stroitel'stva* [3D-design will be used in the field of industrial and civil construction]. [Online] URL:http://minstroyrf.ru/press/3d-proektirovanie-budet-ispolzovatsya-v-oblasti-promyshlennogo-i-grazhdanskogo-stroitelstva/ (date of application: 19.10.2016). (rus)
3. Sharmanov V.V., Mamayev A.Ye., Boleyko A.S., Zolotova Yu.S. Trudnosti poetapnogo vnedreniya BIM [Difficulties of step-by-step implementation of BIM]. *Construction of Unique Buildings and Structures.* 2015. No. 10(37). Pp. 108–120. (rus)
4. Royk V.D. *Professionalnyy risk: otsenka i upravleniye* [Professional risk: assessment and management]. Moscow:

Литература

1. Доклад о реализации государственной политики в области условий и охраны труда в Российской Федерации в 2014 году / Министерство труда и социальной защиты Российской Федерации [Электронный ресурс] URL: http://www.rosmintrud.ru/docs/mintrud/salary/24 (дата обращения: 17.02.2016).
2. 3D-проектирование будет использоваться в области промышленного и гражданского строительства [Электронный ресурс]. URL:http://minstroyrf.ru/press/3d-proektirovanie-budet-ispolzovatsya-v-oblasti-promyshlennogo-i-grazhdanskogo-stroitelstva/ (дата обращения: 19.10.2016).
3. Шарманов В.В, Мамаев А.Е, Болейко А.С, Золотова Ю.С. Трудности поэтапного внедрения BIM // Строительство уникальных зданий и сооружений. 2015. № 10(37). С. 108–120.
4. Ройк В.Д. Профессиональный риск: оценка и управление. М.: АНКИЛ, 2004. 224 с.
5. Бойтуш О.А. Место и роль андеррайтинга в деятельности страховой компании // Управленец. 2012. № 6(46). С. 46–49.

ANKIL, 2004. 224 p. (rus)

5. Boytush O.A. Mesto i rol anderraytinga v deyatelnosti strakhovoy kompanii [The place and the role of underwriting in activities of an insurance company]. *Upravlenets.* 2012. No. 6(46). Pp. 46–49. (rus)
6. Kofanov A.V. Bezopasnost truda v stroitelnom komplekse Rossii [Labor safety in a construction complex of Russia]. *Construction: science and education.* 2011. No. 2. Pp. 1–8. (rus)
7. Levashov S.P. *Monitoring i analiz professionalnykh riskov v Rossii i za rubezhom* [Monitoring and the analysis of professional risks in Russia and abroad]. Kurgan: Publishing house Kurgan state. Un-ty. 2013. 345 p. (rus)
8. Gamayunova O.S., Yershov V.V., Ilin A.A., Li S.I., Sokolov B.V. Obrazovaniye v sfere tekhniki bezopasnosti v stroitelstve [Education in the sphere of safe engineering in a construction]. *Construction of Unique Buildings and Structures.* 2012. No. 5. Pp. 31–35. (rus)
9. Morozova T.F., Lapteva N.A. Otsenka riskov pri realizatsii investitsionno-stroitelnogo proyekta na primere biznes-tsentra [Risks assessment when implementing the investment and construction project on the example of business center]. *Magazine of Civil Engineering*. 2011. No. 2. Pp. 48–51. (rus)
10. Morozova T.F., Kinayat L.A., Kinayat A.Zh. Otsenka riskov v stroitelstve [Risks assessment in a construction]. *Construction of Unique Buildings and Structures.* 2013. No. 5(10). Pp. 68–76. (rus)
11. *MOT-SUOT 2001 (ILO-OSH 2001) Rukovodstvo po sistemam upravleniya bezopasnostyu i okhranoy truda* [ILO- OSH 2001 (ILO-OSH 2001) Guidance on safety management systems and occupational safety and health]. Geneva. ILO. 2003. 28 p.
12. Talapov V.V. *BIM: chto pod etim obychno ponimayut* [BIM: what is usually understood as it]. [Online] URL:http://isicad.ru/ru/articles.php?article_num=14078 (date of application: 23.04.2016). (rus)
13. Kim K., Cho Y., Zhang S. Integrating work sequences and temporary structures into safety planning: Automated scaffolding-related safety hazard identification and prevention in BIM. *Automation in Construction.* 2016. Vol. 70. Pp. 128–142.
14. Zou Y, Kiviniemi A., Stephen W.J. A review of risk management through BIM and BIM-related technologies. *Safety Science*. 2016. No. 1.
15. Zhang S., Sulankivi K., Kiviniemi M., Romo I., Eastman C.M., Teizer J. BIM-based fall hazard identification and prevention in construction safety planning. *Safety Science.* 2015. Vol. 72. Pp. 31–45.
16. Zhang S., Teizer J., Lee J.-K., Eastman C. M.., Venugopal M. Building Information Modeling (BIM) and safety: automatic safety checking of construction models and schedules. *Automation in Construction*. 2013. Vol. 29. Pp. 183–195.
17. Benjaoran V., Bhokha S. An integrated safety management with construction management using 4D CAD model. *Safety Science.* 2010. Vol. 48. No. 3. Pp. 395–403.
18. Zhang S., Boukamp F., Teizer J. Ontology-based semantic modeling of construction safety knowledge: Towards automated safetyplanning for job hazard analysis (JHA). *Automation in Construction*. 2015. Vol. 52. Pp. 29–41.
19. Raheem A.A., Issa R.R.A. Safety implementation framework for Pakistani construction industry. *Safety Science*. 2016. Vol. 82. Pp. 301–314.
20. Smith P. BIM implementation – global strategies. *Procedia Engineering.* 2014. Vol. 85. Pp. 482–492.
21. Tomek A., Matějka P. The Impact of BIM on risk management as an argument for its implementation in a construction company. *Procedia Engineering.* 2014. Vol. 85. Pp. 501–509.

6. Кофанов А.В. Безопасность труда в строительном комплексе России // Строительство: наука и образование. 2011. № 2. С. 1–8.
7. Левашов С.П. Мониторинг и анализ профессиональных рисков в России и за рубежом. Курган: Изд-во Курганского гос. ун-та, 2013. 345 с.
8. Гамаюнова О.С., Ершов В.В., Ильин А.А., Ли С.И., Соколов Б.В. Образование в сфере техники безопасности в строительстве // Строительство уникальных зданий и сооружений. 2012. № 5. С. 31–35.
9. Морозова Т.Ф., Лаптева Н.А. Оценка рисков при реализации инвестиционно-строительного проекта на примере бизнес-центра // Инженерно-строительный журнал. 2011. № 2. С. 48–51.
10. Морозова Т.Ф., Кинаят Л.А., Кинаят А.Ж. Оценка рисков в строительстве // Строительство уникальных зданий и сооружений. 2013. № 5(10). С. 68–76.
11. МОТ-СУОТ 2001 (ILO-OSH 2001) Руководство по системам управления безопасностью и охраной труда. Женева: МОТ, 2003. 28 с.
12. Талапов В.В. BIM: что под этим обычно понимают. [Электронный ресурс] URL http://isicad.ru/ru/articles.php?article_num=14078 (дата обращения: 23.04.2016).
13. Kim K., Cho Y., Zhang S. Integrating work sequences and temporary structures into safety planning: Automated scaffolding-related safety hazard identification and prevention in BIM // Automation in Construction. 2016. Vol. 70. Pp. 128–142.
14. Zou Y, Kiviniemi A., Stephen W.J. A review of risk management through BIM and BIM-related technologies // Safety Science. 2016. № 1.
15. Zhang S., Sulankivi K., Kiviniemi M., Romo I., Eastman C.M., Teizer J. BIM-based fall hazard identification and prevention in construction safety planning // Safety Science. 2015. Vol. 72. Pp. 31–45.
16. Zhang S., Teizer J., Lee J.-K., Eastman C. M.., Venugopal M. Building Information Modeling (BIM) and safety: automatic safety checking of construction models and schedules // Automation in Construction. 2013. Vol. 29. Pp. 183–195.
17. Benjaoran V., Bhokha S. An integrated safety management with construction management using 4D CAD model // Safety Science. 2010. Vol. 48. № 3. Pp. 395–403.
18. Zhang S., Boukamp F., Teizer J. Ontology-based semantic modeling of construction safety knowledge: Towards automated safetyplanning for job hazard analysis (JHA) // Automation in Construction. 2015. Vol. 52. Pp. 29–41.
19. Raheem A.A., Issa R.R.A. Safety implementation framework for Pakistani construction industry // Safety science. 2016. Vol. 82. Pp. 301–314.
20. Smith P. BIM implementation – global strategies // Procedia Engineering. 2014. Vol. 85. Pp. 482–492.
21. Tomek A., Matějka P. The Impact of BIM on risk management as an argument for its implementation in a construction company // Procedia Engineering. 2014. Vol. 85. Pp. 501–509.
22. Czmoch I., Pękala A. Traditional design versus BIM based design // Procedia Engineering. 2014. Vol. 91. Pp. 210–215.
23. Volkov A.A., Sukneva L.V. BIM-Technology in tasks of the designing complex systems of alternative energy supply // Procedia Engineering. 2014. Vol. 91. Pp. 377–380.
24. Lindblad H., Vass S. BIM implementation and organisational change: a case study of a large Swedish public client // Procedia Economics and Finance. 2015. Vol. 21. Pp. 178–184.
25. Tarandi V. A BIM collaboration lab for improved through life support // Procedia Economics and Finance. 2015. Vol. 21.

22. Czmoch I., Pękala A. Traditional design versus BIM based design. *Procedia Engineering.* 2014. Vol. 91. Pp. 210–215.
23. Volkov A.A., Sukneva L.V. BIM-Technology in tasks of the designing complex systems of alternative energy supply. *Procedia Engineering.* 2014. Vol. 91. Pp. 377–380.
24. Lindblad H., Vass S. BIM implementation and organisational change: a case study of a large Swedish public client. *Procedia Economics and Finance.* 2015. Vol. 21. Pp. 178–184.
25. Tarandi V. A BIM collaboration lab for improved through life support. *Procedia Economics and Finance.* 2015. Vol. 21. Pp. 383–390.
26. Tulenheimo R. challenges of implementing new technologies in the world of BIM – case study from construction engineering industry in Finland. *Procedia Economics and Finance.* 2015. Vol. 21. Pp. 469–477.
27. Sørensen N.L, Frandsen A.K., Øien T.B. Architectural competitions and BIM. *Procedia Economics and Finance.* 2015. Vol. 21. Pp. 239–246.
28. Jankowski B., Prokocki J., Krzemiński M. Functional assessment of BIM methodology based on implementation in design and construction company. *Procedia Engineering.* 2015. Vol. 111. Pp. 351–355.
29. Porter S., Tan T., Tan T., West G. Breaking into BIM: Performing static and dynamic security analysis with the aid of BIM. *Automation in Construction.* 2014. Vol. 40. Pp. 84–95.
30. Takim R., Harris M., Nawawi A. Building Information Modeling (BIM): a new paradigm for quality of life within architectural, engineering and construction (AEC), industry. *Procedia – Social and Behavioral Sciences.* 2013. Vol. 101. Pp. 23–32.
31. Motawa I., Carter K. Sustainable BIM-based evaluation of buildings. *Procedia – Social and Behavioral Sciences.* 2013. Vol. 74. Pp. 419–428.
32. Fridrich J., Kubečka K. BIM – the process of modern civil engineering in higher education. *Procedia – Social and Behavioral Sciences*. 2014. Vol. 141. Pp. 763–767.
33. Bargstädt H.-J. Challenges of BIM for construction site operations. *Procedia Engineering.* Vol. 117. Pp. 52–59.
34. Maia L., Mêda P., Freitas J.G. BIM methodology, a new approach - case study of structural elements creation. *Procedia Engineering.* 2015. Vol. 114. Pp. 816–823.
35. Yenumula K., Kolmer C., Pan J., Su X. BIM-controlled signage system for building evacuation. *Procedia Engineering*. 2015. Vol. 118. Pp. 284–289.
36. Luo Y., Wu W. Sustainable design with BIM facilitation in project-based learning. *Procedia Engineering.* 2015. Vol. 118. Pp. 819–826.
37. Juszczyk M., Výskala M., Zima K. Prospects for the use of BIM in Poland and the Czech Republic – preliminary research results. *Procedia Engineering.* 2015. Vol. 123. Pp. 250–259.
38. Plebankiewicz E., Zima K., Skibniewski M. Analysis of the first Polish BIM-based cost estimation application. *Procedia Engineering.* 2015. Vol. 123. Pp. 405–414.
39. Tomek R., Kalinichuk S. Agile PM and BIM: a hybrid scheduling approach for a technological construction project. *Procedia Engineering.* 2015. Vol. 123. Pp. 557–564.
40. Minagawa M., Kusayanagi S. Study on BIM utilization for design improvement of infrastructure project. *Procedia Engineering.* 2015. Vol. 125. Pp. 431–437.
41. Bonenberg W., Wei X. Green BIM in sustainable infrastructure. *Procedia Manufacturing.* 2015. Vol. 3. Pp. 1654–1659.
42. Sharmanov V.V., Mamayev A.Ye., Boleyko A.S., Zolotova Yu.S. BIM i Anderrayting – tochki soprikosnoveniya. [BIM and Underwriting : a common grounds]. *Aktual'nye*

Pp. 383–390.

26. Tulenheimo R. challenges of implementing new technologies in the world of BIM – case study from construction engineering industry in Finland // Procedia Economics and Finance. 2015. Vol. 21. Pp. 469–477.
27. Sørensen N.L, Frandsen A.K., Øien T.B. Architectural competitions and BIM // Procedia Economics and Finance. 2015. Vol. 21. Pp. 239–246.
28. Jankowski B., Prokocki J., Krzemiński M. Functional assessment of BIM methodology based on implementation in design and construction company // Procedia Engineering. 2015. Vol. 111. Pp. 351–355.
29. Porter S., Tan T., Tan T., West G. Breaking into BIM: Performing static and dynamic security analysis with the aid of BIM // Automation in Construction. 2014. Vol. 40. Pp. 84–95.
30. Takim R., Harris M., Nawawi A. Building Information Modeling (BIM): a new paradigm for quality of life within architectural, engineering and construction (AEC), industry // Procedia – Social and Behavioral Sciences. 2013. Vol. 101. Pp. 23–32.
31. Motawa I., Carter K. Sustainable BIM-based evaluation of buildings // Procedia – Social and Behavioral Sciences. 2013. Vol. 74. Pp. 419–428.
32. Fridrich J., Kubečka K. BIM – the process of modern civil engineering in higher education // Procedia – Social and Behavioral Sciences. 2014. Vol. 141. Pp. 763–767.
33. Bargstädt H.-J. Challenges of BIM for construction site operations // Procedia Engineering. Vol. 117. Pp. 52–59.
34. Maia L., Mêda P., Freitas J.G. BIM methodology, a new approach - case study of structural elements creation // Procedia Engineering. 2015. Vol. 114. Pp. 816–823.
35. Yenumula K., Kolmer C., Pan J., Su X. BIM-controlled signage system for building evacuation // Procedia Engineering. 2015. Vol. 118. Pp. 284–289.
36. Luo Y., Wu W. Sustainable design with BIM facilitation in project-based learning // Procedia Engineering. 2015. Vol. 118. Pp. 819–826.
37. Juszczyk M., Výskala M., Zima K. Prospects for the use of BIM in Poland and the Czech Republic – preliminary research results // Procedia Engineering. 2015. Vol. 123. Pp. 250–259.
38. Plebankiewicz E., Zima K., Skibniewski M. Analysis of the first Polish BIM-based cost estimation application // Procedia Engineering. 2015. Vol. 123. Pp. 405–414.
39. Tomek R., Kalinichuk S. Agile PM and BIM: a hybrid scheduling approach for a technological construction project // Procedia Engineering. 2015. Vol. 123. Pp. 557–564.
40. Minagawa M., Kusayanagi S. Study on BIM utilization for design improvement of infrastructure project // Procedia Engineering. 2015. Vol. 125. Pp. 431–437.
41. Bonenberg W., Wei X. Green BIM in sustainable infrastructure // Procedia Manufacturing. 2015. Vol. 3. Pp. 1654–1659.
42. Шарманов В.В., Мамаев А.Е., Болейко А.С., Золотова Ю.С. BIM и Андеррайтинг – точки соприкосновения // Актуальные проблемы гуманитарных и естественных наук. 2016. № 1–3. С. 167–173.
43. МДС 12-28.2006 «Методическое руководство по проведению экспертной оценки безопасности нестационарных рабочих мест на строительных объектах» М.: 2007.

Шарманов В.В., Симанкина Т.Л., Мамаев А.Е. BIM технологии в оценке уровня охраны труда // Инженерно-строительный журнал. 2017. № 1(69). С. 77–88.

problemy gumanitarnyh i estestvennyh nauk. 2016. No. 1–3. Pp. 167–173. (rus)

43. MDS 12-28.2006. Metodicheskoye rukovodstvo po provedeniyu ekspertnoy otsenki bezopasnosti nestatsionarnykh rabochikh mest na stroitelnykh obyektakh. [Guidance Documents in Construction 12-28.2006. A methodical management on carrying out an expert evaluation of safety of non-stationary workplaces on construction objects]. Moscow, 2007. (rus)

Vladimir Sharmanov,
+7(911)1747195; sharmanov_v@mail.ru

Tat'yana Simankina,
+7(952)3991288; talesim@mail.ru

Anton Mamaev,
89117642005; mamaev7@gmail.com

Владимир Владимирович Шарманов,
+7(911)1747195;
эл. почта: sharmanov_v@mail.ru

Татьяна Леонидовна Симанкина,
+7(952)3991288; эл. почта: talesim@mail.ru

Антон Евгеньевич Мамаев,
89117642005; эл. почта: mamaev7@gmail.com

Федеральное государственное автономное образовательное учреждение высшего образования
Санкт-Петербургский политехнический университет Петра Великого

ПОЛИТЕХ
Санкт-Петербургский политехнический университет Петра Великого

Инженерно-строительный институт
Центр дополнительных профессиональных программ

195251, г. Санкт-Петербург, Политехническая ул., 29,
тел/факс: 552-94-60, www.stroikursi.spbstu.ru,
stroikursi@mail.ru

Приглашает специалистов проектных и строительных организаций,
не имеющих базового профильного высшего образования
на курсы профессиональной переподготовки (от 500 часов)
по направлению «Строительство» по программам:

П-01 «Промышленное и гражданское строительство»

Программа включает учебные разделы:

- ***Основы строительного дела***
- ***Инженерное оборудование зданий и сооружений***
- ***Технология и контроль качества строительства***
- ***Основы проектирования зданий и сооружений***
- ***Автоматизация проектных работ с использованием AutoCAD***
- ***Автоматизация сметного дела в строительстве***
- ***Управление строительной организацией***
- ***Управление инвестиционно-строительными проектами. Выполнение функций технического заказчика***

П-02 «Экономика и управление в строительстве»

Программа включает учебные разделы:

- ***Основы строительного дела***
- ***Инженерное оборудование зданий и сооружений***
- ***Технология и контроль качества строительства***
- ***Управление инвестиционно-строительными проектами. Выполнение функций технического заказчика и генерального подрядчика***
- ***Управление строительной организацией***
- ***Экономика и ценообразование в строительстве***
- ***Управление строительной организацией***
- ***Организация, управление и планирование в строительстве***
- ***Автоматизация сметного дела в строительстве***

П-03 «Инженерные системы зданий и сооружений»

Программа включает учебные разделы:

- ***Основы механики жидкости и газа***
- ***Инженерное оборудование зданий и сооружений***
- ***Проектирование, монтаж и эксплуатация систем вентиляции и кондиционирования***
- ***Проектирование, монтаж и эксплуатация систем отопления и теплоснабжения***
- ***Проектирование, монтаж и эксплуатация систем водоснабжения и водоотведения***
- ***Автоматизация проектных работ с использованием AutoCAD***
- ***Электроснабжение и электрооборудование объектов***

П-04 «Проектирование и конструирование зданий и сооружений»

Программа включает учебные разделы:

- ***Основы сопротивления материалов и механики стержневых систем***
- ***Проектирование и расчет оснований и фундаментов зданий и сооружений***
- ***Проектирование и расчет железобетонных конструкций***
- ***Проектирование и расчет металлических конструкций***
- ***Проектирование зданий и сооружений с использованием AutoCAD***
- ***Расчет строительных конструкций с использованием SCAD Office***

П-05 «Контроль качества строительства»

Программа включает учебные разделы:

- ***Основы строительного дела***
- ***Инженерное оборудование зданий и сооружений***
- ***Технология и контроль качества строительства***
- ***Проектирование и расчет железобетонных конструкций***
- ***Проектирование и расчет металлических конструкций***
- ***Обследование строительных конструкций зданий и сооружений***
- ***Выполнение функций технического заказчика и генерального подрядчика***

По окончании курса слушателю выдается диплом о профессиональной переподготовке установленного образца, дающий право на ведение профессиональной деятельности